UNIVERSIDADE FEDERAL DO RIO GRANDE DO SUL
INSTITUTO DE BIOCIÊNCIAS
PROGRAMA DE PÓS-GRADUAÇÃO EM GENÉTICA E BIOLOGIA MOLECULAR

EVOLUÇÃO NA FORMA E TAMANHO DO CRÂNIO NO GÊNERO *CTENOMYS* (RODENTIA: CTENOMYIDAE)

RODRIGO FORNEL

Tese submetida ao Programa de Pós-Graduação em Genética e Biologia Molecular da Universidade Federal do Rio Grande do Sul como requisito parcial para a obtenção do grau de Doutor em Ciências.

Orientador: Dr. Thales Renato O. de Freitas
Co-orientador: Dr. Pedro Cordeiro Estrela de A. Pinto

Porto Alegre
Abril de 2010

Este trabalho foi desenvolvido no Laboratório de Citogenética e Evolução do Departamento de Genética do Instituto de Biociências da Universidade Federal do Rio Grande do Sul, subvencionado por: Conselho Nacional de Desenvolvimento Científico e Tecnológico (CNPq), Coordenação de Aperfeiçoamento de Pessoal de Nível Superior (CAPES) e Fundação de Amparo à Pesquisa do Estado do Rio Grande do Sul (FAPERGS).

À minha esposa Tatiane.

Agradecimentos

Agradeço ao professor Thales R. O. de Freitas pela orientação, amizade, paciência e por todos os ensinamentos acadêmicos e de vida. Obrigado por me deixar fazer parte deste universo à parte dos tuco-tucos.

Ao Pedro Cordeiro Estrela pela co-orientação, motivação, paciência e ensinamentos, principalmente nas áreas de morfometria e evolução. Obrigado por me ensinar programação em *R*, que foi de grande valia nas análises deste trabalho.

Agradeço profundamente a Tatiane Noviski da Silva Fornel, minha esposa, por todo apoio, paciência e carinho incondicional durante esta jornada. Te amo Tatinski!

Agradeço ao meu colega Fabiano A. Fernandes por todo o apoio e incentivo durante o doutorado. Pela "parceria" nas viagens a museus e congressos e pelas agradáveis conversas no RU. Valeu amigão!

Aos meus pais Paulo e Isolde que mesmo na distante e pacata Panambi permanecem como uma fonte sólida de amor e carinho, muito obrigado pela educação que me deram e por todo o apoio.

Aos pesquisadores, estudantes e estagiários da sala 103 e do Laboratório de Citogenética e Evolução do Departamento de Genética, "tucólogos" e "não-tucólogos". Um muito obrigado pela convivência e amizade dos colegas José, Gabriela, Gislene, Simone, Darlise, Lívia, Carla, Camila, Paula, Claiton, Benhur, Chico, Jorge, Josmael, Laura, Patrícia, Tati Trigo, Lígia, Eunice, Daniel, Flávia e Luciano. Bem como àqueles diretamente relacionadas ao grupo, como Binha, Guga, Lessandro, Arthur, Milton, Renata e Caetano. Mesmo convivendo mais com uns do que com outros, foi uma grande honra conhecer todos vocês.

Aos colegas "morfometristas" Daniela, Daniza e Ernesto. Aprendi muito com vocês. Assim como com os professores Leandro R. Monteiro e Gabriel Marroig.

Ao professor Michel Baylac por nos ceder gentilmente a biblioteca *Rmorph*.

Aos sempre dispostos a ajudar Lúcia, Ellen e Elmo, muito obrigado.

Aos chefes e curadores de coleções dos museus que visitei e que foram fundamentais para o trabalho de doutorado: Henrique Gonzales do MUNHINA (*Museo Nacional de Historia Natural y Antropología, Montevideo, Uruguay*); Olga B. Vacaro e Esperança A. Varela do MACN (*Museo Argentino de Ciencias Naturales "Bernardino*

Rivadavia", Buenos Aires, Argentina); Diego H. Verzi e A. Itati Olivares do MLP (*Museo de La Plata, Argentina*); A. Damián Romero do MMP (*Museo Municipal de Ciencias Naturales "Lorenzo Scaglia", Mar del Plata, Argentina*); James L. Patton, Eileen A. Lacey, e Christopher Conroy do MVZ (*Museum of Vertebrate Zoology, University of California, Berkeley, USA*); Eileen Westwig do AMNH (*American Museum of Natural History, New York City, USA*); e Bruce D. Patterson do FMNH (*Field Museum of Natural History, Chicago, USA*).

Aos professores do Departamento de Genética da UFRGS por todos os ensinamentos.

Ao Programa de Pós-Graduação em Genética e Biologia Molecular pelo auxílio financeiro na viagem aos museus da América do Norte.

Ao Conselho Nacional de Desenvolvimento Científico e Tecnológico (CNPq) pela bolsa de doutorado.

Sinceramente, muito obrigado à todos que de alguma forma contribuiram na elaboração desta tese.

Sumário

Lista de Tabelas

Lista de Figuras

Capítulo III

Capítulo IV

Resumo

Ctenomys é um gênero de roedores subterrâneos endêmico ao sul da região Neotropical, que compreende cerca de 60 espécies conhecidas como "tuco-tucos". Este gênero é um exemplo de evolução rápida, que tem uma alta diversidade cariotípica com número diplóide variando de 2n = 10 até 2n = 70. Com exceção de algumas espécies, a variação morfológica quantitativa entre os tuco-tucos é pouco conhecida. Recentemente, estudos usando citocromo *b* propuseram relações filogenéticas para *Ctenomys* e apoiam oito grandes grupos. O objetivo deste estudo é investigar neste gênero, os padrões de evolução morfológica na forma e no tamanho do crânio, assim como diferenças entre sexos, em nível macro e microevolutivo, usando uma abordagem de morfometria geométrica. Em nível macroevolutivo, analisamos padrões de variação em 47 espécies do gênero *Ctenomys* e a variação dentro e entre os grupos *mendocinus* e *torquatus*. Em nível microevolutivo, analisamos mais detalhadamente as espécies *C. minutus* e *C. lami*. Ambas ocorrem na planície costeira do sul do Brasil. A primeira espécie tem 15 cariótipos (2n = 42, 43, 44, 45, 46a, 46b, 47a, 47b, 48a, 48b, 48c, 49a, 49b, 50a e 50b), o maior polimorfismo cromossômico conhecido para o gênero *Ctenomys*. *C. lami* também apresenta uma alta variação cariotípica, com números diplóides de 2n = 54 até 2n = 58. Baseado em diferentes frequências de rearranjos cromossômicos ao longo de sua distribuição geográfica, quatro blocos populacionais foram previamente propostos. Em nível macroevolutivo, a diversificação na forma do crânio parece estar estruturada geograficamente. Encontramos gradientes tanto leste-oeste quanto norte-sul, crânios mais robustos no norte e crânios mais gráceis nas espécies do sul. A mandíbula se mostrou menos variável na forma do que o crânio. Os fenogramas gerados com distâncias de Mahalanobis mostraram um forte sinal filogenético para o grupo *torquatus* e similaridade morfológica entre os dois grupos Bolivianos e entre os grupos *mendocinus* e Patagônico. O grupo *torquatus* é muito congruente na forma e pouco varia em tamanho. Uma relação de ancestralidade comum entre os grupos Patagônico e *mendocinus*, baseada na forma do crânio, é reforçada pela mesma morfologia de espermatozóide assimétrico encontrada nos dois grupos. Em nível microevolutivo, a forma do crânio não parece obedecer ao mesmo padrão. Em *C. minutus* a variação morfológica é estruturada espacialmente por um modelo de isolamento pela distância, por barreiras geográficas antigas (paleo-canais) e

provavelmente por uma inversão cromossômica. Os rearranjos cromossômicos envolvendo fusões e fissões robertsonianas parecem não ser um fator primário que promova a estruturação na variação do crânio. A diferença de habitats também foi um dos fatores detectados como estruturante. Além disso, nós encontramos deriva, seleção diversificadora e seleção estabilizadora atuando na variação da forma do crânio nos quatro blocos populacionais cromossômicos de *C. lami*. O padrão de seleção diversificadora envolve estruturas relacionadas à escavação, que são compatíveis com modelos biomecânicos propostos para *Ctenomys*. O padrão de seleção estabilizadora envolve um ajuste das proporções da bula timpânica, entre a capacidade auditiva e a abertura mandibular. De forma geral, nossos achados sugerem que a evolução do crânio de *Ctenomys* é resultado principalmente de processos históricos regidos pela biologia da espécie em níveis macroevolutivos. Porém, em níveis microevolutivos, a combinação de diversas forças evolutivas e processo históricos produzem padrões mais variáveis do que o esperado e pouco relacionados com a distribuição geográfica.

Abstract

Ctenomys is a genus of subterranean rodents endemic to the southern Neotropical region, which comprise about 60 living species known as "tuco-tucos". This genus is an example of rapid evolution, which have high karyotypic diversity with diploid numbers varying from 2n = 10 to 2n = 70. To the exception of a few species, quantitative morphological variation among tuco-tucos is poorly known. Recently, studies using cytochrome *b* proposed phylogentic relationships for *Ctenomys* and support eight great groups. The goal of this study is to investigate in this genus, the morphological evolution patterns in skull shape and size variation between sexes, in macro and microevolutionary levels, using a geometric morphometrics approach. In macroevolutionay level, we analyze the variation pattern in 47 species of the genus *Ctenomys* and the variation within and between *mendocinus* and *torquatus* groups. In microevolutionary level we analyze in more details *C. lami* and *C. minutus*. Both occurs in coastal plain of southern Brazil. The first species has 15 karyotypes (2n = 42, 43, 44, 45, 46a, 46b, 47a, 47b, 48a, 48b, 48c, 49a, 49b, 50a and 50b), the highest intraspecific chromosomal polymorphism known for the genus *Ctenomys*. *C. lami* also shows high karyotypic variation, with diploid numbers ranging from 2n = 54 to 2n = 58. Based on different chromosome rearrangement frequencies along its geographical distribution, four population blocks were previously proposed. In macroevolutionary level we found that skull evolution appear geographically structured. We found west-east and north-south gradients, skulls more robust in north and skulls more gracile in south species. The mandible is less variable in shape than skull. The phenograms of Mahalanobis distances show strong phylogenetic signal only for *torquatus*-group and morphological similarity between two Bolivian groups, and between *mendocinus* and Patagonico groups. The *torquatus*-group is very congruent in shape and have low variation in size. Common ancestral relationship between Patagonico and *mendocinus* groups based in skull shape is reinforced by the same asymmetry in sperm morphology found in both groups. In microevolutionary level, the skull shape does not follow the same pattern. For *C. minutus* the morphological variation is spatial structured by the isolation-by-distance model by ancient barriers (paleochannels) and probably by a chromosomal inversion. Chromosomal rearrangements involving robertsonians fusions and fissions appear not be a primary factor that promote the structure in skull shape. The habitats difference also a

factor in structure shape change. Moreover, we found drift, diversifying selection and stabilizing selection acting on variation in skull shape in four chromosomal population blocks of *C. lami*. Diversifying patterns involve structures related to digging, that are compatible with biomechanical models proposed for *Ctenomys*. Stabilizing patterns involve a compromise in the proportions of the auditory bulla, between hearing ability and the mandibular opening. In general, our findings suggested that *Ctenomys* skull evolution is a result of historical factors conducted by species biology in macroevolutionary level. However, in microevolutionary level the combination of many forces and historical process producing more variable patterns than expected and weak related to geographical distribution.

Capítulo I - Introdução Geral

I.1. Evolução morfológica

"A diversidade da vida na Terra é produto da evolução: um processo natural e imprevisível de descendência temporal com modificação genética que é afetada por seleção natural, acaso, contingências históricas e alterações ambientais" (NABT 2003).

Desde a época de Charles R. Darwin, um dos temas centrais, mas pouco entendidos, da biologia evolutiva é o modo como morfologias complexas são formadas e evoluem. A evolução destas morfologias complexas, como o crânio de um mamífero, no qual vários caracteres interagem para construir um organismo funcionalmente e morfologicamente integrado, é um tema importante, com implicações em diversos campos da biologia evolutiva (Atchley & Hall 1991, Marroig *et al*. 2004).

O fenótipo não é uma simples "tradução" do genótipo, mas sim, resultado da interação entre genes e o ambiente. Recentemente, alguns trabalhos têm tentado explicar os mecanismos de regulação gênica para o desenvolvimento do plano corporal dos animais através de Redes Regulatórias de Genes (*GRNs – Gene Regulatory Networks*) (Davidson & Erwin 2006, De Robertis 2008, Erwin & Davidson 2009, He & Deem 2010). A evolução dos planos corporais deve depender de mudanças na arquitetura do desenvolvimento dos *GRNs* e essas redes são compostas por diversos componentes que evoluem em diferentes taxas e maneiras (Davidson & Erwin 2006). Assim, nos próximos anos provavelmente passaremos a entender melhor os mecanismos genéticos relacionados com a evolução morfológica. De forma geral, a maioria das mudanças no fenótipo são causadas principalmente por mudanças genéticas e muito poucas como resultado de resposta direta a mudanças ambientais (Lande 1979). O genótipo pode ser resumido como a matriz de variância/covariância genética (Matriz-G) e o fenótipo, como a matriz de variância/covariância fenotípica (Matriz-P) (Lande 1979). Em muitos casos é extremamente difícil a obtenção da matriz-G mas, é possível substituí-la pela sua contra-parte, a matriz-P, obtida através de dados morfológicos, já que em muitas vezes as duas matrizes são similares ou proporcionais (Cheverud 1996, Koots & Gibson 1996, Klingenberg & Leamy 2001, Marroig & Cheverud 2001, 2004). A similaridade entre os padrões de variação genética e fenotípica é de grande importância nas inferências a cerca

das forças evolutivas que atuaram na diferenciação entre populações (Marroig *et al*. 2004). Embora, em muitos casos, seja possível que fatores filogenéticos, ecológicos e relacionados ao desenvolvimento afetem os padrões de variação (Marroig & Cheverud 2001).

Mesmo que a maioria dos biólogos concorde que o processo de seleção natural seja a principal força atuante na diversificação morfológica, e que morfologias complexas, sejam muitas vezes estruturas altamente adaptativas, sempre existe a possibilidade de que evolução neutra, por deriva genética, seja responsável pela diversidade morfológica observada (Marroig & Cheverud 2004). Por exemplo, se presume que em populações, subdivididas em pequenos demes, de pequeno tamanho efetivo, possa ocorrer influência de deriva genética mesmo na presença de seleção (Lessa 2000).

O termo macroevolução foi cunhado pelo geneticista russo Iurii Filipchenko (mentor de Theodosius Dobzhansky), para distinguir a herança Mendeliana que ocorre em espécies, e as mudanças responsáveis pela formação de táxons acima do nível de espécie (Erwin 2000). Macro e microevolução diferem basicamente quanto ao nível em que atuam (Bock 2007). Microevolução é a variação em populações dentro do nível de espécie, já macroevolução é a variação acima do nível de espécie (Erwin 2000, Catley & Novick 2009). Para Bock (2007) os dois modos de evolução não diferem entre si, com exceção apenas da escala de mudança. Já para Erwin (2000) a especiação rápida representa uma descontinuidade entre micro e macroevolução. A principal fonte de discussão nesse debate, se a macroevolução seria apenas sucessivos ciclos de microevolução, vem da paleobiologia. Isso pois a escala de espaço/tempo em que eventos como a especiação e a origem de novos gêneros e famílias é gigantesco perto de eventos de variação intraespecífica (microevolução) (Erwin 2000, Simons 2002, Granthan 2007, Jablonski 2007).

I.2. A quantificação da forma biológica

Estima-se que a forma dos organismos seja um dos mais antigos temas investigados na biologia (Monteiro & Reis 1999). Entretanto, a palavra morfologia só foi cunhada no século XVIII pelo poeta e naturalista alemão Goethe (1749-1832), que caracterizou a morfologia como sendo o estudo das formas orgânicas (Kardong 1995).

O estudo que visava quantificar a forma dos organismos recebeu o nome de morfometria por R. Blackith em 1965 (Monteiro & Reis 1999). Entretanto, a morfometria, ou biometria, teve seu início no final do século XIX com os trabalhos de Francis Galton, W. F. R. Weldon e Karl Pearson, os quais estudaram a variação na forma dos organismos através de correlações entre medidas de distâncias em estruturas biológicas. Outros personagens que contribuíram para os avanços na morfometria foram G. Teissier e R. A. Fisher nos anos 30 do século XX. O primeiro criou a análise de componentes principais e o segundo a análise da variância, a análise multivariada da variância e a análise discriminante (Marcus *et al*. 1996, Monteiro & Reis 1999). Só no início dos anos 80 Bookstein propôs um método geométrico para estudar diferenças de forma com a criação de um espaço multivariado para análises morfométricas em configurações de marcos anatômicos. Ainda no final dos 80 Bookstein conceituou forma como sendo "todas as propriedades de uma configuração de pontos que não se alteram por efeitos de tamanho, posição e orientação". Mas a maior popularização dos métodos de morfometria geométrica só veio a ocorrer no início dos anos 90 quando F. James Rohlf começou a desenvolver uma série de programas de análise geométrica para microcomputadores (Marcus *et al*. 1996, Monteiro & Reis 1999).

O campo da morfometria tem especial interesse nos métodos de descrição, na análise estatística da variação da forma entre organismos e na análise das mudanças na forma em função do crescimento. Também preocupa-se com estudos relacionados com tratamentos experimentais e evolução (Rohlf & Marcus 1993). Morfologias complexas podem ser descritas por um conjunto de caracteres de distribuição contínua, permitindo que diferenças entre populações possam ser testadas estatisticamente (Marroig & Cheverud 2004, Marroig *et al*. 2004).

A chamada morfometria tradicional consiste na aplicação de métodos de estatística multivariada em um conjunto de variáveis. Essas variáveis geralmente correspondem a uma série de medidas tomadas de um organismo. As medidas são na maioria comprimentos e larguras de estruturas e distâncias entre certos pontos de referência. Algumas vezes também podem ser usados ângulos, áreas e razões entre distâncias (Monteiro & Reis 1999). É usada geralmente para estudos de alometria (mudanças na forma em função do tamanho) e estudos de mudanças na forma ajustados para um mesmo tamanho entre organismos. Os resultados podem ser mostrados de maneira numérica e

gráfica em termos de combinações lineares de variáveis mensuráveis. Esta abordagem não pode recriar a forma a partir dos dados coletados, mas apenas indicar regiões de possível variação (Rohlf & Marcus 1993, Marcus *et al*. 1996).

A morfometria geométrica, como o próprio nome sugere, captura a geometria da estrutura em estudo através das coordenadas de marcos anatômicos, que podem ser bi ou tridimensionais e permite a separação dos componentes forma e tamanho (Rohlf & Marcus 1993, Monteiro & Reis 1999). Esta nova morfometria é capaz de localizar e descrever regiões de mudanças na forma de maneira mais precisa, e também de reconstruir graficamente tais mudanças. Esta descrição é feita através do estabelecimento de pontos anatômicos que servem de referência em estruturas homólogas, os chamados marcos anatômicos. As coordenadas cartesianas destas configurações de marcos são as variáveis utilizadas no estudo geométrico das estruturas de interesse. A estatística da nova morfometria é a mesma estatística multivariada usada nas medidas lineares, só que agora aplicada a coordenadas de marcos anatômicos alinhados adequadamente. Então, as mesmas análise de componentes principais, análise fatorial e análise de variáveis canônicas podem ser aplicadas a dados de pontos de referência. As coordenadas apresentam vantagens, pois incluem informações sobre as posições relativas, permitindo assim a reconstrução da forma após as análises uni e multivariadas. A morfometria geométrica tem maior robustez na análise integrada e exclui fatores de posição, orientação e tamanho na análise da forma (Bookstein 1991, Rohlf & Marcus 1993, Marcus *et al*. 1996, Monteiro & Reis 1999, Adams *et al*. 2004).

A análise de contornos também é atribuída à nova morfometria. Tais contornos podem ser tanto abertos quanto fechados, dependendo da estrutura a ser analisada. Apesar dos contornos não compartilharem a noção de homologia dos marcos anatômicos, eles podem ser bastante úteis no estudo da forma em organismos onde a localização dos marcos anatômicos é muito difícil ou praticamente impossível. (Marcus *et al*. 1996, Monteiro & Reis 1999, Adams *et al*. 2004).

As diferentes técnicas morfométricas vêm sendo utilizadas em estudos que visam testar e descrever a existência de variação na forma dos organismos, seja em nível de dimorfismo sexual, variação geográfica, variação inter e intra-populacional, variação entre espécies filogeneticamente próximas, trajetórias ontogenéticas, zonas híbridas, paleontologia, sistemática e evolução. Além disso, a gama de estruturas anatômicas e

grupos taxonômicos que vêm sendo estudadas com estes métodos é bastante ampla. Ela vai desde conchas de moluscos e asas de insetos, passando por cascos de tartarugas e toda a sorte de estruturas ósseas de peixes a mamíferos, até estruturas vegetais como nervuras de folhas e partes florais (Marcus *et al*. 1996, Adams *et al*. 2004).

Entre os estudos que vêm sendo feitos com morfometria geométrica para análise da forma do crânio de roedores podem ser destacados alguns trabalhos. Entre eles, Corti *et al*. (1996) examinaram a variação morfométrica tridimensional na forma e tamanho da mandíbula em quatro espécies cromossômicas de *Spalax ehrenbergi*. Esses autores concluíram que diferenças no tamanho entre espécies são relacionadas ao número cromossômico e a ecogeografia, mas a significância biomecânica na diferença da forma não foi facilmente interpretada. Reis *et al*. (2002) estudaram a variação geográfica na forma do crânio de *Thrichomys apereoides* no Brasil e das três vistas do crânio analisadas a que melhor se ajustou com a atual distribuição geográfica desta espécie foi a vista lateral. Nicola *et al*. (2003) investigaram a congruência entre variação na forma do crânio e árvores filogenéticas baseadas em dados moleculares para o gênero roedor *Trinomys* e das vistas do crânio usadas no estudo apenas a vista lateral foi congruente com os dados moleculares. Cardini & O'Higgins (2004) estudaram os padrões de evolução morfológica em marmotas no contexto filogenético (a partir de dados de citocromo *b*), o objetivo não era de reconstruir filogenias com dados morfológicos, mas sim de examinar a variação na forma do crânio no contexto filogenético. Klingenberg & Leamy (2001) combinaram métodos de morfometria geométrica e genética quantitativa para estudar os padrões de variação fenotípica e genética na forma da mandíbula de *Mus musculus* e mostraram correspondência entre os dados morfológicos e genéticos. Monteiro & Reis (2005) estimaram padrões evolutivos na mudança da forma da mandíbula do gênero *Trinomys*, combinando dados de desenvolvimento, quantificação da variação da forma e filogenia a partir de dados moleculares.

Atualmente trabalhos usando dados tridimensionais (3D) vêm sendo realizados. Esses dados, na maioria das vezes, são mais difíceis de serem adquiridos que os bidimensionais (2D) e são necessários equipamentos mais dispendiosos para determinar a posição (coordenadas 3D) de cada marco anatômico. Cardini & Thorington (2006) usando crânios de marmotas testaram as duas metodologias (bi- e tridimensional) e apesar da técnica em 3D ser considerada como a mais precisa, os dados de variação na forma do

crânio pouco diferiram dos resultados obtidos pelos métodos de 2D para diferenciar populações. Mas para descrever as mudanças na forma do crânio os dados em 3D ainda são mais ricos.

I.3. A ordem Rodentia

Considerado o grupo mais diverso entre os mamíferos, os roedores compreendem 2.277 espécies, distribuídas em 481 gêneros, organizados em 34 famílias (Honeycutt 2009). A ordem Rodentia é tradicionalmente dividida em três subordens: Sciuromorpha, Myomorpha e Hystricomorpha, todas elas baseadas na musculatura da mandíbula e em estruturas associadas ao crânio. Apesar desses três termos ainda serem usados, novos estudos mostram que a sistemática de Rodentia é mais complexa e reconhecem apenas duas subordens: Sciurognathi e Hystricognathi, distinguidas basicamente pela estrutura da mandíbula (Emmons & Feer 1990, Nowak 1999, Marivaux *et al*. 2002).

Os roedores são animais facilmente reconhecidos através de seus dentes. Estes animais possuem dois pares de incisivos de crescimento contínuo, um par na maxila superior e outro na inferior. A ausência de caninos e de três a quatro pré-molares formam um espaço (diastema) entre os incisivos e os dentes do fundo da boca. Os incisivos têm um forte esmalte na superfície anterior e dentina mais macia e de desgaste mais rápido na parte posterior; esse arranjo garante que mesmo com o desgaste pelo uso, os dentes estejam sempre afiados. Estes incisivos são ferramentas bastante versáteis e podem ser usados para cortar gramíneas, raspar a casca de árvores, cavar túneis, aprisionar e matar presas, ou até mesmo segurar e transportar a prole com delicadeza (Emmons & Feer 1990, Nowak 1999).

A origem mais provável dos roedores data do final do Cretáceo, início do Paleoceno, por volta de 88 a 66 milhões de anos atrás, quando divergiram da linhagem Lagomorpha. Os fósseis mais antigos de roedores que se tem registro foram encontrados na Ásia central (Nowak 1999, Marivaux *et al*. 2002, Honeycutt 2009).

Com distribuição em praticamente todos os continentes do Globo, com exceção da Antártica, os roedores são os únicos mamíferos placentários que colonizaram naturalmente a Austrália e Nova Guiné sendo depois introduzidos pelo homem em outras ilhas oceânicas. Os roedores ocupam uma grande variedade de habitats: eles podem ser terrestres, especializados na vida arborícola, saltadores, semi-aquáticos, subterrâneos e existem até os que são capazes de planar em vôos curtos (Nowak, 1999).

I.4. Os roedores subterrâneos

Os vertebrados que passam toda, ou a maior parte de suas vidas sob o solo, são denominados subterrâneos. Muitos desses animais constroem túneis, sendo também chamados de escavadores. Outros vertebrados são ativos na superfície mesmo sendo aptos para cavar em busca de alimento ou abrigo. Todos esses são descritos como fossoriais, ou seja, animais especializados na escavação (Hildebrand 1995, Lacey *et al*. 2000).

Entre os mamíferos, a ordem Rodentia é a que possui o maior número de representantes escavadores, que ocorrem em todos os continentes com exceção da Austrália e Antártica (Hildebrand 1995, Lacey *et al*. 2000).

Lacey *et al*. (2000) consideram oito grupos de roedores como sendo subterrâneos: as subfamílias Arvicolinae, Myospalacinae, Rhyzomyinae e Spalacinae, todas pertencentes à família Muridae; e ainda as famílias Bathyergidae, Geomyidae, Octodontidae e Ctenomyidae. A subfamília Arvicolinae é representada por dois gêneros: *Prometheomys* e *Ellobius* com uma e cinco espécies descritas respectivamente, encontradas na Eurásia, da Turquia ao Cazaquistão. Myospalacinae, do centro da Rússia até o nordeste da China, possui apenas um gênero, *Myospalax* com sete espécies. A subfamília Rhyzomyinae é dividida em *Cannomys,* com uma espécie, ocorrendo do leste do Nepal à Indochina; *Rhizomys* com três espécies encontradas do norte da Índia e China central até Sumatra, e o gênero *Tachyoryctes* com onze espécies encontradas na África, do sul da Etiópia até a Tanzânia. A subfamília Spalacinae é dividida em dois gêneros: *Nannospalax* com três espécies, e *Spalax* com cinco. O primeiro é encontrado do sul da Ucrânia passando por Turquia e parte do Oriente Médio até a costa do Egito e Líbia. O segundo (*Spalax*), ocorre na Rússia e leste da Ucrânia até o oeste da costa do Mar Cáspio. A família Bathyergidae é representada por cinco gêneros: *Bathyergus*, *Cryptomys*, *Georychus*, *Heliophobius* e *Heterochephalus*, com um total de 12 espécies, distribuídas da África equatorial até a África do Sul. A família Geomyidae, encontrada nas Américas Central e do Norte é dividida em cinco gêneros: *Geomys*, *Orthogeomys*, *Pappogeomys*, *Zygogeomys* e *Thomomys* com cinco, onze, nove, uma e nove espécies respectivamente. A família Octodontidae com um gênero monoespecífico *Spalacopus* que ocorre no centro do Chile. E finalmente, a família Ctenomyidae é representada por um único gênero, *Ctenomys* com cerca de 60 espécies descritas para a metade meridional da América do Sul.

De maneira geral o nicho subterrâneo é considerado como sendo relativamente pouco variável comparado com habitats de superfície, devido à diversidade de áreas geográficas e de habitats na superfície nos quais ocorrem os roedores subterrâneos. Isso tem sido reforçado pela similaridade morfológica encontrada entre os diferentes grupos que reflete as restrições impostas pelo estilo de vida subterrâneo (Lacey *et al*. 2000). O sistema de túneis, geralmente é caracterizado pela ausência de luz, alta umidade relativa do ar, baixa amplitude térmica e altos níveis de concentração de dióxido de carbono (Lacey *et al*. 2000). Estas condições nos fazem crer que os roedores subterrâneos tenham uma série de adaptações fisiológicas, comportamentais e morfológicas para sobreviverem em galerias debaixo da superfície do solo. As modificações morfológicas estão entre as mais notáveis alterações ao modo de vida imposto pelo nicho subterrâneo (Reig *et al*. 1990, Lacey *et al*. 2000).

As condições do solo podem limitar a distribuição geográfica destes animais quanto à escavação de túneis o que pode resultar em uma distribuição fragmentada das populações. Essa distribuição pode representar restrições à dispersão e ao fluxo gênico, criando assim novas oportunidades para diversificação evolutiva. Casos de convergência e paralelismo na morfologia externa, entre diferentes gêneros de roedores subterrâneos, demonstram a existência de tal variabilidade em seu sistema muscular-esquelético, a despeito de histórias filogenéticas independentes (Lacey *et al*. 2000, Stein 2000).

I.5. O gênero *Ctenomys*

Descrito por H. M. D. Blainville em 1826, esse gênero compreende roedores subterrâneos que habitam a região Neotropical sub-região Patagônica, estendendo-se do sul da Argentina e Chile, passando pelo Uruguai até o sul do Brasil e chegando até o Paraguai, Bolívia e sul do Peru. São encontrados desde o nível do mar, na costa do Oceano Atlântico, até mais de 4.000 metros de altitude no Altiplano Boliviano. Vivem em galerias escavadas no solo e possuem adaptações morfológicas para esse modo de vida, como o corpo e cabeça robustos, cauda relativamente curta, olhos e ouvidos reduzidos, patas munidas de grandes garras e incisivos fortes e proeminentes (Reig *et al*. 1990, Nowak 1999, Lacey *et al*. 2000). O gênero *Ctenomys* apresenta uma grande diversidade no tamanho corporal (220-430mm), variando em peso de 90-100g em *C. pundti* e *C. chasiquensis* até 700-1100g em *C. tuconax* e *C. conoveri* (Reig *et al*. 1990, Vassalo 1998, Mora *et al*. 2003). São

herbívoros, ocupam regiões arenosas, campos abertos, pradarias e estepes. De distribuição fragmentada, são na grande maioria solitários, territoriais e apresentam baixa taxa de dispersão. O gênero *Ctenomys* compreende atualmente cerca de 60 espécies (Tabela 1), (Reig *et al*. 1990, Nowak 1999, Lacey *et al*. 2000, Wilson & Reeder 2005).

Também conhecidos como tuco-tucos, devido aos sons que produzem, esses pequenos roedores apresentam alta diversidade cariotípica interespecífica, de 2n = 10 em *C. steinbachi* até 2n = 70 em *C. pearsoni*, sendo considerada a mais ampla variação entre os mamíferos (Tabela 1), (Reig *et al*. 1990, Bidau *et al*. 1996, Nowak 1999). Quanto ao número fundamental (NF: número total de braços cromossômicos das fêmeas), *Ctenomys* também apresenta uma ampla variação que vai de NF = 16 a NF = 90 (Tabela 1), (Bidau *et al*. 1996, Cook & Salazar-Bravo 2004).

Há até pouco tempo, a origem provável desse gênero era estimada para o Plioceno tardio - Pleistoceno (há cerca de 1,8 milhão de anos atrás), segundo o registro fóssil de sítios paleontológicos na Argentina e Bolívia (Azurduy 2005). Recentemente Verzi *et al*. (2010) descreveram um fóssil de Ctenomyidae datado em torno de 3,5 milhões de anos, encontrado na Formação Uquía no noroeste da Argentina.

As altas taxas de evolução cromossômica tem sido sugeridas para explicar a alta diversidade de *Ctenomys*, tornando o grupo um excelente modelo evolutivo para o estudo de eventos de especiação rápida. Talvez junto com Arvicolinae, Ctenomyinae apresente a mais rápida diversificação entre todos os grupos de roedores subterrâneos (Reig & Kiblisky 1969, Reig *et al*. 1990, Lessa & Cook 1998, Lacey *et al*. 2000). Ainda, Verzi (2002) destacou que os roedores Ctenomyideos representam um modelo excepcional para estudos macroevoutivos.

Tabela 1. Lista de espécies do gênero *Ctenomys* com indicação do autor, região de ocorrência, número diplóide (2n) e número fundamental (NF) de cromossomos segundo Cook & Salazar-Bravo (2004), Woods & Kilpatrick (2005) e Fernandes *et al*. (2009a, b).

Espécie	Autor(es)	Região de ocorrência	Cariótipo
C. argentinus	Contreras & Berry, 1982	Argentina, Prov. Chaco	2n = 44 e NF = 50-54
C. australis	Rusconi, 1934	Argentina, Prov. Buenos Aires	2n = 48, NF = 76-80
C. azarae	Thomas, 1903	Argentina, Prov. La Pampa	2n = 46-48, NF = 68-78
C. bergi	Thomas, 1902	Argentina, Prov. Córdoba	2n = 48, NF = 90
C. boliviensis	Waterhouse, 1848	Bolívia, Dep. Santa Cruz	2n = 36-46, NF = 64-68
C. bonettoi	Contreras & Berry, 1982	Argentina, Prov. Chaco	-
C. brasiliensis	Blainville, 1826	Brasil, Minas Gerais	-
C. budini	Thomas, 1913	Argentina, Prov. Jujuy	-
C. colburni	Allen, 1903	Argentina, Prov. Santa Cruz	2n = 34, NF = 64
C. coludo	Thomas, 1920	Argentina, Prov. Catamarca	-
C. conoveri	Osgood, 1946	Paraguai, Dep. Boqueron	2n = 48-50, NF = 70
C. coyhaiquensis	Kelt & Gallardo, 1994	Chile, Prov. General Carrera	2n = 28, NF = 42-44
C. dorbignyi	Contreras & Contreras, 1984	Argentina, Prov. Corrientes	2n = 70, NF = 80-84
C. dorsalis	Thomas, 1900	Paraguai, Prov. Boqueron	-
C. emilianus	Thomas & Leger, 1926	Argentina, Prov. Neuquén	-
C. famosus	Thomas, 1920	Argentina, Prov. Rioja	-
C. flamarioni	Travi, 1981	Brasil, Est. Rio Grande do Sul	2n = 48, NF = 50-78
C. fochi	Thomas, 1919	Argentina, Prov. Catamarca	-
C. fodax	Thomas, 1910	Argentina, Prov. Chubut	2n = 28, NF = 42-46
C. frater	Thomas, 1902	Bolivia, Prov. Potosí	2n = 52, NF = 76-78
C. fulvus	Philippi, 1860	Chile, Prov. Antofagasta	2n = 25-26, NF = 48-52
C. goodfellowi	Thomas, 1921	Bolívia, Prov. Santa Cruz	2n = 46, NF = 68
C. haigi	Thomas, 1917	Argentina, Prov. Chubut	2n = 50, NF = 66
C. johannis	Thomas, 1921	Argentina, Prov. San Juan	-
C. juris	Thomas, 1920	Argentina, Prov. Jujuy	-
C. knighti	Thomas, 1919	Argentina, Prov. Catamarca	2n = 36, NF = 64-68
C. lami	Freitas, 2001	Brasil, Est. Rio Grande do Sul	2n = 54-58, NF = 76-82
C. latro	Thomas, 1918	Argentina, Prov. Tucumán	2n = 40-42, NF = 46-50
C. leucodon	Waterhouse, 1848	Bolívia, Prov. La Paz	2n = 36, NF = 68
C. lewisi	Thomas, 1926	Bolívia, Dept. Tarija	2n = 56, NF = 74
C. magellanicus	Bennett, 1835	Chile, Dept. Magallanes	2n = 34-36, NF = 64
C. maulinus	Philippi, 1872	Chile, Prov. Talca e Cautin	2n = 26, NF = 48-50
C. mendocinus	Philippi, 1869	Argentina, Prov. Mendoza	2n = 47-48, NF = 75-80
C. minutus	Nehring, 1887	Brasil, Est. Rio Grande do Sul	2n = 42-50, NF = 74-78
C. occultus	Thomas, 1920	Argentina, Prov. Tucumán	2n = 22, NF = 38-40
C. opimus	Wagner, 1848	Bolívia, Prov. Oruro	2n = 26, NF = 46-52
C. osvaldoreigi	Contreras, 1995	Argentina, Prov. Cordoba	2n = 52, NF = 56
C. pearsoni	Lessa & Langguth, 1983	Uruguai, Dept. Colônia	2n = 56-70, NF = 60-88
C. perrensi	Thomas, 1898	Argentina, Prov. Corrientes	2n = 50-58, NF = 80-84
C. peruanus	Sanborn & Pearson, 1947	Peru, Dept. Puno	-
C. pilarensis	Contreras, 1993	Paraguai, Dept. Nembucú	2n = 48-50, NF = 50
C. pontifex	Thomas, 1918	Argentina, Prov. Mendoza	-
C. porteousi	Thomas, 1916	Argentina, Prov. Buenos Aires	2n = 46-48, NF = 71-73
C. pundti	Nehring, 1900	Argentina, Prov. Cordoba	2n = 50, NF = 66-86
C. rionegrensis	Langguth & Abella, 1970	Uruguai, Dept. Rio Negro	2n = 48-56, NF = 68-80
C. roigi	Contreras, 1988	Argentina, Prov. Corrientes	2n = 48, NF = 76-80*
C. saltarius	Thomas, 1912	Argentina, Prov. Salta e Jujuy	-
C. scagliai	Contreras, 1999	Argentina, Prov. Tucumán	2n = 36, NF = 64
C. sericeus	Allen, 1903	Argentina, Prov. Santa Cruz	-
C. sociabilis	Pearson & Christie, 1985	Argentina, Prov. Neuquén	2n = 56, NF = 72
C. steinbachi	Thomas, 1907	Bolívia, Dept. Santa Cruz	2n = 10, NF = 16
C. sylvanus	Thomas, 1919	Argentina, Prov. Salta e Jujuy	-
C. talarum	Thomas, 1898	Argentina, Prov. Buenos Aires	2n = 46-50, NF = 65-86
C. torquatus	Lichtenstein, 1830	Brasil, Est. Rio Grande do Sul	2n = 40-46, NF = 72
C. tuconax	Thomas, 1925	Argentina, Prov. Tucumán	2n = 58-61, NF = 80
C. tucumanus	Thomas, 1900	Argentina, Prov. Tucumán	2n = 28, NF = 52-56
C. tulduco	Thomas, 1921	Argentina, Prov, San Juan	-
C. validus	Contreras et al. 1977	Argentina, Prov. Mendoza	-
C. viperinus	Thomas, 1926	Argentina, Prov. Tucumán	-
C. yolandae	Contreras & Berry, 1984	Argentina, Prov. Santa Fé	2n = 50, NF = 74-78

Algumas espécies possuem alta diversidade cariotípica intra-específica, como no caso de *C. minutus*. Endêmica da planície costeira do Rio Grande do Sul e Santa Catarina essa espécie possui populações com 2n = 42, 43, 44, 45, 46a, 46b, 47a, 47b, 48a, 48b, 48c, 49a, 49b, 50a and 50b (Freitas 1995, 1997, 2006; Freygang *et al.* 2004). Ainda para esse gênero há registro da ocorrência de zonas híbridas intra e interespecíficas. Duas delas ocorrem entre diferentes populações cromossômicas de *C. minutus* (2n = 46a × 48a e 2n = 42 × 48a) e existe uma zona híbrida interespecífica no encontro das distribuições de *C. minutus* (2n = 48a) e *C. lami* (2n = 56b) a oeste da Lagoa dos Barros no Rio Grande do Sul (Gava & Freitas 2002, 2003). Este e outros exemplos mostram a complexidade dos modelos de evolução cromossômica no gênero *Ctenomys*, com algumas espécies tendo alta diversidade cariotípica (por exemplo *C. perrensi* e *C. pearsoni*), enquanto outras apresentam uniformidade cromossômica (por exemplo *C. flamarioni* e *C. australis*) (Tabela 1).

Além da diversidade cromossômica foram descritas três morfologias distintas de espermatozóides para o gênero *Ctenomys*: simétrico, simples-assimétrico e duplo-assimétrico (Vitullo *et al*. 1988). O primeiro apresenta cabeça e flagelo normais, o segundo tem uma extensão nuclear paralela ao flagelo e o último possui duas extensões nucleares paralelas à cauda. A distribuição geográfica destas três formas segue um padrão. O tipo simétrico ocorre em espécies mais ao norte da distribuição do gênero e o tipo simples-assimétrico é encontrado na porção meridional da América do Sul. Na região entre a província de Buenos Aires e o norte da Argentina ocorre um misto de espécies com uma ou outra forma espermática. No Uruguai e sul do Brasil também há registros das duas formas de espermatozóides. O tipo duplo-assimétrico é reportado para *C. yolandae*, uma espécie encontrada na porção norte da Argentina. Este polimorfismo espermático encontrado em *Ctenomys* não é observado em outros mamíferos (Vitullo *et al*. 1988, Freitas 1995a, Contreras 1996).

Massarini *et al*. (1991) introduziram o termo "grupo-*mendocinus*" para tratar de um grupo que diferia das demais espécies de *Ctenomys*. Formado inicialmente por cinco espécies: *C. australis*, *C. porteousi*, *C. azarae*, *C. mendocinus* e *C. chasiquensis*. Este grupo compartilha uma série de características em comum: possui o mesmo número cariotípico (2n = 48), o mesmo tipo assimétrico de espermatozóides, grande similaridade

morfológica, o mesmo padrão de heterocromatina e de braços cromossômicos. Mais tarde foram adicionadas a este grupo *C. flamarioni* e *C. rionegrensis* devido à íntima relação filogenética entre estas duas espécies e o grupo *mendocinus* (Massarini & Freitas 2005).

Recentemente filogenias moleculares, baseadas em análises de regiões de DNA nuclear (sequências de íntrons) e regiões de DNA mitocondrial (citocromo *b*), vêm sendo propostas para ajudar a esclarecer as relações evolutivas entre as espécies de *Ctenomys* (Lessa & Cook 1998, D'Elía *et al*. 1999, Castillo *et al*. 2005).

Nas últimas décadas, estudos baseados no polimorfismo cromossômico, em dados morfológicos e moleculares têm contribuído na formulação de grupos de espécies dentro do gênero *Ctenomys*. Foram propostos os seguintes grupos: *mendocinus*, Boliviano-Matogrossense, Boliviano-Paraguaio, Chaco, *opimus-fulvus* e *pundti-talarum* (Massarini *et al*. 1991, Freitas 1994, Lessa & Cook 1998, D'Elia *et al*. 1999, Mascheretti *et al*. 2000, Slamovits 2001, Castillo *et al*. 2005, Tiranti *et al*. 2005). Recentemente mais dois grupos foram propostos: Patagônico e *torquatus* (Parada 2007).

Segundo Bidau *et al*. (1996) os roedores escavadores do gênero *Ctenomys* são um paradigma de multiformidade cromossômica e especiação rápida com uma escassa diferenciação morfológica. Porem, estudos quantificando a variabilidade inter e intraespecíficas são escassos (Mora *et al*., 2003).

I.6. Crânio e mandíbula de *Ctenomys*

O crânio é uma estrutura de grande importância, pois protege e sustenta o encéfalo e órgãos dos sentidos e contribui para a eficiência dos mecanismos alimentares e respiratórios (Hildebrand 1995). Além disso, o crânio de *Ctenomys* mostra adaptações ao estilo de vida subterrâneo, servindo para apoiar um forte arranjo muscular e sustentar os dentes incisivos em cinzel, que em alguns casos são utilizados na escavação junto com as garras (Agrawal 1967, Stein 2000, Mora *et al*. 2003).

A origem embrionária do crânio e mandíbula dos mamíferos tem profunda relação com as células da crista neural e do mesoderma paraxial (Moore 1981, Morriss-Kay 2001, Noden & Trainor 2005). As células mesenquimais, originárias da crista neural, após a migração agregam-se e diferenciam-se, dando origem às chamadas unidades morfogenéticas. Estas unidades, por sua vez, interagem durante a ontogenia, resultando em uma estrutura de determinado tamanho e forma no indivíduo adulto (Osumi-Yamashita &

Eto 1990, Atchley & Hall 1991, Monteiro & Reis 1999, Noden & Trainor 2005). As células da crista neural formam os ossos da face, como os nasais, os lacrimais, os jugais, os pré-maxilares, os maxilares e os frontais (estes últimos fazem parte do neurocrânio) entre outros, enquanto as células provenientes do mesoderma paraxial formam os ossos do neurocrânio, tais como os parietais, o occipital, o basisfenóide e outros (Moore 1981, Leamy *et al*. 1999, Morriss-Kay 2001, Noden & Trainor 2005).

O crescimento coordenado do cérebro e do crânio dos mamíferos é obtido através de uma série de interações de tecidos entre o cérebro em desenvolvimento, os ossos do crânio em crescimento e as suturas que unem estes ossos, integrando a expansão do cérebro ao crescimento dos ossos nas suturas (Kim *et al*. 1998).

Como no caso de outros roedores fossoriais, o crânio de *Ctenomys* é maciço e achatado dorso-ventralmente (Figura 1). Possui algumas características gerais como presença de cristas parietais e ausência de crista sagital. Arcos zigomáticos intensamente curvados lateralmente, os jugais têm processos dorsal e ventral bem desenvolvidos e não fazem contato com os lacrimais. Os ctenomyideos são hystricomorfos, ou seja, possuem um amplo forame infra-orbital sem forames acessórios. As bulas timpânicas são muito grandes e por trás delas estendem-se grandes processos paraoccipitais. Em muitas espécies o interparietal é fusionado aos parietais, tornando difícil sua identificação em animais adultos. O crânio alarga-se posteriormente, promovendo um aumento da região cervical que, somado ao maior tamanho da crista lambdoidal (nucal), aumenta a área de inserção dos músculos do pescoço, que é curto e robusto (Reig *et al*. 1966, Agrawal 1967, Anderson & Jones, 1985, Stein 2000, Verzi 2002, Verzi & Olivares 2006). Na maioria das espécies o comprimento do crânio fica em torno de 3,5 - 5,0cm, mas pode passar dos 8,0cm em espécies fósseis, como no caso de *C. cotocaensis* (Azuruy 2005).

A mandíbula (Figura 1) é bem desenvolvida, típica de roedores hystricognathos com processos coronóide e condilóide (articular) bem desenvolvidos e com uma profunda separação entre as cristas massetéricas e o corpo da mandíbula (Anderson & Jones 1985). Essas modificações aumentam a superfície de fixação de uma ampla e poderosa musculatura (Vassallo 1998, Lacey *et al*. 2000, Stein 2000, Mora *et al*. 2003, Verzi & Olivares 2006).

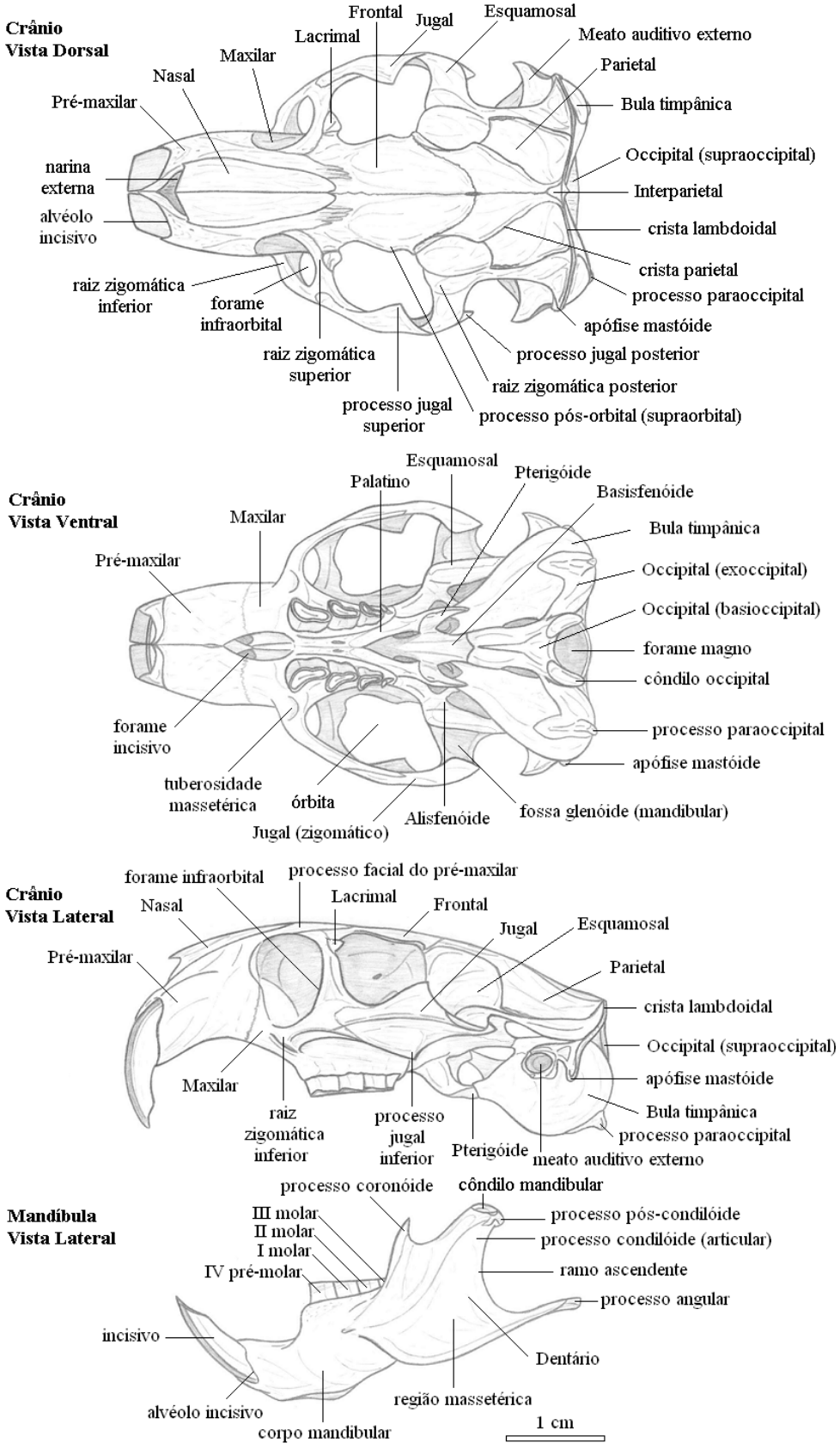

Figura 1. Crânio e mandíbula de *Ctenomys lami* com indicação dos ossos (em maiúsculo) e das principais características anatômicas (em minúsculo).

Alguns trabalhos analisaram a morfometria do crânio e mandíbula de *Ctenomys*. Entre eles, Freitas (1990) analisou uma série de medidas lineares tomadas do crânio de três espécies de *Ctenomys* provenientes do estado do Rio Grande do Sul e demonstrou variação morfológica significativa entre elas. Vassallo (1998) mostrou variação no crânio, ângulo de procumbência dos incisivos e mudanças na ulna de duas espécies (*C. talarum* e *C. australis*) mostrando adaptações morfológicas associadas ao tipo de escavação adotado por cada espécie e ao tipo de habitat. Marinho & Freitas (2000) exploraram a variação craniométrica em uma zona híbrida cromossômica descrita para *C. minutus*, e mostraram que a forma híbrida também possui características intermediárias em relação às formas parentais. Mora *et al*. (2003) fizeram estudos sobre a variação morfológica e funcional do crânio de 23 espécies de *Ctenomys* provenientes da Argentina e sugeriram que a forma do crânio tende a ser mais constante do que o tamanho, devido a sua direta relação com a escavação. Freitas (2005) estudou a variação morfológica no crânio de 15 espécies provenientes do Brasil, Argentina, Chile e Peru e constatou que o tamanho do crânio é o aspecto mais informativo e que a forma é pouco variável. Em contrapartida, no mesmo estudo, foram pesquisadas 18 populações de *C. minutus* e verificou-se variação na forma correlacionada com variação cariotípica e distribuição geográfica. Verzi & Olivares (2006) analisaram a relação cranio-mandibular de 15 espécies de Ctenomyidae e sugerem restrição mecânica na forma e tamanho da bula timpânica relacionada a abertura da mandíbula. Vassallo & Mora (2007) investigaram alometria e trajetória ontogenética no crânio de 21 espécies de *Ctenomys* e sugerem que o traço mais variável é o tamanho corporal. Todos estes trabalhos foram feitos utilizando morfometria tradicional.

Recentemente, D'Anatro & Lessa (2006) publicaram o primeiro trabalho de variação na forma do crânio de *Ctenomys* utilizando morfometria geométrica. Esses autores investigaram a relação da forma do crânio de *C. rionegrensis* com a variação geográfica e a variação genética. Apesar de seus resultados não mostrarem correlação significativa entre distância morfológica e as distâncias geográfica e genética para esta espécie, a técnica mostrou-se capaz de discriminar populações locais. Além deste último, Fernandes *et al*. (2009a) fizeram um estudo sobre a variação na forma do crânio dentro e entre duas espécies do gênero *Ctenomys*, *C. torquatus* e *C. pearsoni*, e mostraram diferenças entre populações. Existe então uma grande escassez de trabalhos que abordem a variação na forma do crânio de espécies do gênero *Ctenomys* utilizando morfometria

geométrica, e ainda, uma ausência quase que total de estudos com este gênero de roedor que busquem relacionar dados morfológicos com geográficos e dados morfológicos com filogenéticos (contexto evolutivo).

Portanto, as controvérsias que ainda existem quanto a multiformidade cromossômica associada a variação morfológica, os pouco abrangentes estudos craniométricos com técnicas mais precisas e a escassez de estudos que associem a diversidade morfológica ao contexto evolutivo em tuco-tucos são a base para justificar este trabalho. Assim, podemos justificar a importância deste estudo tendo em vista a importância do gênero *Ctenomys* como modelo evolutivo, principalmente no que se refere a relação entre os dados moleculares, cromossômicos e morfológicos, vistos de uma maneira integrada.

I.7. Objetivos

Objetivo geral

Analisar a variação na forma e tamanho do crânio e mandíbula de *Ctenomys* em dois níveis principais. O primeiro ao nível de gênero, analisando um grande número de espécies que melhor representem a diversidade e distribuição geográfica desse grupo na América do Sul. Já o segundo nível está concentrado no nível intra-específico em duas espécies que ocorrem na planície costeira do Rio Grande do Sul: *C. minutus* e *C. lami*.

Objetivos específicos

1. Quantificar e descrever a variação na forma do crânio e mandíbula no gênero *Ctenomys*;
2. Testar se a variação na forma do crânio tem correlação com a variação de tamanho (se espécies com crânios de dimensões diferentes também diferem na forma do crânio);
3. Verificar se há existência de congruência entre as topologias de árvores geradas a partir de dados morfológicos e moleculares (disponíveis na literatura) para o gênero *Ctenomys*;
4. Testar associação entre polimorfismo cromossômico e variação na forma e tamanho do crânio dentro e entre os grupos *mendocinus* e *torquatus*;
5. Analisar a variação na forma e tamanho do crânio no nível intra-específico em *Ctenomys minutus* em relação à variação geográfica, cromossômica e ambiental (duna e campo).
6. Testar se a variação morfológica tem associação com a variação cromossômica em populações de *Ctenomys lami* e investigar a ação de seleção natural e deriva na forma do crânio.

Capítulo II

Manuscrito em preparação

Patterns of morphological evolution in skull shape and size in the genus *Ctenomys* (Rodentia: Ctenomyidae) in a phylogenetic context

Rodrigo Fornel[1,2], Pedro Cordeiro-Estrela[1,2], & Thales Renato O. de Freitas[1,2]

[1]Programa de Pós-Graduação em Genética e Biologia Molecular – Universidade Federal do Rio Grande do Sul, Av. Bento Gonçalves 9500, CEP 91501-970, Porto Alegre, RS, Brazil.
[2]Departamento de Genética, Instituto de Biociências, Universidade Federal do Rio Grande do Sul, Av. Bento Gonçalves 9500, CEP 91501-970, Porto Alegre, RS, Brazil.

Email addresses:

RF: rodrigofornel@hotmail.com

PCE: pedroestrela@yahoo.com

TROF: thales.freitas@ufrgs.br

Running Title: Skull evolution of *Ctenomys*

Keywords: cranial form; geometric morphometrics; phenotypic evolution, tuco-tuco.

Abstract

Ctenomys is a genus of subterranean rodents endemic to the southern Neotropical region, and comprises about 60 living species known as “tuco-tucos”. This genus is an example of rapid evolution, and its members have high karyotypic diversity with diploid numbers varying from 2n = 10 to 2n = 70. Except for a few species, quantitative morphological variation among tuco-tucos is poorly known. Recently, studies using cytochrome *b* have proposed phylogenetic relationships for *Ctenomys* and supported eight great clades. Our goal in the present study was to investigate skull shape and size variation between the sexes, and among groups and species in a phylogenetic context. Were analyzed 1344 skulls from 47 living species and a subsample of 820 mandibles of *Ctenomys*. Our results showed a large diversification in skull shape in genus *Ctenomys*. We found a geographical structure in skull shape among groups along east-west and north-south morphological gradients. The mandible is less variable in shape (conserved) than the skull. The phenograms of Mahalanobis distances show a strong phylogenetic signal only for the *torquatus*-group, and morphological similarity between the two Bolivian groups, and between the *mendocinus* and Patagonico groups. The *torquatus*-group is very congruent in shape and has low variation in size. A common ancestral relationship between the Patagonico and *mendocinus* groups based on skull shape is reinforced by the same asymmetry in sperm morphology found in both groups. In addition, *C. sociabilis* is very similar to the *mendocinus* and Patagonico species, and may be a case of convergence or common ancestry.

Introduction

Ctenomys is a genus of subterranean rodents endemic to the southern Neotropical region, from the Andes to the Atlantic and, from southern Peru to Tierra del Fuego in Argentina (Figure 1). Also known as "tuco-tucos", this genus is an example of explosive cladogenesis that occurred during the Pleistocene and nowadays comprises about 60 extant species (Reig *et al*. 1990, Nowak & Paradiso 1991, Woods 1993, Lacey *et al*. 2000, Verzi 2002, Wilson & Reeder 2005, Verzi 2008, Verzi *et al*. 2010). The members of *Ctenomys* have a high karyotypic diversity, with diploid number varying from 2n = 10 (*C. steinbachi*) to 2n = 70 (*C. dorbignyi* and *C. pearsoni*), which may be the highest rate of chromosomal evolution among mammals (Reig & Kiblisky 1969, Reig *et al*. 1990, Bidau *et al*. 1996, Cook & Salazar-Bravo 2004).

Three different sperm morphologies occur in tuco-tucos: symmetric, simple asymmetric, or complex-asymmetric due to a nuclear caudal extension being absent, simple, or double, respectively (Vitullo *et al*. 1988). The asymmetric forms were derived from the symmetric sperm, and are not observed in any other mammal (Feito & Gallardo 1982, Vitullo *et al*. 1988, Freitas 1995a). Besides chromosomal polymorphism and sperm variation, most of the species differ in size (from the small *C. pundti* with 100 g body weight and 220 mm total length, to the large *C. conoveri* with 1100 g and 430 mm), color (from pale yellow-grayish to black), and the angle of incisor procumbency (Reig *et al*. 1990, Vassallo 1998, Mora *et al*. 2003). *Ctenomys* has been characterized as a scratch (claws) and chisel-tooth (incisors) digger. They use these tools to build their tunnel systems, and are considered a good model to investigate functional morphological adaptations to the subterranean niche (Vassallo 1998, Lessa *et al*. 2008). Ctenomyidae have evolved independently from other fossorial and subterranean rodents, and are highly convergent in ecology and external morphology with the families Geomyidae, Bathyergidae, and Spalacidae (Nevo 1979, Lessa 1990, Stein 2000, Lessa *et al*. 2008).

Factors including their patchy distribution, limited vagility, territoriality, small effective numbers, and high karyotypic polymorphism associated with the subterranean lifestyle and the changes at the end of the Pliocene could be responsible for the rapid evolution in *Ctenomys* (Reig *et al*. 1990).

Many studies have explored the morphological skull variation in *Ctenomys*, at both intra- and interspecific levels (i.e., Vassallo 1998, Marinho & Freitas 2000, Mora *et al*. 2003, Freitas 2005, D'Anatro & Lessa 2006, Verzi & Olivares 2006, Fernandes *et al*. 2009a). Mora *et al*. (2003) showed significant morphological variation in skull size and in angle of incisor procumbency (AIP), both could be related to adaptation to digging. However, a broad view of the morphological variation in the genus is not yet available (Lessa *et al*. 2008).

Studies based on chromosomal polymorphism, morphological, and molecular data in recent decades have contributed to the formulation of groups of species within the genus *Ctenomys* (Figure 1). The following groups have been proposed: *mendocinus*, Boliviano-Matogrossense, Boliviano-Paraguaio, Chaco, *opimus-fulvus*, and *pundti-talarum* (Massarini *et al*. 1991, Freitas 1994, Lessa & Cook 1998, D'Elia *et al*. 1999, Mascheretti *et al*. 2000, Slamovits 2001, Castillo *et al*. 2005, Tiranti *et al*. 2005). Recently, two additional groups were proposed, Patagonico and *torquatus* (Parada 2007, see Appendix I).

Therefore, *Ctenomys* offers an opportunity to investigate the evolution of skull morphology at the interspecific level. The aims of this study were to (1) test if the eight groups proposed for *Ctenomys* are supported by skull and mandible morphology; (2) test if tree topologies based on morphometric data are congruent with molecular data; and (3) test if the changes in skull size are related to the changes in shape.

Material and Methods

Sample – Skulls of 1344 adult specimens of 47 living species and a subsample of 820 mandibles of *Ctenomys* were examined (Table 1). We used a reduced number of mandibles in relation to skull number due a damages in some processes of mandibles that prejudice landmark localization. The skulls and mandibles were obtained from the following museums and scientific collections: Departamento de Genética, Universidade Federal do Rio Grande do Sul, Porto Alegre, Brazil (UFRGS); Museo Nacional de História Natural y Antropología, Montevideo, Uruguay (MUNHINA); Museo Argentino de Ciencias Naturales "Bernardino Rivadavia", Buenos Aires, Argentina (MACN); Museo de La Plata, La Plata, Argentina (MLP); Museo de Ciencias Naturales "Lorenzo Scaglia", Mar del Plata, Argentina (MMP); Museum of Vertebrate Zoology, University of

California, Berkeley, USA (MVZ); American Museum of Natural History, New York, USA (AMNH); and Field Museum of Natural History, Chicago, USA (FMNH).

Geometric Morphometrics – Each cranium was photographed in the dorsal, ventral, and left lateral views of the skull and on the left lateral side of the mandible, with a digital camera with 3.1 megapixels (2048 × 1536) of resolution, with macro function and without flash. We used 29 two-dimensional landmarks for the dorsal, 30 for ventral, and 21 for lateral views of the skull, the same proposed by Fernandes *et al*. (2009a) and added 13 more landmarks for the lateral view of the mandible (Figure 2; Appendix II). Anatomical landmarks were digitized for each specimen, using TPSDig version 1.40 software (Rohlf 2004, http://life.bio.sunysb.edu/morph). All landmarks were taken by the same person (R.F.). Coordinates were superimposed using a generalized Procrustes analysis (GPA) algorithm (Dryden & Mardia 1998). GPA removes differences unrelated to the shape, such as scale, position, and orientation (Rohlf & Slice 1990, Rohlf & Marcus 1993, Bookstein 1996a, 1996b, Adams *et al*. 2004). We symmetrized both sides of the landmarks in the dorsal and ventral views of the skull, and only the symmetric part of the variation was analyzed (Kent & Mardia 2001, Klingenberg *et al*. 2002, Evin *et al*. 2008). The size of each skull was estimated using its centroid size, the square root of the sum of the squares of the distances of each landmark from the centroid (mean of all coordinates) of the configuration (Bookstein 1991).

Statistical Analysis – Size difference was tested between sexes and among groups and species with analysis of variance (ANOVA), and for multiple comparisons we used Tukey's test. Size differences between species were visualized through box plots. Shape differences between sexes and among groups and species, as well as their interactions, were tested through multivariate analysis of variance (MANOVA). The Bonferroni correction for multiple comparisons was applied when needed (Wright 1992). Because of the small sample size for mandibles, we used them solely in sexual-dimorphism and group comparisons.

Principal components analysis (PCA) was carried out using the variance-covariance matrix of generalized least-squares superimposition residuals. PCs of the covariance matrix of superimposition residuals were used as new shape variables, to reduce the dimensionality of the data set as well as to work on independent variables (Baylac & Friess 2005, Evin *et al*. 2008). The matrices of PCA scores for each view of the cranium were

combined in one total matrix, and a subsequent matrix was used for a PCA to pool dorsal, ventral, and lateral information in the same analysis (Cordeiro-Estrela *et al*. 2006, Fernandes *et al*. 2009a).

To choose the number of PCs to be included in the linear discriminant analysis (LDA), we computed correct classification percentages with each combination of PCs (Baylac & Friess 2005). We selected the subset of PCs giving the highest overall correct classification percentage. We used a leave-one-out cross-validation procedure that allows an unbiased estimate of classification percentages (Ripley 1996, Baylac & Friess 2005). Cross-validation was used to evaluate the performance of classification by LDA. Differences in shape between species were explored by canonical variate analysis (CVA). We performed an LDA on PCs in combination with and without the sum of the logarithms of dorsal, ventral, and lateral centroid sizes (Cordeiro-Estrela *et al*. 2006). We used LDA for computed correct classification percentages among groups and species.

Mahalanobis's D^2 distances were used with Neighbour-joining to compute trees to visualize the morphological relationships among groups and species, with and without size information. The visualization of shape differences for the skull views was obtained through multivariate regression of shape variables on discriminant axes. We used Pearson's correlation to test the association between size and shape.

For all statistical analyses and to generate the graphs, we used the "R" language and environment for statistical computing version 2.9.0 for Windows (R Development Core Team, http://www.R-project.org), and the following libraries: MASS (Venables & Ripley 2002), ape version 1.8-2 (Paradis *et al*. 2004), stats (R Development Core Team, 2009), and ade4 (Dray & Dufour 2007). Geometric morphometrics procedures were carried out with the Rmorph package: a geometric and multivariate morphometrics library for R (Baylac 2008).

Results

Size – Males and females differed significantly in both skull and mandible size. The results of the ANOVA for centroid size were highly significant for the three views of the skull and for the lateral view of the mandible (Table 2). Males are larger on average than the females.

Results from ANOVA showed significant differences among groups for centroid size (Table 2). The Tukey test confirmed the change in skull and mandible size, and the Boliviano-Matogrossense group proved to be larger than the Chaco and *pundti-talarum* groups ($P < 0.05$). We found a large variation in skull centroid size among species and *C. conoveri* is twice bigger than second biggest species (Figure 3a). Also the species showed great variation in skull size within each group (Figure 3b). The exception was *torquatus*-group, with six species, which showed no significant differences among them (Figure 3b).

Shape – The MANOVA showed highly significant sexual dimorphism in shape for the dorsal, ventral, and lateral views of the skull, as well as for the three views pooled and for the mandible (Table 3). The interaction between sex and species effects was significant for shape (Table 3).

For groups, Table 3 shows the significant difference in skull and mandible shape. For MANOVA comparisons between different effects, the highest *F* value was found for groups. The percentages of correct classification were lowest for the *pundti-talarum* group (mean 74.04%) and highest for the *torquatus*-group (mean 98.66%). Considering only skull data, the correct classification for the *torquatus*-group in mean was 100% (Table 4).

Because of the significant interaction between sex and species effects, the Canonical Variate Analysis (CVA) was carried out only for females, because the sample size was larger than for males. Figures 4 and 5 summarize the graphs of CVAs for females, using data from the dorsal, ventral, and lateral views of the skull and the lateral view of the mandible. All four graphs show the first axis (CV1) following a west-east direction, with the *torquatus*-group with the highest scores (Figures 4 and 5). The second axis, following the north-south direction, shows the Bolivian groups with the highest scores and the Patagonico group with the lowest ones (Figures 4 and 5).

The Neighbor-joining trees of Mahalanobis distances among *Ctenomys* groups for different views of the skull and mandible are very similar (Figure 6 - 9). In general, the Bolivian groups are on branches at one extreme, and the *mendocinus* and Patagonico groups at the other. For the mandible view, the tree topology shows the two Bolivian branches separated by the *torquatus*-group, which differs from other skull views (Figure 9).

Interspecific differences in shape were significant in both the skull and mandible (Table 3). The percentages of correct classification were relatively higher for the majority

of species (Table 5). On average, the lowest percentage was 90.22% for the ventral view, and the highest was 93.64% for the three views pooled. When we used the size plus shape (form), the percentage of correct classification was 94.84% on average (Table 5).

The phenogram for 47 species of *Ctenomys* shows the largest branch for *C. conoveri*, and the most morphologically constrained group was *torquatus* for both trees using shape and form (Figure 10 and 11). The Chaco group was congruent using form data, and the *mendocinus* and Patagonico groups were little congruent. In skull shape *C. sociabilis* was associated with the *mendocinus* species (Figure 10), and for the form data was associated with *C. magellanicus* and *C. maulinus* (Figure 11). Our results showed a significant correlation between shape and size for the dorsal (r = -0.47; $P < 0.001$), ventral (r = -0.419; $P < 0.001$), and lateral (r = -0.264; $P < 0.001$) views of the skull.

Discussion

The skull is an important structure that harbors the trophic apparatus, brain, and sense organs (Hanken & Thorogood 1993). In the case of *Ctenomys*, the skull is also part of the digging apparatus, the incisors (Vassallo 1998, Mora *et al*. 2003). Our data suggest that this genus shows high morphological variation in skull and mandible shape and size. Similarly to other works, we found strong sexual dimorphism in the skull; and at the present no clear hypothesis can completely explain the causes of this dimorphism (Pearson *et al*. 1968, Malizia & Busch 1991, Gastal 1994, El Jundi & Freitas 2004, Marinho & Freitas 2006, Fernandes *et al*. 2009a). Ecological and, mainly, sexual selection are suggested to be responsible for the sexual dimorphism in *Ctenomys* (Zenuto & Busch 1998, Zenuto *et al*. 2001). We found a highly significant interaction between sex and species factors. This significant interaction found in both skull shape and size may result from our larger sample size, and the partial overlap in variation observed for species and for sexes. Therefore, the lower F scores obtained by ANOVA and MANOVA can be neglected (Tables 2 and 3).

We found a high variation in size within *Ctenomys* groups, with the exception of the *torquatus*-group (Figure 3A). Apparently, size shows a similar range of variation within groups but is constrained to intermediate values in the *torquatus*-group. *C. conoveri* is the sole species with extreme values that falls outside the range of other species. The

eight groups proposed for *Ctenomys* are, on average, different in shape. The graphs from the CVA (Figures 4 and 5) and mainly the phenograms based on Mahalanobis distance among groups (Figure 6 - 9) show that morphology follows a geographical pattern. The Mahalanobis trees from the different views, with the exception of the mandible, show the Bolivian groups at one extreme and the Patagonico group at the other, on a north-south gradient (Figures 6, 7, 8). This result is congruent with an isolation-by-distance pattern that was proposed for *Ctenomys* at the intraspecific level with molecular data (Mora *et al*. 2006, 2007). In this interspecific scenery, the allopatric and parapatric speciation models are acceptable, and this skull shape variation could be the result of adaptive radiation because *Ctenomys* occur in a wide variety of habitats (Reig *et al*. 1990).

Moreover, our results show a large difference between northern and southern and between eastern and western species of *Ctenomys*. Indeed, we found a gradient from north to south with more-robust species in the north and more-delicate species in the south. The Bolivian groups in the north have a skull with strong and enlarged zygomatic arches with long processes and a deep rostrum, the "robust form"; whereas the members of the Patagonico group have a more delicate skull with a thin zygomatic arch and a narrow rostrum, the "gracile form" (Figures 4, 5, and 6).

The main question of this study was whether morphological topologies are congruent with trees made by molecular data. The answer is no, not completely. The morphological trees for the species are only partially congruent with the molecular data (Figures 10 and 11). The only completely congruent group was *torquatus*, in which all the species (*C. lami*, *C. minutus*, *C. torquatus*, *C. pearsoni*, *C. perrensi*, *C. roigi*) always fell out together (Figures 10 and 11). Moreover, our results showed that *C. dorbignyi* is associated with the *torquatus* species, as also found by Mascheretti *et al*. (2000) using a molecular analysis. These authors suggested that *C. dorbignyi* and *C. roigi* belong to the old Corrientes group. Therefore, we propose the inclusion of *C. dorbignyi* in the *torquatus*-complex, based on molecular and skull-morphological similarities.

The Chaco group (*C. argentinus*, *C. tucumanus*, *C. occultus* and *C. latro*) is partially congruent for shape data (Figure 10) and congruent for form data (Figure 11). The Patagonico group is only partially congruent, because *C. magellanicus* is not associated with other species of this group. We propose that *C. coulburni* be integrated with the Patagonico group, because the skull form and geographical distribution are very similar to

the species from this group. The *opimus-fulvus* group is congruent only with the form tree, and *pundti-talarum* is not congruent. The *mendocinus*-group is divided into two groups, the closely associated *C. flamarioni* and *C. australis*, and the other species that form another group.

There is a partial overlap in species of the Patagonico and *mendocinus* groups, related to skull morphology. The species of these two groups and also *C. maulinus* have the same sperm morphology (Feito & Gallardo 1982, Vitullo *et al*. 1988). Thus, the association between *C. magellanicus* and *C. maulinus* may be due to a common ancestry. D'Elia *et al*. (1999) proposed that the asymmetric sperm form evolved twice, but the skull data agree with the sperm morphology. Thus, we suggest that the *mendocinus* and Patagonico groups could be share the same ancestor (with asymmetric sperm), and are paraphyletic to other species of the genus *Ctenomys*. *C. sociabilis* is similar to the Patagonico and *mendocinus* species.

The most singular *Ctenomys* skull belongs to *C. conoveri*; this species is the most distinct in both shape and size (Figures 3 and 10). Besides the strong morphological difference observed in the phenograms, *C. conoveri* is associated with *C. peruanus* (Figures 10 and 11). This high morphological divergence in *C. conoveri* was noted by Osgood (1946), who proposed a new subgenus *Chacomys* to accommodate only *C. conoveri* (Lessa & Cook 1998). The subgenus *Haptomys* was proposed by Thomas (1916) to comprise only *C. leucodon*, which differs from other tuco-tucos because the incisors are extremely proodont. Our results for skull morphology do not support the *Haptomys* group, because in the phenograms *C. leucodon* was associated with other groups.

Cardini (2003) tested the congruence between molecular and morphological information using marmot mandible data, and showed that the congruence was very low. However, the mandible morphology supported the main subgenus as well as the marmot skull shape (Cardini & O'Higgins 2004). We found a similar result in the genus *Ctenomys*, low congruence at the interspecific level and a certain support for some groups. Cardini (2003) enumerated several factors that might explain the lack of correspondence between phenotypic and phylogenetic trees, such as sampling error, retention of plesiomorphic traits, genetic drift, morphological convergence, and misrepresentation of the phylogenetic analysis. This last factor occurs in *Ctenomys* which lacks a complete gene tree representing all species of the genus (Lessa & Cook 1998, Mascheretti *et al*. 2000).

We found a regular but significant correlation between size and shape, and the percentages of correct classification for species increased only 1.2% on average when size was added. The skull size is highly variable within groups (the *torquatus*-group is an exception). Thus, the relationship between size and shape in the genus *Ctenomys* seems very weak in the phylogenetic context, and the interspecific allometries are negligible.

Medina *et al*. (2007) found that body size and weight follow the converse Bergmann's rule at the interspecific level in *Ctenomys*. The authors suggested that this pattern could be related to seasonality, ambient energy, primary productivity, or predation pressure. Our data show significant variation in skull size, but this difference apparently do not follow a clear pattern.

Chromosomal diploid number (2n) also appears no relationship with morphological distances for *Ctenomys* skull among species (Figures 10, 11). Tomasco & Lessa (2007) studied molecular polymorphism in *C. pearsoni* and suggested that there is no correlation between chromosomal rearrangements and speciation.

Furthermore taxonomic revisions are needed, as well as more complete phylogenies to elucidate the phenotypic evolution of *Ctenomys*.

Figure Legends

Figure 1. Map of South America with indication of type localities of 60 *Ctenomys* species, according to Woods & Kilpatrick (2005) and groups according to Parada (2007).

Figure 2. Locations of landmarks on skull of *Ctenomys* for dorsal (a), ventral (b), and lateral (c) views of the cranium and lateral view of the mandible (d).

Figure 3. Skull centroid size variability in *Ctenomys*. (a) Among species with sample size larger than 1. (b) Within and between groups. B-M (Boliviano-Matogrossense), B-P (Boliviano-Paraguaio), O-F (*opimus-fulvus*), P-T (*pundti-talarum*), Pat (Patagonico).

Figure 4. Scatter plot of first versus second canonical variate axes (CV1 and CV2) for dorsal and ventral views of the skull, for *Ctenomys* groups using females. The shape change for each axis is given, solid lines indicate positive scores and dashed lines negative ones. The percentage explained by each axis is given in parentheses.

Figure 5. Scatter plot of first versus second canonical variate axes (CV1 and CV2) for lateral view of the skull and lateral view of the mandible, for *Ctenomys* groups using females. The shape change for each axis is given, solid lines indicate positive scores and dashed lines negative ones. The percentage explained by each axis is given in parentheses.

Figure 6. Neighbor-joining tree of Mahalanobis distances among *Ctenomys* groups for dorsal view of the cranium. Scale bar = 1cm.

Figure 7. Neighbor-joining tree of Mahalanobis distances among *Ctenomys* groups for ventral view of the cranium. Scale bar = 1cm.

Figure 8. Neighbor-joining tree of Mahalanobis distances among *Ctenomys* groups for lateral view of the cranium. Scale bar = 1cm.

Figure 9. Neighbor-joining tree of Mahalanobis distances among *Ctenomys* groups for lateral view of the mandible. Scale bar = 1cm.

Figure 10. Neighbor-joining tree of Mahalanobis distances among *Ctenomys* species for three views of the skull using shape data pooled from males and females. In parentheses chromosomal diploid number (2n) according with Woods & Kilpatrick (2005).

Figure 11. Neighbor-joining tree of Mahalanobis distances among *Ctenomys* species for three views of the skull pooled, using form data (size plus shape) for males and females. In parentheses chromosomal diploid number (2n) according with Woods & Kilpatrick (2005).

Tables

Table 1 - The *Ctenomys* species examined in this study.

Species	Group	N_{FEMALE}	N_{MALE}	N_{TOTAL}*
C. argentinus	Chaco	2	1	3
C. australis	Mendocinus	20	11	35
C. azarae	Mendocinus	18	11	32
C. boliviensis	Boliviano-Matogrossense	43	17	60
C. bonettoi	-	-	2	2
C. budini	-	-	-	1
C. coludo	-	-	2	2
C. conoveri	Boliviano-Paraguaio	3	1	4
C. coulburni	-	16	11	30
C. coyhaiquensis	Patagonico	-	1	1
C. dorbignyi	-	6	7	13
C. dorsalis	-	4	2	6
C. flamarioni	Mendocinus	17	15	34
C. fochi	-	3	-	3
C. fodax	Patagonico	1	-	1
C. frater	Boliviano-Paraguaio	8	3	11
C. fulvus	Opimus-Fulvus	15	11	26
C. haigi	Patagonico	37	37	74
C. knighti	-	1	1	2
C. lami	Torquatus	53	36	89
C. latro	Chaco	5	3	8
C. leucodon	-	8	-	8
C. lewisi	Boliviano-Paraguaio	8	5	13
C. magellanicus	Patagonico	11	12	23
C. maulinus	-	18	14	34
C. mendocinus	Mendocinus	10	14	24
C. minutus	Torquatus	107	90	197
C. minutus (Bolivia)	-	1	1	2
C. occultus	Chaco	3	3	6
C. opimus	Opimus-Fulvus	52	28	80
C. pearsoni	Torquatus	51	26	77
C. perrensi	Torquatus	5	4	9
C. peruanus	-	8	6	14
C. porteousi	Mendocinus	21	9	30
C. pundti	Pundti-Talarum	3	2	5
C. rionegrensis	-	1	1	2
C. roigi	Torquatus	2	5	7
C. scagliai	-	-	1	1
C. sericeus	Patagonico	2	-	2
C. sociabilis	-	11	4	15
C. steinbachi	-	6	6	12
C. sylvanus	-	5	1	6
C. talarum	Pundti-Talarum	33	29	76
C. torquatus	Torquatus	159	63	222
C. tuconax	-	13	4	17
C. tucumanus	Chaco	13	10	23
C. yolandae	-	1	1	2
Total		804	511	1344

*Including specimens of unknown sex.

Table 2 - ANOVA for skull and mandible centroid size in *Ctenomys* for sex, groups, and species.

Effect (Skull-Dorsal)	Sum of squares	*d.f.*	*F*	*P*
Sex	692372	1	44.831	3.362×10^{-11}
Group	7657264	7	116.44	2.2×10^{-16}
Species	16227451	46	64.677	2.2×10^{-16}
Sex × species	336809	41	1.937	0.00041
Effect (Skull-Ventral)	Sum of squares	*d.f.*	*F*	*P*
Sex	757218	1	48.261	6.253×10^{-12}
Group	7244132	7	102.84	2.2×10^{-16}
Species	15998846	46	57.218	2.2×10^{-16}
Sex × species	342703	41	1.746	0.00268
Effect (Skull-Lateral)	Sum of squares	*d.f.*	*F*	*P*
Sex	690685	1	39.113	5.64×10^{-10}
Group	8589149	7	113.62	2.2×10^{-16}
Species	17760991	46	60.782	2.2×10^{-16}
Sex × species	393618	41	1.892	0.00065
Effect (Mandible)	Sum of squares	*d.f.*	*F*	*P*
Sex	246306	1	26.21	3.834×10^{-7}
Group	3236279	7	80.81	2.2×10^{-16}
Species	5454583	24	75.623	2.2×10^{-16}
Sex × species	178344	24	3.338	1.652×10^{-7}

Table 3 - MANOVA for skull and mandible shape in *Ctenomys* for sex, groups, and species.

Effect (Skull-Dorsal)	λ_{Wilks}	*d.f.*	*F*	*P*
Sex	0.746	1	19.079	2.2×10^{-16}
Group	0.005	7	63.311	2.2×10^{-16}
Species	7.123×10^{-6}	46	18.409	2.2×10^{-16}
Sex × species	0.383	41	1.488	2.2×10^{-16}
Effect (Skull-Ventral)	λ_{Wilks}	*d.f.*	*F*	*P*
Sex	0.688	1	23.057	2.2×10^{-16}
Group	0.004	7	60.351	2.2×10^{-16}
Species	4.99×10^{-5}	47	20.502	2.2×10^{-16}
Sex × species	0.479	41	1.26	2.19×10^{-6}
Effect (Skull-Lateral)	λ_{Wilks}	*d.f.*	*F*	*P*
Sex	0.733	1	13.496	2.2×10^{-16}
Group	0.004	7	46.814	2.2×10^{-16}
Species	3.995×10^{-6}	46	15.502	2.2×10^{-16}
Sex × species	0.406	41	1.157	0.00053
Effect (Skull-3 views)	λ_{Wilks}	*d.f.*	*F*	*P*
Sex	0.736	1	14.776	2.2×10^{-16}
Group	0.003	7	53.296	2.2×10^{-16}
Species	3.037×10^{-6}	46	17.401	2.2×10^{-16}
Sex × species	0.287	41	1.427	2.2×10^{-16}
Effect (Mandible)	λ_{Wilks}	*d.f.*	*F*	*P*
Sex	0.71	1	15.975	2.2×10^{-16}
Group	0.049	7	21.2256	2.2×10^{-16}
Species	0.0019	24	12.336	2.2×10^{-16}
Sex × species	0.428	24	1.347	9.505×10^{-7}

Table 4 - Percentage of correct classification from discriminant analysis for shape for dorsal, ventral, and lateral views of the skull, as well as the three views combined and for the lateral view of the mandible for *Ctenomys* groups.

Group	Dorsal	Ventral	Lateral	3 views	Mandible
Boliviano-Matogrossense	100.00	94.91	100.00	100.00	66.66
Boliviano-Paraguaio	89.28	85.71	82.14	89.28	69.23
Chaco	92.50	87.50	92.50	92.50	56.00
Mendocinus	83.56	86.30	84.93	88.35	82.05
Opimus-Fulvus	85.84	87.73	93.39	87.73	83.33
Patagonico	89.69	96.90	84.53	94.84	70.12
Pundti-Talarum	73.13	77.61	73.13	76.11	70.21
Torquatus	100.00	100.00	100.00	100.00	93.29
Average	89.25	89.58	88.82	91.00	73.86

Table 5 - Percentage of correct classification from discriminant analysis for shape for dorsal, ventral, and lateral views of the skull, individually, combined, and with size plus shape (form) for *Ctenomys* species.

Species	Dorsal	Ventral	Lateral	3 views Shape	3 views Form
C. argentinus	100.00	66.66	66.66	66.66	100.00
C. australis	100.00	97.14	94.28	100.00	100.00
C. azarae	84.37	90.62	93.75	90.62	93.75
C. boliviensis	96.66	98.33	98.33	96.66	96.66
C. bonettoi	100.00	100.00	100.00	100.00	100.00
C. budini	100.00	100.00	100.00	100.00	100.00
C. coludo	100.00	100.00	100.00	100.00	100.00
C. conoveri	100.00	100.00	100.00	100.00	100.00
C. coulburni	93.33	90.00	83.33	93.33	93.33
C. coyhaiquensis	100.00	100.00	100.00	100.00	100.00
C. dorbignyi	100.00	84.61	100.00	100.00	100.00
C. dorsalis	100.00	100.00	100.00	100.00	100.00
C. flamarioni	100.00	100.00	100.00	100.00	100.00
C. fochi	66.66	100.00	33.33	66.66	66,66
C. fodax	100.00	100.00	100.00	100.00	100.00
C. frater	90.90	90.90	90.90	90.90	90.90
C. fulvus	76.92	42.30	84.61	80.76	80.76
C. haigi	90.54	93.24	86.48	91.89	95.94
C. knighti	100.00	100.00	100.00	100.00	100.00
C. lami	86.51	83.14	82.02	85.39	85.39
C. latro	100.00	100.00	75.00	100.00	100.00
C. leucodon	100.00	100.00	100.00	100.00	100.00
C. lewisi	100.00	92.30	100.00	100.00	100.00
C. magellanicus	91.30	100.00	95.65	91.30	95.65
C. maulinus	91.17	94.11	91.17	91.17	94.11
C. mendocinus	70.83	58.3	37.50	70.83	66.66
C. minutus	91.87	92.38	93.40	92.38	92.89
C. minutus (Bol)	100.00	50.00	50.00	100.00	100.00
C. occultus	100.00	83.33	83.33	100.00	100.00
C. opimus	92.50	97.50	98.75	95.00	97.50
C. pearsoni	83.11	90.90	96.10	84.41	85.71
C. perrensi	88.88	100.00	88.88	88.88	88.88
C. peruanus	100.00	100.00	100.00	100.00	100.00
C. porteousi	60.00	80.00	70.00	70.00	76.66
C. pundti	80.00	60.00	80.00	80.00	80.00
C. rionegrensis	100.00	100.00	100.00	100.00	100.00
C. roigi	100.00	71.42	100.00	100.00	100.00
C. scagliai	100.00	100.00	100.00	100.00	100.00
C. sericeus	100.00	100.00	100.00	100.00	100.00
C. sociabilis	100.00	100.00	100.00	100.00	100.00
C. steinbachi	100.00	100.00	100.00	100.00	100.00
C. sylvanus	100.00	83.33	83.33	100.00	100.00
C. talarum	86.84	82.89	85.52	86.84	88.15
C. torquatus	96.39	95.04	95.49	96.84	97.29
C. tuconax	94.11	94.11	94.11	100.00	100.00
C. tucumanus	91.30	78.26	95.65	91.30	91.30
C. yolandae	100.00	100.00	100.00	100.00	100.00
Average	93.69	90.22	90.37	93.64	94.84

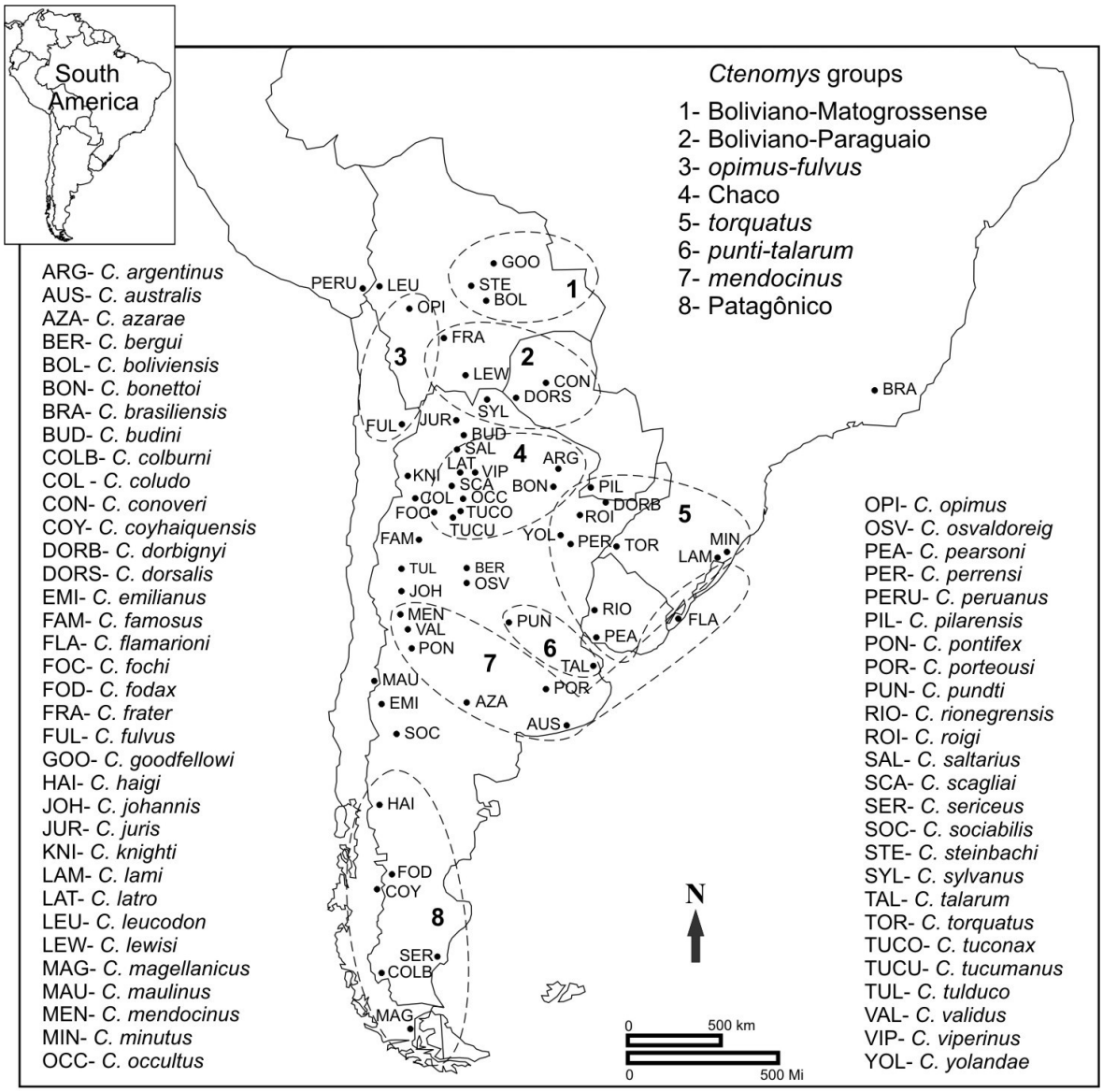

Figure 1. Map of South America with indication of type localities of 60 *Ctenomys* species, according to Woods & Kilpatrick (2005) and groups according to Parada (2007).

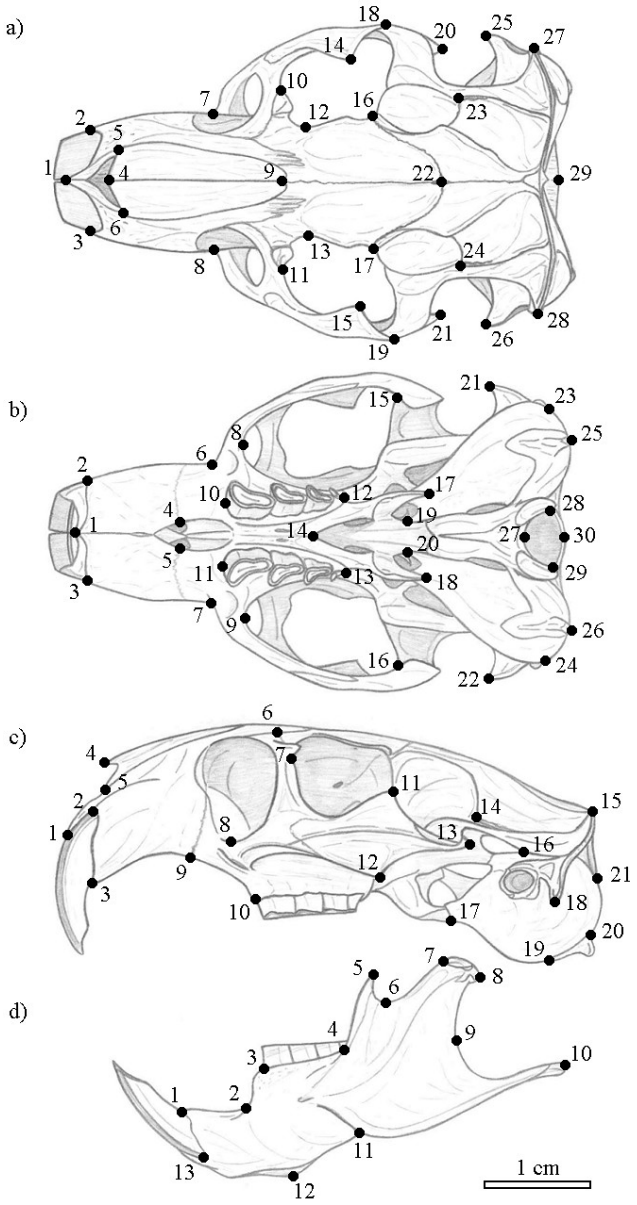

Figure 2. Locations of landmarks on skull of *Ctenomys* for dorsal (a), ventral (b), and lateral (c) views of the cranium and lateral view of the mandible (d).

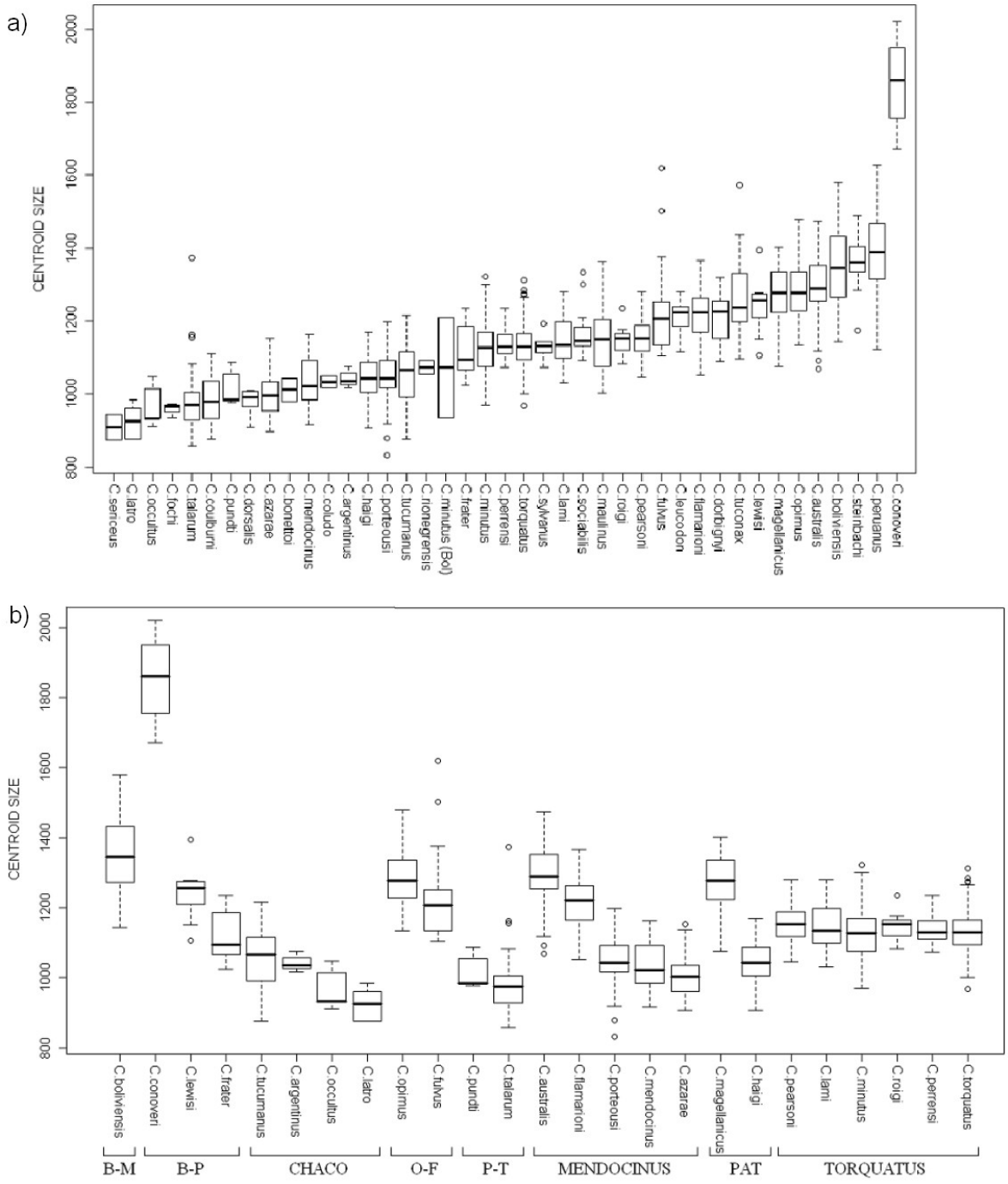

Figure 3. Skull centroid size variability in *Ctenomys*. (a) Among species with sample size larger than 1. (b) Within and between groups. B-M (Boliviano-Matogrossense), B-P (Boliviano-Paraguaio), O-F (*opimus-fulvus*), P-T (*pundti-talarum*), Pat (Patagonico).

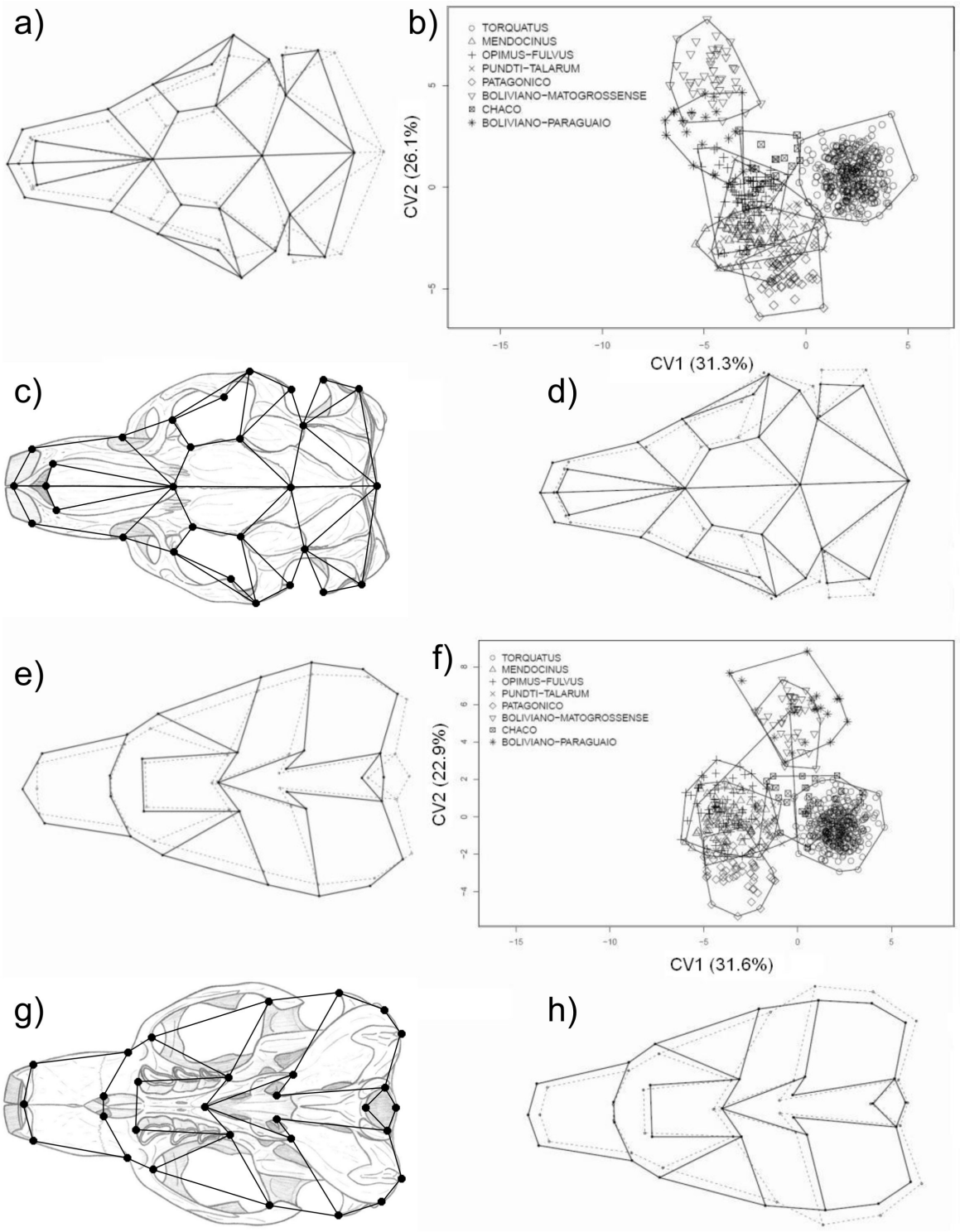

Figure 4. Scatter plot of first versus second canonical variate axes (CV1 and CV2) for dorsal and ventral views of the skull, for *Ctenomys* groups using females. The shape change for each axis is given, solid lines indicate positive scores and dashed lines negative ones. The percentage explained by each axis is given in parentheses.

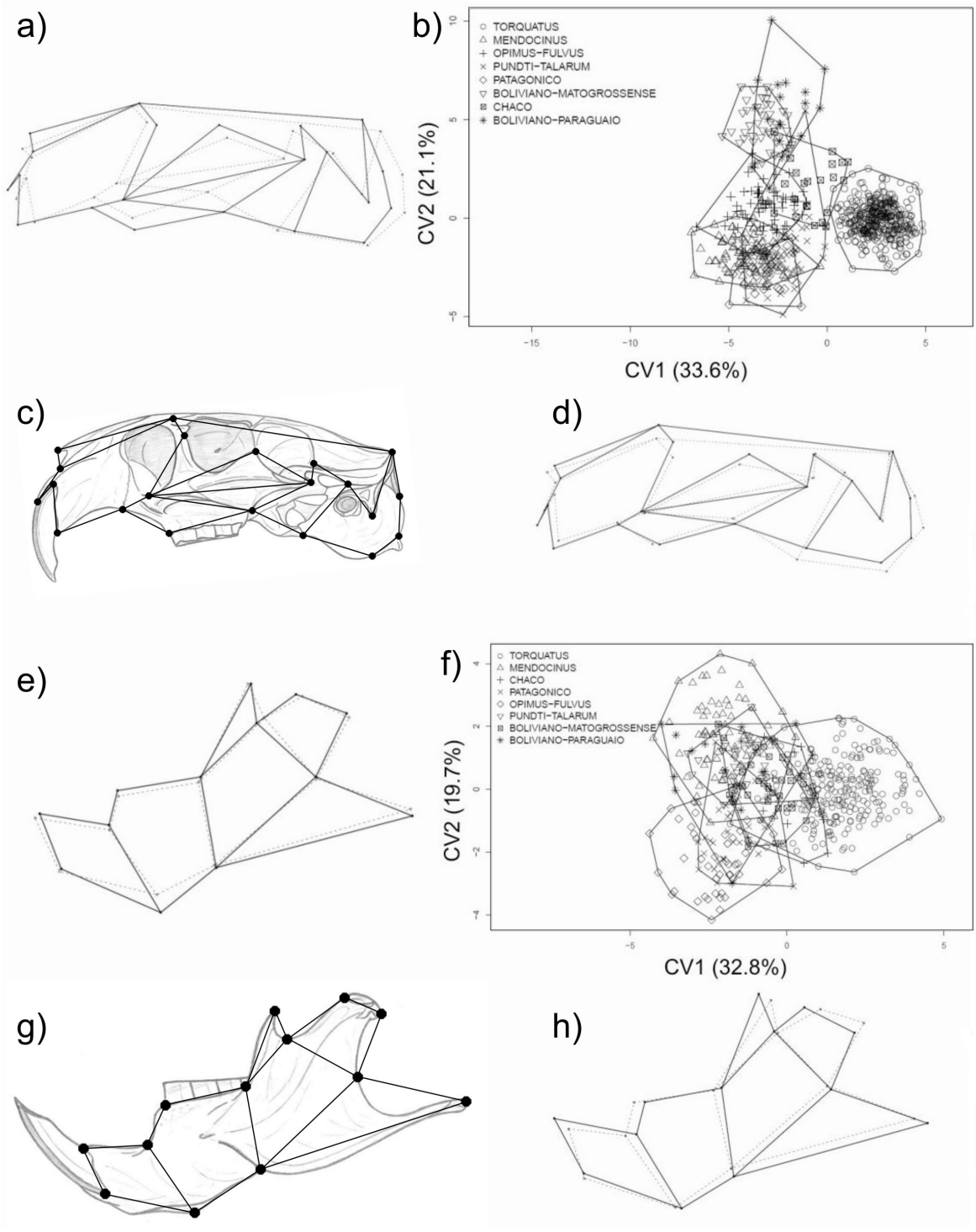

Figure 5. Scatter plot of first versus second canonical variate axes (CV1 and CV2) for lateral view of the skull and lateral view of the mandible, for *Ctenomys* groups using females. The shape change for each axis is given, solid lines indicate positive scores and dashed lines negative ones. The percentage explained by each axis is given in parentheses.

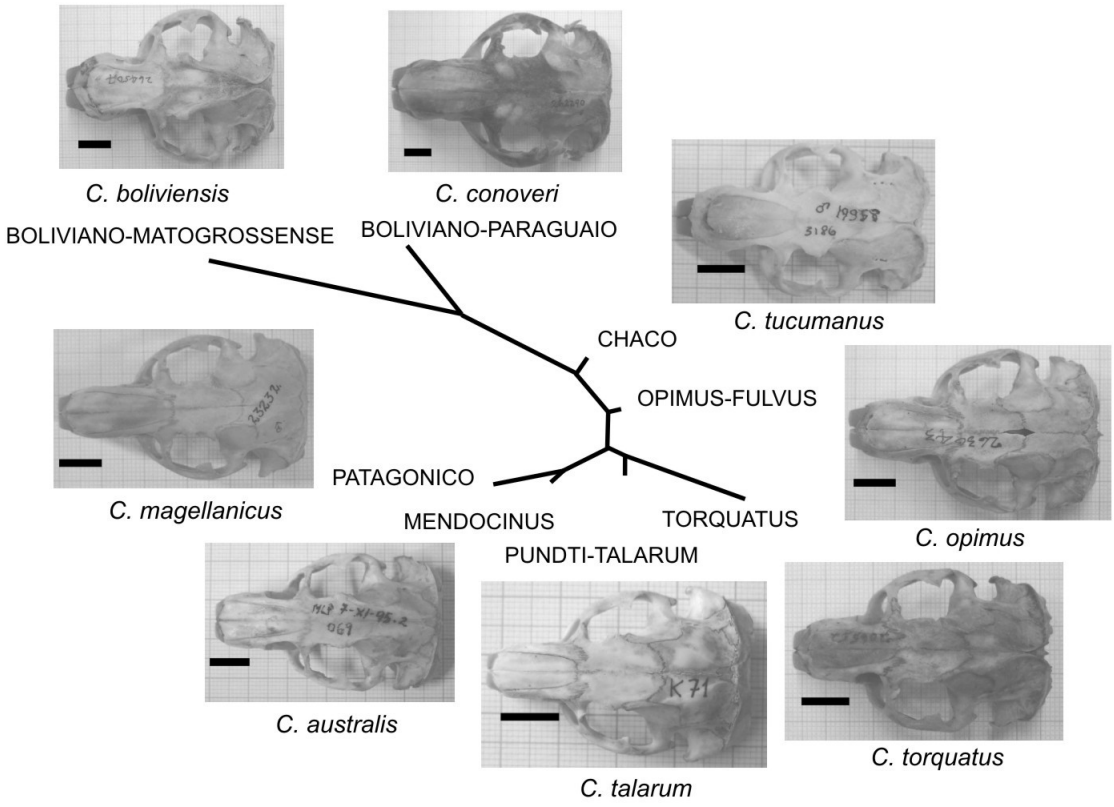

Figure 6. Neighbor-joining tree of Mahalanobis distances among *Ctenomys* groups for dorsal view of the cranium. Scale bar = 1cm.

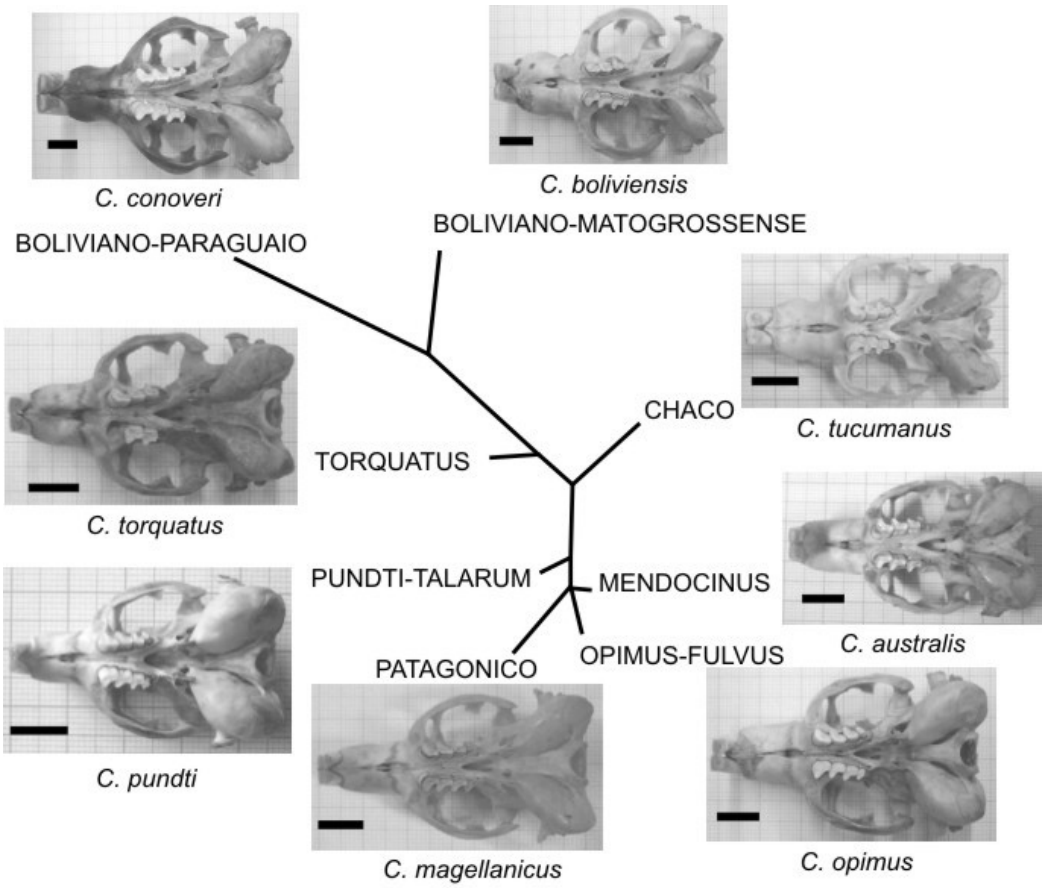

Figure 7. Neighbor-joining tree of Mahalanobis distances among *Ctenomys* groups for ventral view of the cranium. Scale bar = 1cm.

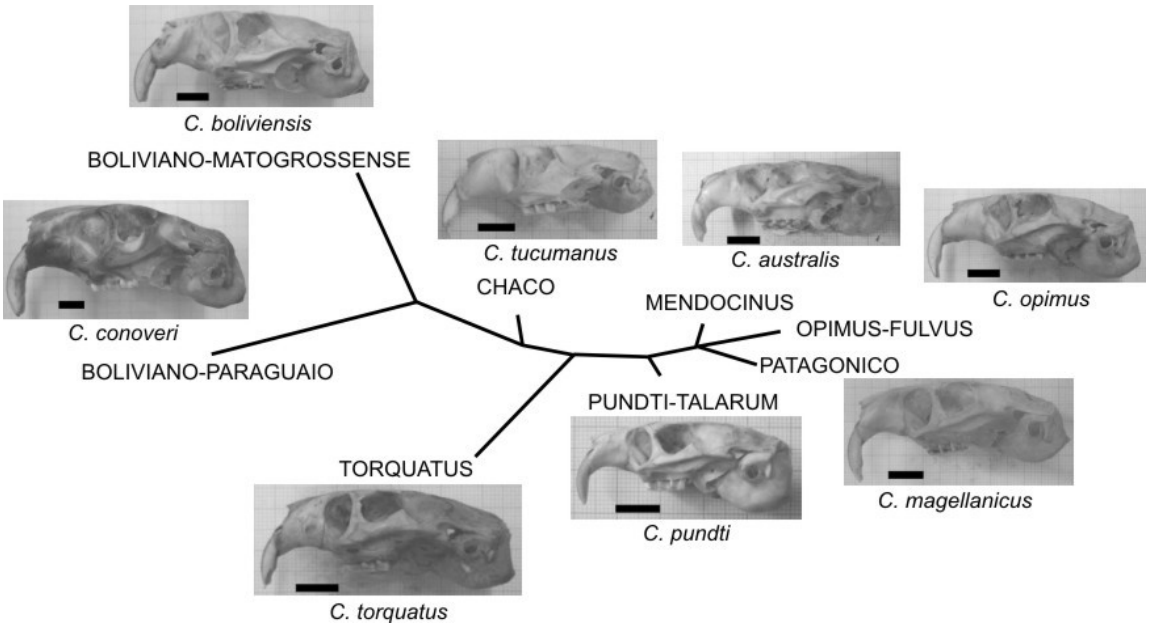

Figure 8. Neighbor-joining tree of Mahalanobis distances among *Ctenomys* groups for lateral view of the cranium. Scale bar = 1cm.

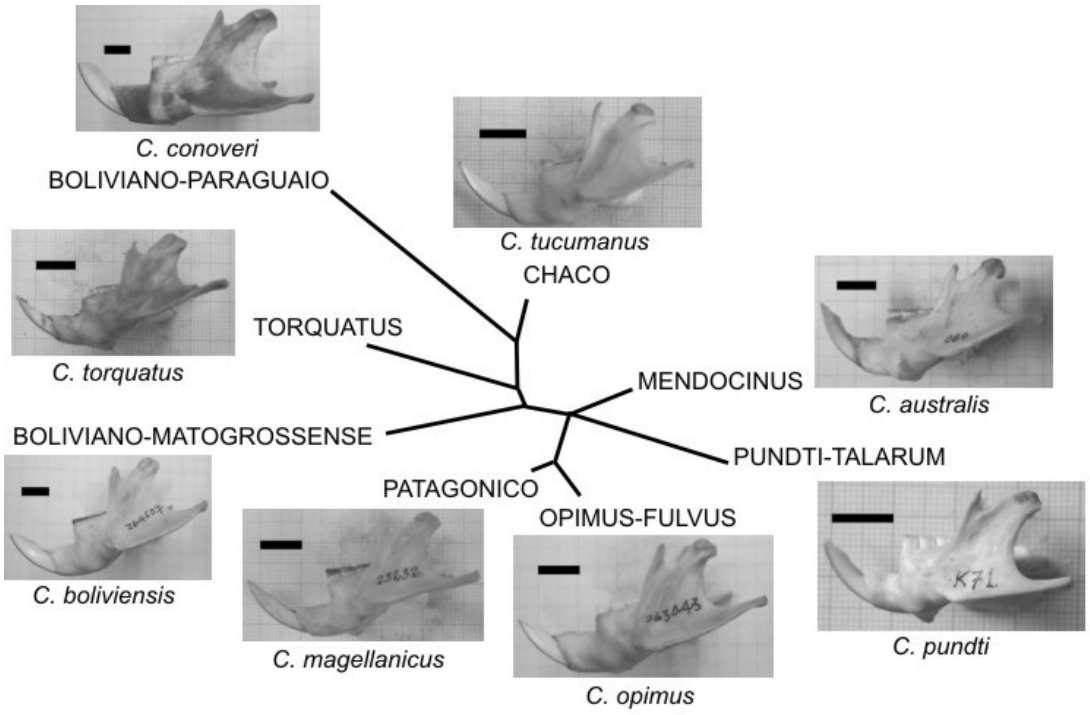

Figure 9. Neighbor-joining tree of Mahalanobis distances among *Ctenomys* groups for lateral view of the mandible. Scale bar = 1cm.

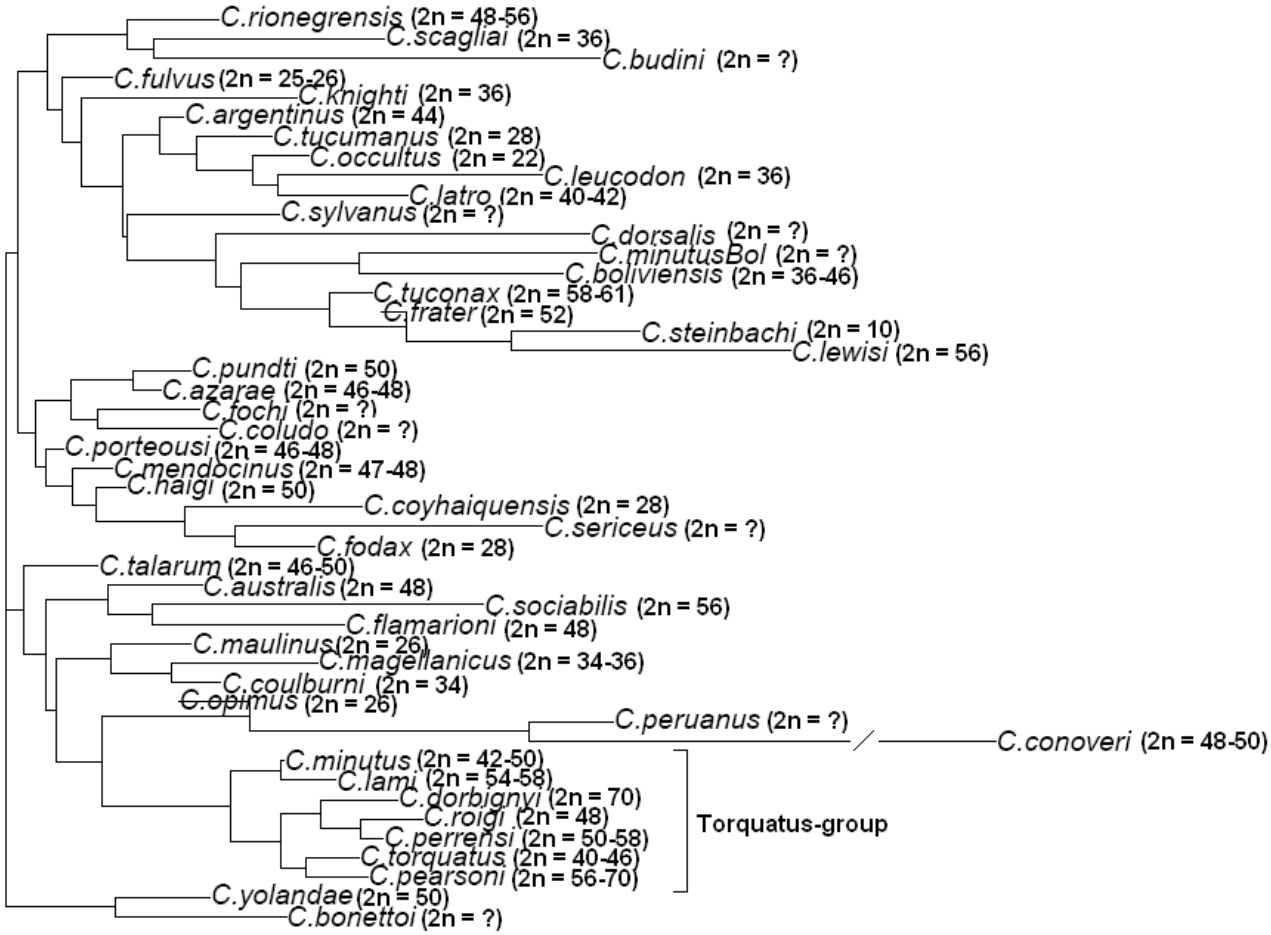

Figure 10. Neighbor-joining tree of Mahalanobis distances among *Ctenomys* species for three views of the skull using shape data pooled from males and females. In parentheses chromosomal diploid number (2n) according with Woods & Kilpatrick (2005).

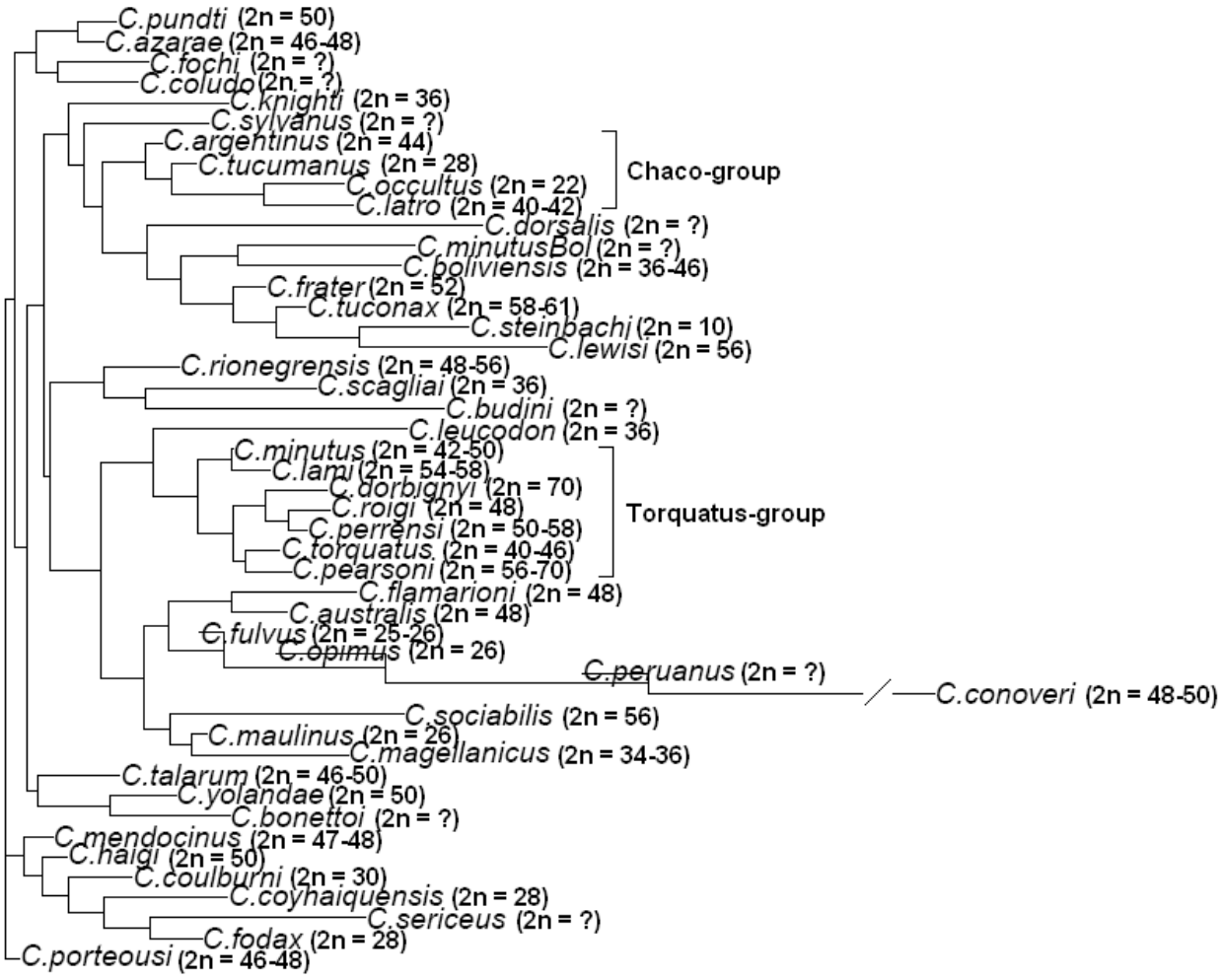

Figure 11. Neighbor-joining tree of Mahalanobis distances among *Ctenomys* species for three views of the skull pooled, using form data (size plus shape) for males and females. In parentheses chromosomal diploid number (2n) according with Woods & Kilpatrick (2005).

Appendix I

Árvore filogenética - tese de mestrado Parada (2007)

Figura 4.1. Consenso estabilizado durante la búqueda del árbol más parsimonioso (de 184 árboles). Se adjuntan los valores de bootstrap >50% (obtenidos con 1000 pseudorrélicas y presentados como Grupo presente/contradicho) e índices de Bremer (BP/iB) para los nodos separados por "/". En el caso de valores de BP menores a 50% el iB se indica precedido de un punto. Se señalan los grupos de especies comentados en esta y las siguientes secciones. Con n 1 y n 2 se indican dos nodos referidos en la sección V.

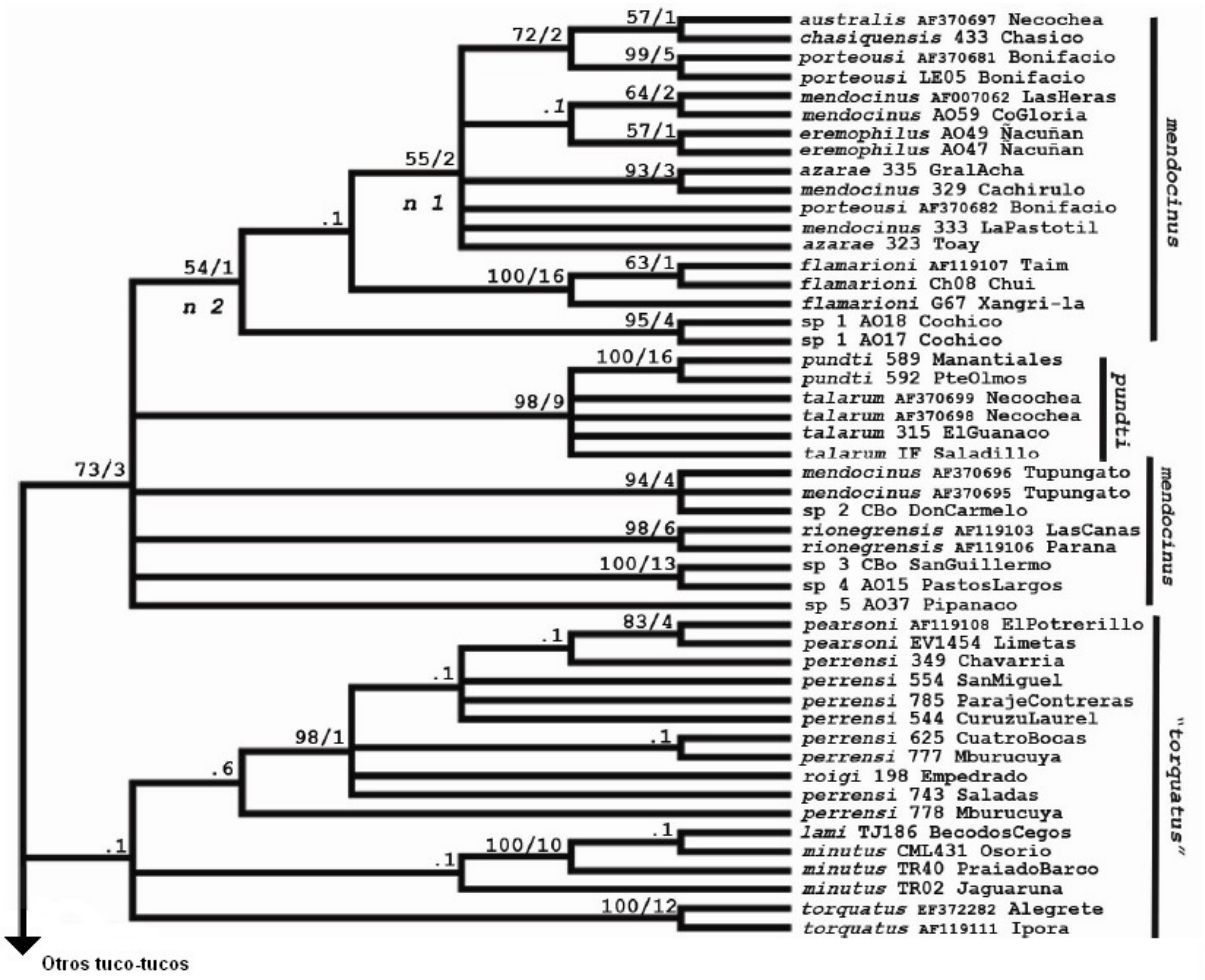

Figura 4.1 cont. Consenso estabilizado durante la búsqueda del árbol más parsimonioso (de 184 árboles). Se adjuntan los valores de bootstrap >50% (obtenidos con 1000 pseudorréplicas y presentados como Grupo presente/contradicho) e índices de Bremer (BP/ iB) para los nodos. Se señalan los grupos de especies comentados en esta y las siguientes secciones.

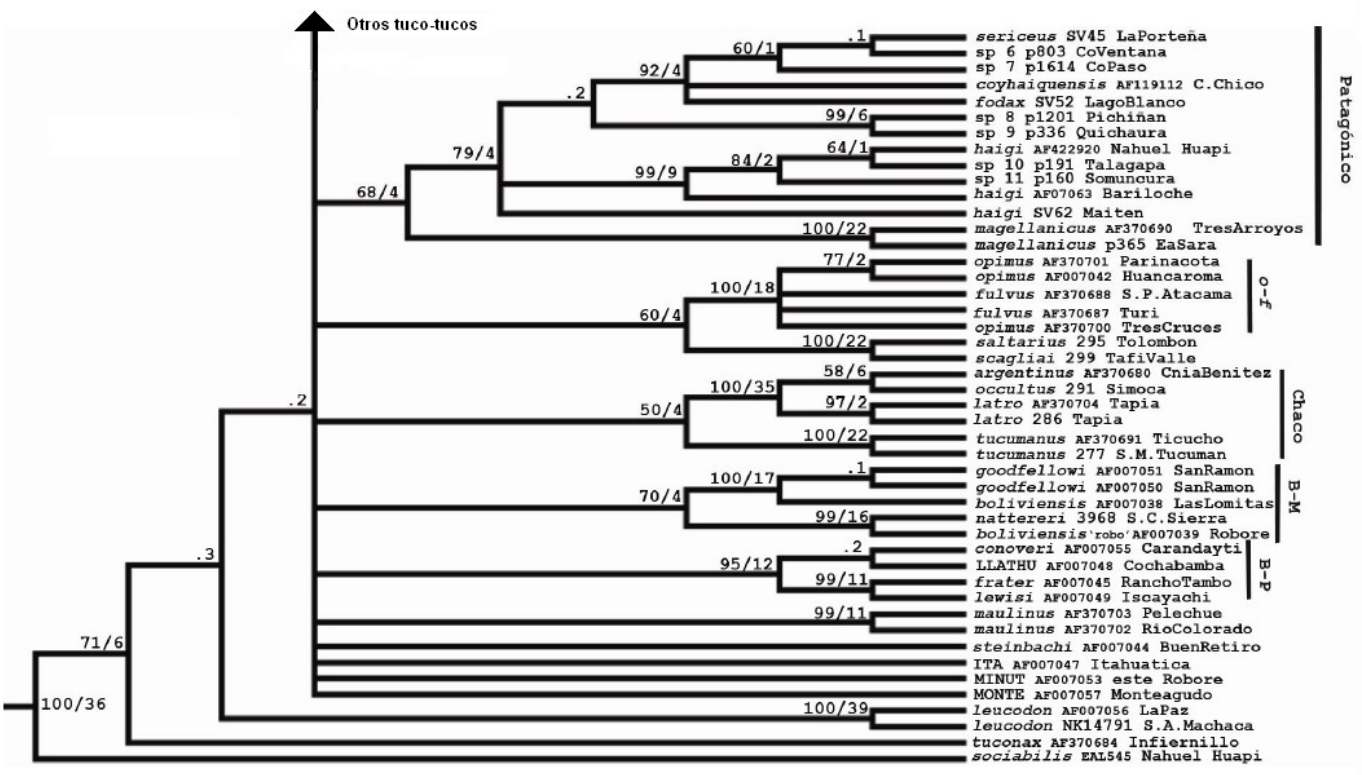

Appendix II

Definition of landmarks with numbers and locations for each view of the cranium and lower jaw of *Ctenomys* (represented in Figure 2).

Dorsal view of the cranium: 1. anterior tip of the suture between premaxillas; 2-3. anterolateral extremity of incisor alveolus; 4. anterior extremity of the suture between nasals; 5-6. anteriormost point of the suture between nasal and premaxilla; 7-8. anteriormost point of the root of zygomatic arch; 9. suture between nasals and frontals; 10-11. anterolateral extremity of lacrimal bone; 12-13. point of least width between frontals; 14-15. tip of extremity of superior jugal process; 16-17. anterolateral extremity of suture between frontal and squamosal; 18-19. lateral extremity of suture between jugal and squamosal; 20-21. tip of posterior process of jugal; 22. suture between frontals and parietals; 23-24. anterolateral extremity of suture between parietal and squamosal; 25-26. anterior tip of external auditory meatus; 27-28. point of maximum curvature on mastoid apophysis; 29. posteriormost point of occipital along the midsagittal plane.

Ventral view of the cranium: 1. anterior tip of suture between premaxillas; 2-3. anterolateral extremity of incisor alveolus; 4-5. lateral edge of incisive foramen in suture between premaxilla and maxilla; 6-7. anteriormost point of root of zygomatic arch; 8-9. anteriormost point of orbit in inferior zygomatic root;10-11. anteriormost point of premolar alveolus; 12-13. posterior extremity of III molar alveolus; 14. posterior extremity of suture between palatines; 15-16. anteriormost point of intersection between jugal and squamosal; 17-18. posteriormost point of pterygoid; 19-20. anterior extremity of tympanic bulla; 21-22. anterior tip of external auditory meatus; 23-24. posterior extremity of mastoid apophysis; 25-26. posterior extremity of paraoccipital apophysis; 27. anteriormost point of foramen magnum; 28-29. posterior extremity of occipital condyle in foramen magnum; 30. posteriormost point of foramen magnum along midsagittal plane.

Lateral view of the cranium: 1. anteriormost point of premaxilla; 2. posteriormost point of incisor alveolus; 3. inferiormost point of incisor alveolus; 4. anterior tip of nasal; 5. anteriormost point of the suture between nasal and premaxilla; 6. suture between premaxilla, maxilla and frontal in superior zygomatic root; 7. inferiormost point of suture between lacrimal and maxilla; 8. inferiormost point of infraorbital foramen in inferior zygomatic root; 9. inferiormost point of suture between premaxilla and maxilla; 10. anteriormost point of premolar alveolus; 11. extremity of superior jugal process; 12. extremity of inferior jugal process; 13. tip of posterior jugal process; 14. medial point of suture between parietal and squamosal; 15. superior extremity of lambdoidal crest; 16. posterior extremity of postglenoid fossa; 17. inferior extremety in suture between pterygoid and tympanic bulla; 18. inferior extremity of mastoid apophysis; 19. anteriormost margin of paraoccipital apophysis; 20. posteriormost margin of paraoccipital apophysis; 21. posterior extremity of intersection between occipital and tympanic bulla.

Lateral view of the mandible: 1. upper extreme anterior border of incisor alveolus; 2. extreme of the diastema invagination; 3. anterior edge of the premolar alveolus; 4. intersection between molar alveolus and coronoid process; 5. tip of the coronoid process; 6. maximum of curvature between the coronoid and condylar processes; 7. anterior edge of the articular surface of the condylar process; 8. tip of the postcondyloid process; 9. maximum curvature between condylar and angular processes; 10. tip of the angular process; 11. intersection between mandibular body and masseteric crest; 12. posterior extremity of the mandibular symphysis; 13. posterior extremity border of incisor alveolus.

Capítulo III

Manuscrito em preparação

Skull shape and size variation within and between *mendocinus* and *torquatus* groups in the genus *Ctenomys* (Rodentia: Ctenomyidae) in chromosomal polymorphism context

Rodrigo Fornel[1,2], Pedro Cordeiro-Estrela[1,2], & Thales Renato O. de Freitas[1,2]

[1]Programa de Pós-Graduação em Genética e Biologia Molecular – Universidade Federal do Rio Grande do Sul, Av. Bento Gonçalves 9500, CEP 91501-970, Porto Alegre, RS, Brazil.
[2]Departamento de Genética, Instituto de Biociências, Universidade Federal do Rio Grande do Sul, Av. Bento Gonçalves 9500, CEP 91501-970, Porto Alegre, RS, Brazil.

Email addresses:

RF: rodrigofornel@hotmail.com

PCE: pedroestrela@yahoo.com

TROF: thales.freitas@ufrgs.br

Running Title: Skull variation in *mendocinus* and *torquatus* groups in genus *Ctenomys*
Keywords: chromosomal polymorphism, cranium, geometric morphometrics, phenotypic evolution.

Abstract

We tested the association between chromosomal polymorphism and skull shape and size variation in two groups of the subterranean rodent *Ctenomys*. This hypothesis is based on the premise that chromosomal rearrangements in small populations, as how occurs in *Ctenomys*, produce reproductive isolation and allow the independent diversification of populations. The m*endocinus*-group has species with low chromosomal diploid number variation (2n = 46-48), while species from *torquatus*-group had a higher karyotype variation (2n = 42-70). We analyzed morphological variation of the skull and mandible with geometric morphometrics approach in 11 species from *mendocinus* and *torquatus* groups of the genus *Ctenomys*. In this way, more phenotypic variation was expected to be found in *torquatus*-group than *mendocinus*. However, our results reject the hypothesis of association between chromosomal polymorphism and skull shape and size variation. Moreover, *torquatus*-group is not more variable than *mendocinus* and heterogeneity of habitat associated to biomechanical constraints and other factors like geography, phylogeny, and demography may be affect the skull morphological evolution in *Ctenomys*.

Introduction

The genus *Ctenomys* is composed of approximately 60 species that occur in South America (Reig *et al.* 1990, Lacey *et al.* 2000, Woods & Kilpatrick 2005). These subterranean rodents show the largest chromosomal polymorphism among mammals, with diploid number varying from 2n = 10 in *C. steinbachi* to 2n = 70 in *C. pearsoni* (Reig *et al*. 1990, Ortells & Barrantes 1994). Because of this large karyotypic variation, chromosomal speciation has been proposed as a probable, or the main, mechanism of cladogenesis within the genus *Ctenomys* (King 1993, Ortells & Barrantes 1994). Adaptive radiation driven by key inovations to the underground niche (Nevo 1979) and patchy population structure (Reig *et al*., 1990) have been proposed as alternative or concurrent mechanisms to explain high rates of diversification. However, most of these mechanisms have been seriously challenged by analyses based on molecular data. The mere fact that *Ctenomys* presents high rates of diversification has failed to receive significant support compared to Hystricognathous sister lineages (Cook & Lessa 1998). More recently, Tomasco & Lessa (2007) have shown that chromosomal populations are polyphyletic relative to mitochondrial DNA in *C. pearsoni*. Adding to this fact no sign of negative heterosis has been found in hybrid zones of *Ctenomys* (Freitas 1997, Gava & Freitas 2002, 2003). Negative heterosis would be required in traditional model of chromosomal speciation to disrupt gene flow between populations. Its absence seriously undermines traditional models of chromosomal speciation as a main mechanism of diversification in *Ctenomys*. However, Navarro & Barton (2003) and Rieseberg & Livingstone (2003) have proposed that the reduced recombination of rearranged chromosomes might to favour the accumulation of adaptive differences on rearranged regions. Within this article we analyse an adaptive structure, the skull, within two clades of *Ctenomys* that differ radically in number of chromosomal rearrangements.

Some works with morphological, cytogenetic and molecular data had proposed different lineages or main groups within the genus *Ctenomys* (Lessa & Cook 1998, Contreras & Bidau 1999, D'Elia *et al.* 1999, Mascheretti *et al.* 2000, Slamovits *et al.* 2001, Parada 2007). Two of these groups, *mendocinus* and *torquatus*, are very different in chromosomal polymorphism.

The *mendocinus*-group suggested by Massarini *et al.* (1991), is known by the low variation in chromosomal diploid number. The majority of species have 2n = 46 to 2n = 48, the exception is *C. rionegrensis* with 2n = 48-56 (Reig *et al.* 1992). This group is formed by seven species: *C. mendocinus* (2n = 47-48), *C. azarae* (2n = 46-48), *C. chasiquensis*, *C. rionegrensis* (2n = 48-56), *C. porteousi* (2n = 47-48), *C. australis* (2n = 48), and *C. flamarioni* (2n = 48) (Massarini *et al.* 1991, Reig *et al.* 1992, Freitas 1994, Massarini *et al*. 1998, D'Elia *et al.* 1999, Massarini & Freitas 2005). All species from this group shown the asymmetric sperm form (Vitullo *et al.* 1988, Freitas 1994, 1995, Massarini *et al.* 1998). The *mendocinus*-group occurs in central west of Argentina, west of Uruguay, and in coastal plain of southern Brazil (Massarini *et al*. 1991, Massarini & Freitas 2005) (Fig. 1).

The *torquatus*-group proposed by Parada (2007), show a high chromosomal diploid number variation from 2n = 40 to 2n = 70. Is formed by *C. torquatus* with 2n = 40-46 (Fernandes *et al.* 2009a, 2009b), *C. lami* with 2n = 54-58 (Freitas 2001, 2007), *C. minutus* with 2n = 42-50 (Freitas 2006), *C. perrensi* with 2n = 50-58 (Ortells *et al.* 1990, Reig *et al.* 1992), *C. pearsoni* with 2n = 56-70 (Novello & Altuna 2002), and *C. roigi* with 2n = 48 (Ortells *et al.* 1990). All species from this group show symmetric sperm form (Vitullo *et al.* 1988, Freitas 1995). The *torquatus*-group occurs in northern and southern Uruguay, southern Brazil, and northeastern Argentina (Freitas 1994, 2006, Parada 2007) (Fig. 1).

Both groups occupy heterogeneous habitats, from dunes of the Atlantic coast to low valleys of the west (Reig *et al*. 1990) (Fig. 1). The molecular phylogenetic analysis support *mendocinus* and *torquatus* groups as two monophyletic clades (D'Elia *et al*. 1999, Castillo *et al*. 2005). Contreras & Bidau (1999) proposed that chromosomal rearrangements could play an important role in the source of reproductive isolation in small populations (common in several species of genus *Ctenomys*). Thus, if chromosomal rearrangements act in reproductive isolation and allows populations to evolve independently from each other (by natural selection or genetic drift), we expect that *torquatus*-group, that had higher chromosomal polymorphism, shows more variable skull shape and size than *mendocinus*-group that had lower chromosomal polymorphism.

Much controversy remains on the role of chromosomal diploid number variation related to the speciation of the genus *Ctenomys*. Thus, the aim of this study is to investigate skull shape and size variation within and between *mendocinus* and *torquatus* groups and

test the association of chromosomal polymorphism and skull morphological variation in these two groups.

Material and Methods

Sample – We analyzed 747 skulls and 505 mandibles of adults representing 11 species from *mendocinus* and *torquatus* groups (Table 1). The skulls and mandibles were obtained from following museums and scientific collections: Departamento de Genética, Universidade Federal do Rio Grande do Sul, Porto Alegre, Brazil (UFRGS); Museo Nacional de História Natural y Antropología, Montevideo, Uruguay (MUNHINA); Museo Argentino de Ciencias Naturales "Bernardino Rivadavia", Buenos Aires, Argentina (MACN); Museo de La Plata, La Plata, Argentina (MLP); Museo de Ciencias Naturales "Lorenzo Scaglia", Mar del Plata, Argentina (MMP); Museum of Vertebrate Zoology, University of California, Berkeley, USA (MVZ); American Museum of Natural History, New York, USA (AMNH); and Field Museum of Natural History, Chicago, USA (FMNH).

Geometric Morphometrics – Each cranium was photographed in the dorsal, ventral and lateral left views of the skull and on lateral left side of the mandible with a digital camera with 3.1 megapixels (2048 × 1536) of resolution, with macro function and without flash. We used 29 two-dimensional landmarks for dorsal, 30 for ventral and 21 for lateral views of the skull, the same proposed by Fernandes *et al*. (2009a) and added more 13 landmarks for lateral view of the mandible (Figure 2; Appendix I). Anatomical landmarks were digitized for each specimen using TPSDig version 1.40 software (Rohlf 2004, http://life.bio.sunysb.edu/morph). All landmarks were taken by the same person (R.F.) Coordinates were superimposed using a generalized Procrustes analysis (GPA) algorithm (Dryden & Mardia 1998). GPA removes differences unrelated to the shape such as scale, position and orientation (Rohlf & Slice 1990, Rohlf & Marcus 1993, Bookstein 1996a, 1996b, Adams *et al*. 2004). We symmetrized both sides of landmarks in dorsal and ventral views of the skull and only the symmetric part of the variation was analyzed (Kent & Mardia 2001, Klingenberg *et al*. 2002, Evin *et al*. 2008). The size of each skull was estimated using its centroid size, the square root of the sum of the squares of the distances

of each landmark from the centroid (mean of all coordinates) of the configuration (Bookstein 1991).

Statistical Analysis – For test the skull size differences we used analysis of variance (ANOVA) of the centroid size, the square root of the sum of the squares of the distance of each landmark from the centroid (mean of all coordinates) of the configuration (Bookstein, 1991). For multiple comparisons of centroid size we used Tukey test and Box plots to visualize centroid size variation.

For skull shape we used principal component analysis (PCA) and multivariate analysis of variance (MANOVA) of the principal components. To choose the number of PCs to be included in the linear discriminant analysis (LDA), we computed correct classification percentages with each combination of PCs (Baylac & Friess 2005). We selected the subset of PCs giving the highest overall correct classification percentage. We used a leave-one-out cross validation procedure that allows an unbiased estimate of classification percentages (Ripley 1996, Baylac & Friess 2005). Cross-validation is used to evaluate the performance of classification by LDA. We used LDA for computed correct classification percentages among groups and species. The Mahalanobis's D^2 distances were used to generate phenograms with neighbor-joining method. Finally, we used Procrustes distances to measure the variation in skull shape within *mendocinus* and *torquatus* groups and used Levene's test to assess the equality of variances in different groups.

For all statistical analyses and to generate graphics we used the "R" language and environment for statistical computing version 2.9.0 for Windows (R Development Core Team, http://www.R-project.org) and the following libraries: MASS (Venables & Ripley 2002), ape version 1.8-2 (Paradis *et al*. 2006), stats (R Development Core Team, 2009), and ade4 (Dray & Dufour 2007). Geometric morphometrics procedures were carried with the Rmorph package: a geometric and multivariate morphometrics library for R (Baylac 2008).

Results

Size – Males are in average bigger than females for centroid size of the skull (ANOVA: $P < 0.001$) (dorsal: $F = 108.77$; ventral: $F = 103.56$; lateral: $F = 85.81$; and mandible: $F = 65.69$). The two groups, *mendocinus* and *torquatus*, do not differ

significantly in skull centroid size (ANOVA: $P > 0.05$). We found significant differences among species for size (ANOVA: $P < 0.001$) (dorsal: $F = 46.82$; ventral: $F = 42.79$; lateral: $F = 42.61$; and mandible: $F = 38.7$). However, the Tukey test showed no significant differences among species that belong to the *torquatus*-group ($P > 0.05$) (Fig. 3). The species from *mendocinus*-group were more variable in skull centroid size than *torquatus*-group, *C. australis* were significantly bigger than other species of both groups (Tukey: $P < 0.001$ in all pairwise comparisons) (Fig. 3). The ANOVA interaction among the three factors (sex, group, and species) were significant only between sex and species for dorsal view of the skull ($P < 0.05$).

Shape – Sexual Dimorphism – Males and females differ significantly in skull shape (MANOVA: $P < 0.001$) (dorsal: $\lambda_{Wilks} = 0.653$, $F = 25.81$; ventral: $\lambda_{Wilks} = 0.657$, $F = 17.96$; lateral: $\lambda_{Wilks} = 0.608$, $F = 14.34$; mandible: $\lambda_{Wilks} = 0.674$, $F = 11.67$). The MANOVA interaction among the three factors (sex, group, and species) were significant only between sex and species ($P < 0.05$).

Two Groups – The principal components analysis (PCA) for the lateral view of the cranium showed structure in the data, indicating two groups corresponding to *mendocinus* and *torquatus* groups (Fig. 4).

The linear discriminant analysis (LDA) for three views of the skull and mandible showed the higher percentage of correct classification for the *torquatus*-group (Table 2). The lateral view of the skull had the highest (100%) and the mandible the lowest (94.87% for *mendocinus* and 97.16% for *torquatus*-group) percentage of correct classification in LDA (Table 2).

The MANOVA for comparison between two groups were significant for all views of the skull ($P < 0.001$) (dorsal: $\lambda_{Wilks} = 0.17$, $F = 372.12$; ventral: $\lambda_{Wilks} = 0.18$, $F = 256.94$; lateral: $\lambda_{Wilks} = 0.2$, $F = 580.66$; mandible: $\lambda_{Wilks} = 0.31$, $F = 84.22$). Skull shape differences between two groups are given in Figure 5. The *torquatus*-group (solid lines in Fig. 5) has a proportionally bigger rostrum, larger zygomatic arch, deeper skull and proportionally larger coronoid process in mandible than *mendocinus*-group. The *mendocinus* have a longer nasals and larger tympanic bulla than *torquatus*-group (dotted lines in Fig. 5).

Species – The MANOVA were highly significant ($P < 0.001$; *d.f.* = 10) among species (dorsal: $\lambda_{Wilks} = 0.002$, $F = 32.92$; ventral: $\lambda_{Wilks} = 0.002$, $F = 35.26$; lateral: $\lambda_{Wilks} = 0.002$, $F = 36.36$; mandible: $\lambda_{Wilks} = 0.017$, $F = 16.68$).

The linear discriminant analysis (LDA) for dorsal view of the skull showed the highest percentage of correct classification for *C. australis*, *C. flamarioni*, and *C. roigi* (100%, Table 3). The species *C. mendocinus* and *C. perrensi* showed the lowest value of correct classification (75% and 77.7% respectively, Table 3). Almost all of specimens were classified in correct group, the only exception was *C. porteousi*, that belong to *mendocinus*-group, showed two individuals classified erroneously in *torquatus*-group (Table 3).

The phenogram using morphological data for dorsal, ventral, and lateral view of the skull showed a large separation between *mendocinus* and *torquatus* groups (Fig. 6). Moreover, the Mahalanobis distances in cladogram indicate a subdivision within *mendocinus*-group with strong morphological association between *C. australis* and *C. flamarioni*, separated from *C. mendocinus*, *C. porteousi*, and *C. azarae* (Fig. 6). In the same way, in *torquatus*-group, *C. lami* and *C. minutus* were strongly associated.

Intra Group Variation – The amplitude of variation of Procrustes distances not differ significantly between *mendocinus* and *torquatus* groups for dorsal, ventral, and lateral views of the skull, as well for the mandible view (Levene's test: $F = 0.221$, $P = 0.64$; $F = 0.005$, $P = 0.94$; $F = 0.083$, $P = 0.77$; $F = 0.082$, $P = 0.78$ respectively).

Discussion

We analyzed skull shape and size within and between *mendocinus* and *torquatus* groups that belong to the genus *Ctenomys*. Our results agree with other studies and support two groups with very different skull morphologies. There is no evidence of convergence among species from different groups.

Contreras & Bidau (1999) suggest that chromosomal rearrangements could be reduce gene flow and until promote the isolation among populations. Nevertheless, some works demonstrated the occurrence of hybrid zones between different chromosomal rearrangements (Freitas 1997, Gava & Freitas 2002, 2003). Moreover, Fernandes *et al*. (2009a) found that there is not necessarily association between chromosomal evolution and phenotypic variation. We refute the hypothesis that a high chromosomal polymorphism is associated to a high morphological variation at the interspecific level in the *mendocinus*-group. Our data show that besides *mendocinus* and *torquatus* groups been very different in

chromosomal polymorphisms, there is no evidence for association between chromosomal diploid number and skull shape variation. Rieseberg & Livingstone (2003) have proposed that the reduced recombination of rearranged chromosomes might favour the accumulation of adaptive differences on rearranged regions. Our data do not support this hypothesis in genus *Ctenomys*, because the *mendocinus*-group that had low chromosomal diploid polymorphism, showed skull shape variation (amplitude of variation) like *torquatus*-group that had high chromosomal polymorphism. These agree with Tomaco & Lessa (2007) that argue that chromosomal speciation could be not the main force in *Ctenomys* diversification.

The *mendocinus*-group occur in a heterogeneous habitats, from coastal dunes to the proximity of the Andes. Several species of *Ctenomys* are characterized as a scratch (claws) and chisel-tooth (incisors) digger. These incisors can be used for building tunnel systems and soil hardness could be influencing the incisor procumbency and affect skull morphology (Vassallo 1998, Mora *et al*. 2003, Verzi & Olivares 2006). In species of *mendocinus*-group we found a pattern in skull centroid size. Populations near the ocean coast are bigger than those inner the continent (see Fig. 1 and Fig. 3). Thus, different types of soil hardness could have a role in biomechanical constraints and diversification in skull morphology of *Ctenomys*. Small skulls to harder soils and bigger skulls in softy soils. Nevertheless, these gradient ocean coast-continent inner in size could be a reflect in skull morphology by different vegetable dietary types. *Ctenomys* are herbivorous and feeds on a variety of grasses, eating both the subterranean and subaereal parts of gramineae (Reig *et al*., 1990). Thus, primary productivity, food quality and abundance may influence body size (Medina *et al*., 2007). Nevertheless, we do not have knowledge about the ecology of all species from the *mendocinus*-group such as vegetable richness data along the total distribution to contribute with a satisfactory explanation about the difference in skull size among *mendocinus* species. The *mendocinus*-group occupies a larger distribution than the *torquatus*-group and the distribution among species is more fragmented (Fig. 1). This more intensive isolation among species of *mendocinus* could permit largest differentiation among species.

We found a strong association between *C. australis* and *C. flamarioni*. Both occurs in sand dunes in Atlantic coast and are more distant than other *mendocinus* species (Fig. 6).

Thus, both ecological and phylogenetic constraints allows *C. australis* and *C. flamarioni* very close.

Medina *et al*. (2007) found that the genus *Ctenomys* follows the converse of Bergmann's rule. This agrees with our data that larger species occupy warm areas while smaller species occupy cold areas and inner continent near Andes mountain range.

New studies about the association between morphological and geographical distances, about several aspects of ecological, demographic, and historical factors of *Ctenomys* species will help in the better understand about evolution of this group of rodents.

Figure Legends

Figure 1. Map with distribution of 11 *Ctenomys* species belong to *mendocinus* and *torquatus* groups, with exception of *C. rionegrensis* and *C. chasiquensis*. *Mendocinus*-group in black: *C. flamarioni* (2n = 48), *C. australis* (2n = 48), *C. porteousi* (2n = 47-48), *C. azarae* (2n = 46-48), and *C. mendocinus* (2n = 47-48). *Torquatus*-group in grey: *C. minutus* (2n = 42-50), *C. lami* (2n = 54-58), *C. torquatus* (2n = 40-46), *C. pearsoni* (2n = 56-70), *C. perrensi* (2n = 50-58), and *C. roigi* (2n = 48).

Figure 2. Landmark location on skull of *Ctenomys* for dorsal (a), ventral (b), and lateral (c) views of the cranium and lateral view of the mandible (d).

Figure 3. Skull centroid size variability among 11 species of *Ctenomys* from *mendocinus* and *torquatus* groups for dorsal view of the skull. The horizontal line represents the mean, box margins are at the 25th and 75th percentils, bars extend to 5th and 95th percentiles, and circles are outliers. Abreviations of species name are given in table 1.

Figure 4. First two axes of principal component analysis (PCA) of the two groups of *Ctenomys*, *mendocinus* and *torquatus* for lateral view of the skull.

Figure 5. Skull shape differences between two groups of *Ctenomys*, the *mendocinus* (dotted lines) and *torquatus* (solid lines) groups for dorsal (a), ventral (b), and lateral (c) views of the cranium, and lateral view of the mandible (d).

Figure 6. Phenogram using neighbor-joining method and Mahalanobis distances from lateral view of the skull for 11 species of *Ctenomys* from *mendocinus* and *torquatus* groups.

Tables

Table 1 - Sample size of skulls and mandibles of 11 species of *Ctenomys* from *mendocinus* and *torquatus* groups.

Species (abreviation)	Group	N_{Skull}	$N_{Mandible}$
C. australis (aus)	*mendocinus*	31	27
C. azarae (aza)	*mendocinus*	29	26
C. flamarioni (fla)	*mendocinus*	32	22
C. porteousi (por)	*mendocinus*	30	28
C. mendocinus (men)	*mendocinus*	24	14
C. lami (lam)	*torquatus*	89	66
C. minutus (min)	*torquatus*	197	122
C. pearsoni (pea)	*torquatus*	77	60
C. perrensi (per)	*torquatus*	9	9
C. roigi (roi)	*torquatus*	7	7
C. torquatus (tor)	*torquatus*	222	124
Total		747	505

Table 2 - Percentage of correct classification for *mendocinus* and *torquatus* groups using linear discriminant analysis (LDA) for dorsal, ventral, and lateral views of the skull, and lateral view of the mandible.

	Group	
	mendocinus	*torquatus*
Dorsal	99.31	100
Ventral	98.63	100
Lateral	100	100
Mandible	94.87	97.16

Table 3 - Classification of 11 species of *Ctenomys* from *mendocinus* and *torquatus* groups for dorsal view of the skull using linear discriminant analysis (LDA). The diagonal line shows the exemplars that were correctly classified to species. The percentage of correct classification is given in the last line. The species abreviations follow the same order in the first column and table 1.

Group	*mendocinus*					*torquatus*					
Species	*aus*	*aza*	*fla*	*por*	*men*	*lam*	*min*	*pea*	*per*	*roi*	*tor*
C. australis	31										
C. azarae		28		1							
C. flamrioni			32								
C. porteousi	1	2		24	1		2				
C. mendocinus		2			18						
C. lami						78	11				
C. minutus						6	186	2			3
C. pearsoni							1	66			10
C. perrensi									7	1	1
C. roigi										7	
C. torquatus							3	4	1		214
Percentage	100	96.6	100	80	75	87.6	94.4	85.7	77.7	100	96.4

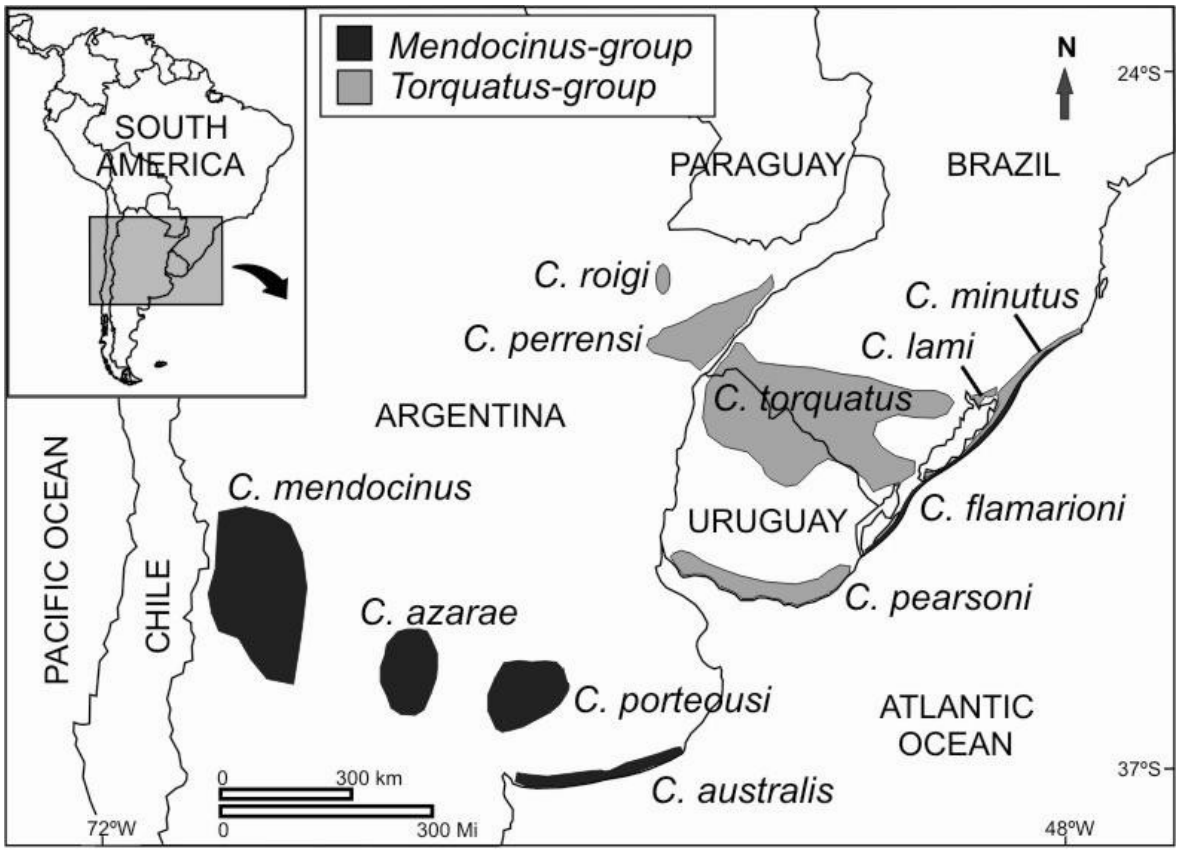

Figure 1. Map with distribution of 11 *Ctenomys* species belong to *mendocinus* and *torquatus* groups, with exception of *C. rionegrensis* and *C. chasiquensis*. *Mendocinus*-group in black: *C. flamarioni* (2n = 48), *C. australis* (2n = 48), *C. porteousi* (2n = 47-48), *C. azarae* (2n = 46-48), and *C. mendocinus* (2n = 47-48). *Torquatus*-group in grey: *C. minutus* (2n = 42-50), *C. lami* (2n = 54-58), *C. torquatus* (2n = 40-46), *C. pearsoni* (2n = 56-70), *C. perrensi* (2n = 50-58), and *C. roigi* (2n = 48).

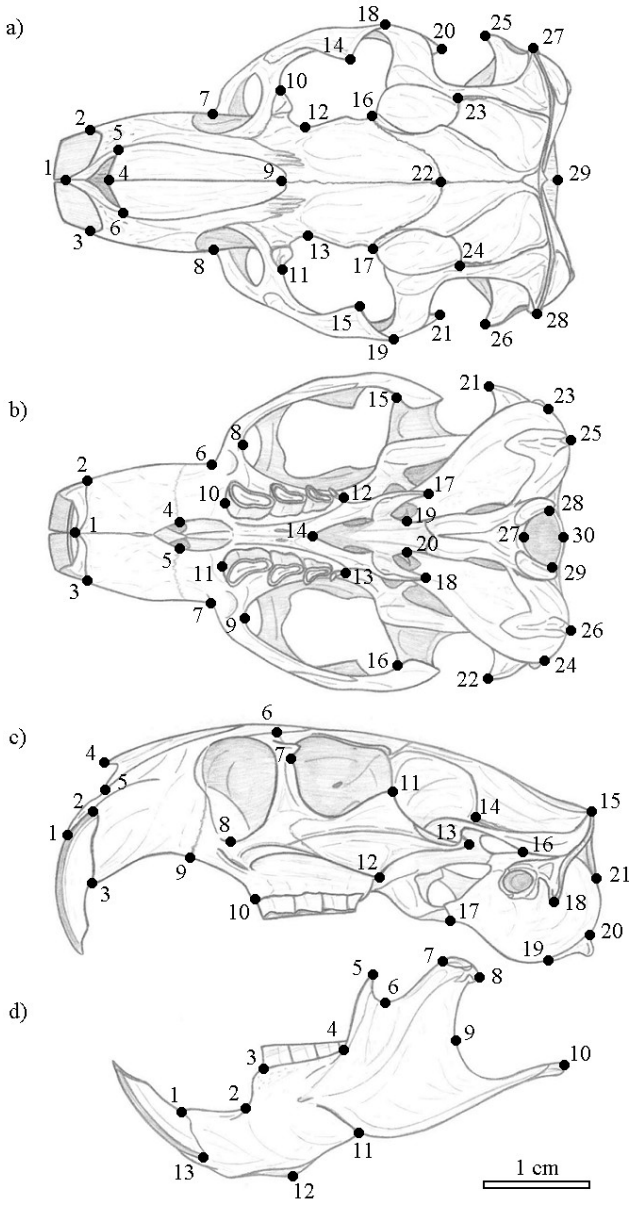

Figure 2. Landmark location on skull of *Ctenomys* for dorsal (a), ventral (b), and lateral (c) views of the cranium and lateral view of the mandible (d).

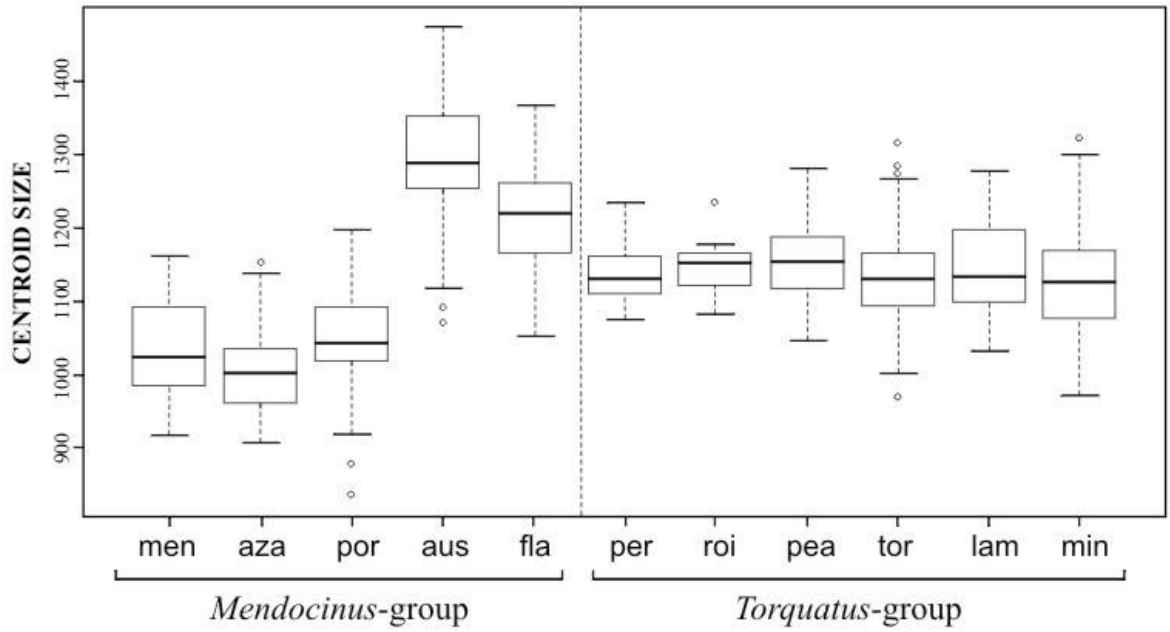

Figure 3. Skull centroid size variability among 11 species of *Ctenomys* from *mendocinus* and *torquatus* groups for dorsal view of the skull. The horizontal line represents the mean, box margins are at the 25th and 75th percentils, bars extend to 5th and 95th percentiles, and circles are outliers. Abreviations of species name are given in table 1.

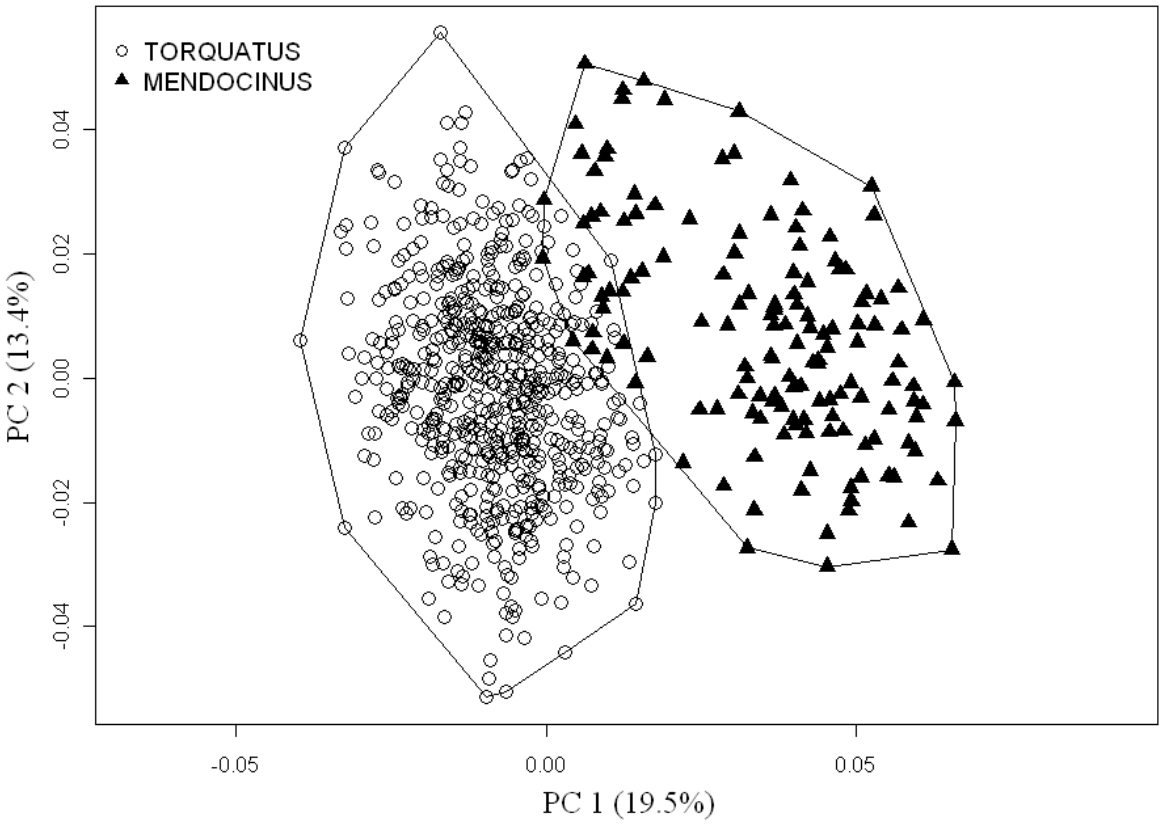

Figure 4. First two axes of principal component analysis (PCA) of the two groups of *Ctenomys*, *mendocinus* and *torquatus* for lateral view of the skull.

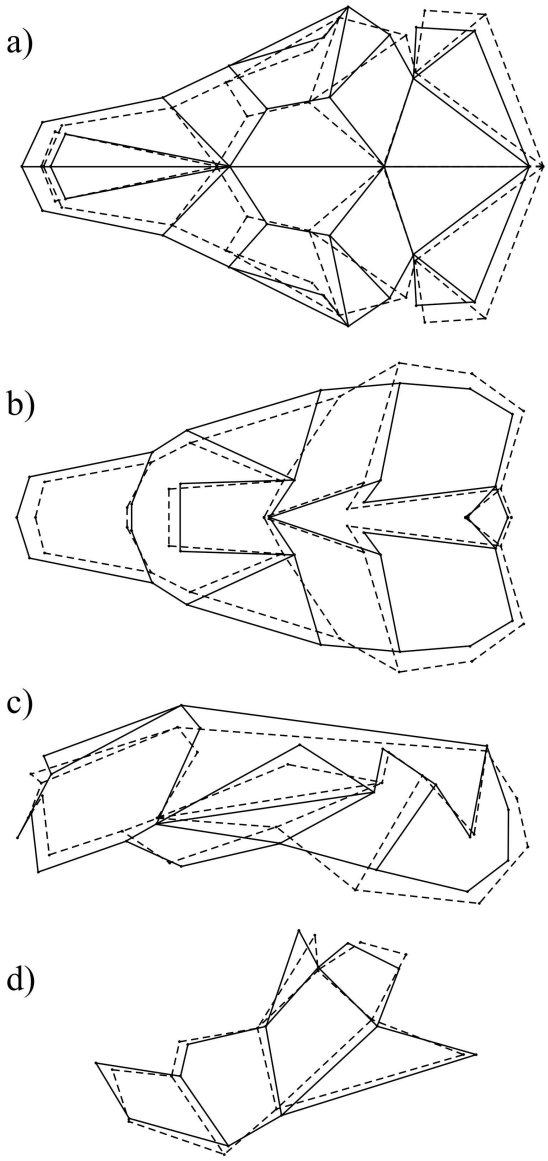

Figure 5. Skull shape differences between two groups of *Ctenomys*, the *mendocinus* (dotted lines) and *torquatus* (solid lines) groups for dorsal (a), ventral (b), and lateral (c) views of the cranium, and lateral view of the mandible (d).

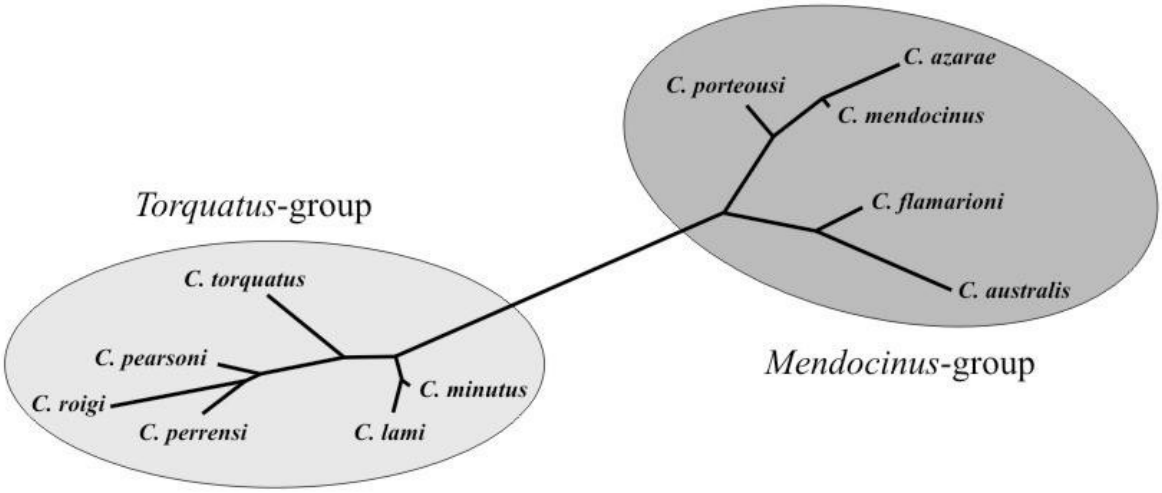

Figure 6. Phenogram using neighbor-joining method and Mahalanobis distances from lateral view of the skull for 11 species of *Ctenomys* from *mendocinus* and *torquatus* groups.

Appendix I

Definition of landmarks with numbers and locations for each view of the cranium and lower jaw of *Ctenomys* (represented in Figure 2).

Dorsal view of the cranium: 1. anterior tip of the suture between premaxillas; 2-3. anterolateral extremity of incisor alveolus; 4. anterior extremity of the suture between nasals; 5-6. anteriormost point of the suture between nasal and premaxilla; 7-8. anteriormost point of the root of zygomatic arch; 9. suture between nasals and frontals; 10-11. anterolateral extremity of lacrimal bone; 12-13. point of least width between frontals; 14-15. tip of extremity of superior jugal process; 16-17. anterolateral extremity of suture between frontal and squamosal; 18-19. lateral extremity of suture between jugal and squamosal; 20-21. tip of posterior process of jugal; 22. suture between frontals and parietals; 23-24. anterolateral extremity of suture between parietal and squamosal; 25-26. anterior tip of external auditory meatus; 27-28. point of maximum curvature on mastoid apophysis; 29. posteriormost point of occipital along the midsagittal plane.

Ventral view of the cranium: 1. anterior tip of suture between premaxillas; 2-3. anterolateral extremity of incisor alveolus; 4-5. lateral edge of incisive foramen in suture between premaxilla and maxilla; 6-7. anteriormost point of root of zygomatic arch; 8-9. anteriormost point of orbit in inferior zygomatic root;10-11. anteriormost point of premolar alveolus; 12-13. posterior extremity of III molar alveolus; 14. posterior extremity of suture between palatines; 15-16. anteriormost point of intersection between jugal and squamosal; 17-18. posteriormost point of pterygoid; 19-20. anterior extremity of tympanic bulla; 21-22. anterior tip of external auditory meatus; 23-24. posterior extremity of mastoid apophysis; 25-26. posterior extremity of paraoccipital apophysis; 27. anteriormost point of foramen magnum; 28-29. posterior extremity of occipital condyle in foramen magnum; 30. posteriormost point of foramen magnum along midsagittal plane.

Lateral view of the cranium: 1. anteriormost point of premaxilla; 2. posteriormost point of incisor alveolus; 3. inferiormost point of incisor alveolus; 4. anterior tip of nasal; 5. anteriormost point of the suture between nasal and premaxilla; 6. suture between premaxilla, maxilla and frontal in superior zygomatic root; 7. inferiormost point of suture between lacrimal and maxilla; 8. inferiormost point of infraorbital foramen in inferior zygomatic root; 9. inferiormost point of suture between premaxilla and maxilla; 10. anteriormost point of premolar alveolus; 11. extremity of superior jugal process; 12. extremity of inferior jugal process; 13. tip of posterior jugal process; 14. medial point of suture between parietal and squamosal; 15. superior extremity of lambdoidal crest; 16. posterior extremity of postglenoid fossa; 17. inferior extremety in suture between pterygoid and tympanic bulla; 18. inferior extremity of mastoid apophysis; 19. anteriormost margin of paraoccipital apophysis; 20. posteriormost margin of paraoccipital apophysis; 21. posterior extremity of intersection between occipital and tympanic bulla.

Lateral view of the mandible: 1. upper extreme anterior border of incisor alveolus; 2. extreme of the diastema invagination; 3. anterior edge of the premolar alveolus; 4. intersection between molar alveolus and coronoid process; 5. tip of the coronoid process; 6. maximum of curvature between the coronoid and condylar processes; 7. anterior edge of the articular surface of the condylar process; 8. tip of the postcondyloid process; 9. maximum curvature between condylar and angular processes; 10. tip of the angular process; 11. intersection between mandibular body and masseteric crest; 12. posterior extremity of the mandibular symphysis; 13. posterior extremity border of incisor alveolus.

Capítulo IV

Manuscrito aceito pelo periódico *Biological Journal of the Linnean Society*

Skull shape and size variation in *Ctenomys minutus* (Rodentia: Ctenomyidae) in geographical, chromosomal polymorphism, and environmental contexts

Rodrigo Fornel[1,2], Pedro Cordeiro-Estrela[1,2], & Thales Renato O. de Freitas[1,2]

[1]Programa de Pós-Graduação em Genética e Biologia Molecular – Universidade Federal do Rio Grande do Sul, Av. Bento Gonçalves 9500, CEP 91501-970, Porto Alegre, RS, Brazil.
[2]Departamento de Genética, Instituto de Biociências, Universidade Federal do Rio Grande do Sul, Av. Bento Gonçalves 9500, CEP 91501-970, Porto Alegre, RS, Brazil.

Email addresses:

RF: rodrigofornel@hotmail.com
PCE: pedroestrela@yahoo.com
TROF: thales.freitas@ufrgs.br

Running Title: Skull shape variation in *Ctenomys minutus*

Keywords: chromosomal rearrangements, cranial morphology, geometric morphometrics, isolation by distance, partial least-squares, Q_{ST}.

Abstract

We tested the influence of migration and drift (isolation-by-distance model), and differences in micro-habitat on phenotypic traits, and correlated it with chromosomal polymorphism, at the intraspecific level, with geometric descriptors of the cranium and mandible over the entire range of subterranean rodent *Ctenomys minutus*. This species occurs in two different environments, dunes and sandy fields, along a strip extending for 470 km on the coastal plain of southern Brazil. *C. minutus* has 7 parental chromosomal diploid numbers, several intraspecific hybrid zones and up to 15 different karyotypes structured almost linearly along the coastline. Chromosomal populations show significant overall differences in size and shape, intraspecific hybrids are phenotypically intermediate between parental forms and clustering suggests four groups delimited by chromosomal inversions and riverine barriers. Dune and field morphologies were significantly different in cranial shape. A significant but weak correlation between morphological and geographic distances along the complete distribution was found supporting the isolation-by-distance model. The intraspecific phenotypic differences seem to arise as a combination of selection and drift acting as diversifying forces. Chromosomal inversions, rivers and paleochannels seem to be acting as barriers to gene flow unlike robertsonian fusions and fissions.

Introduction

Geographic variation in morphological traits in natural populations may provide the basis for the development of studies as well as for testing hypotheses in evolutionary biology. Intraspecific morphological differences may provide the first evidence of ongoing differentiation processes, ultimately leading to speciation. This variation arises from the combined effects of gene mutation, migration, genetic drift, selection, and historical factors (Cwynar & MacDonald 1987).

As partioning the effects of evolutionary forces, demographical and historical factors is far from trivial, very early, simple models where formulated. In population genetics, the isolation-by-distance model (Wright 1943) predicts that, in the absence of selection, there is a significant correspondence between geographic distance and genetic variation. Under this model, genetic similarity between populations will decrease exponentially as the geographic distance between them increases at neutral loci, because of the limiting effect of geographic distance on rates of gene flow (Crow & Kimura 1970, Morton 1973, Relenthford 2004). Any departure from this model tends to indicate selective forces or historical factors as determinants of population structure.

Mathematical models for the evolution of quantitative traits have been derived based on quantitative genetics and population genetic theories (Lande 1991, Nagylaki 1994) to provide predictions of the expected patterns of geographical variation under genetic drift and mild stabilizing selection. The theoretical expectation of equilibrium variance has been derived for different migration model and spatial arrangements including the unbounded linear stepping-stone model (Nagylaki, 1994) which yields a good approximation to our biological model. Further work has derived the expectation of variance and means of clines of polygenic traits under different theoretical models (Barton, 1999). Although the application of these models to empirical data in a hypothesis testing framework is limited by an independent parameter estimation (population effective size, the additive genetic variance of traits, the mutational variance, the neighborhood size or selection coefficients), the quantitative genetic variance among populations, Q_{ST}, has been shown to be equal to F_{ST} under a neutral and additive model (Whitlock 1999). Thus, it is particularly interesting to test the isolation-by-distance model with quantitative characters

as we propose in this contribution. Furthermore, these tests can significantly contribute to the knowledge of evolutionary forces acting on the diversification of the genus *Ctenomys*.

Know as tuco-tucos, *Ctenomys* is a genus of subterranean rodents endemic to the southern Neotropical region, which comprises about 60 extant species (Reig *et al*. 1990, Nowak & Paradiso 1991, Woods 1993, Woods & Kilpatrick 2005). *Ctenomys* is by far the most speciose lineage of subterranean rodents, and its members have high karyotypic diversity, with diploid numbers ranging from 2n = 10 to 2n = 70 (Reig *et al*., 1990). The species *Ctenomys minutus*, Nehring, 1887, has up to 15 different karyotypes with 7 different described parental diploid numbers (2n = 42, 46a, 46b, 48a, 48b, 50a and 50b). Furthermore there are the hybrid karyotypes (2n = 43, 44, 45, 47a, 47b, 49a, and 49b) and the yet underscribed 2n = 48c (Lopes *et al*., in prep). This combination of karyotypes and diploid numbers is the highest intraspecific chromosomal polymorphism known for the genus. These karyotypes are distributed almost linearly along a 470 km strip on the coastal plain of Rio Grande do Sul and Santa Catarina states in southern Brazil (Fig. 1). The 2n = 50 karyotype is found at both extremes of the geographical range, and reduces progressively down to 2n = 42, through chromosomal rearrangements (mostly through Robertsonian rearrangements and tandem fusions) at the approximate center of its geographic distribution (Freitas 1995, 1997, 2006, Gava & Freitas 2003, Freygang *et al*. 2004; Marinho & Freitas 2006). The difference between karyotype system "a" (2n = 46a, 47a, 48a, 49a and 50a) and system "b" (2n = 46b, 47b, 48b, 49b, and 50b) is due to the presence of a pericentric inversion in chromosome 2p (Freygang *et al*. 2004). Populations with 2n = 48c, which belong to neither chromosomal system "a" nor "b" due to a fusion of chromosomes 20 and 17 from 2n = 50a, occur in the extreme north of the distribution (Fig. 1). Therefore, the high speciation rates of *Ctenomys* and the high number of intraspecific diploid numbers lead us to expect that the karyotype might act as a structuring force in the phenotype of *C. minutus* by limiting gene flow between karyotypes and between chromosomal systems (Reig *et al*. 1990).

Chromosomal rearrangements, even if they have little or no effect on hybrid fitness, might reduce gene flow through the suppression of recombination (Rieseberg 2001). Navarro & Barton (2003) suggested that chromosomal rearrangements cause genetic barriers to gene flow and promote parapatric speciation in primates. Nevertheless, in subterranean rodents, particularly in *Ctenomys*, the chromosomal evolution remains

controversial (Lessa 2000). Steinberg & Patton (2000) have argued that chromosomal polymorphism plays a minor role in the speciation of subterranean rodents. Moreover, Tomasco & Lessa (2007) studied molecular polymorphism in *C. pearsoni* and suggested no evidence for fixation by drift of negatively heterotic chromosomal rearrangements in this species, in other words, there is no correlation between chromosomal rearrangements and speciation.

Ecological differentiation process have been less studied as a possible speciation mechanism. *C. minutus* occurs in two different habitats, sand dunes at the extreme north of the range until Praia do Barco (locality 24 in Fig. 1), and fields and pastures from the extreme south until Capão Novo (locality 26 in Fig. 1) (Freitas 1997, Marinho & Freitas 2000, Gava & Freitas 2003) which vary in soil hardness. The genus *Ctenomys* has been characterized as a scratch (claws) and chisel-tooth (incisors) digger, and uses these tools for building its tunnel systems. It is considered a good model to investigate functional morphological adaptations to the subterranean niche (Vassallo 1998, Stein 2000, Lessa *et al*. 2008). Changes in the skull shape in *Ctenomys* are associated (among other factors) with this chisel-tooth digging model, mainly related to the angle of incisor procumbency, rostral allometry, and zygomatic arch proportions, which change with soil hardness (Vassallo 1998, Mora *et al*. 2003, Verzi & Olivares 2006). Therefore, we expected to find differences in skull shape located in biomechanically meaningful regions between the dune and sand-field populations. In addition, environmental heterogeneity over the range of the species might also act as a selective factor producing phenotypic differences in the skull.

Conversely, if karyotypes and environmental differences play little role in interpopulation differentiation, *Ctenomys* characteristics including their patchy distribution, territoriality, limited vagility, and small effective population size (Reig *et al*. 1990) are expected to be among the main determinants of population structure, which should follow an isolation-by-distance model.

The aim of the present study was the examination of skull shape variation in *C. minutus* using different statistical techniques based on geometric morphometrics data. We tested factors that might generate intraspecific structure in the shape and size of the skull of populations of *C. minutus*. We tested karyotypic and environmental factors against a null model of isolation-by-distance.

Material and Methods

Sample – The material examined consisted of 210 skulls (96 males and 114 females) and 122 mandibles (48 males and 74 females) of karyotyped adult specimens of *C. minutus* from 40 localities (Fig. 1 and Appendix I). All of the samples are from the collection of the Departamento de Genética, Instituto de Biociências, Universidade Federal do Rio Grande do Sul, Porto Alegre, Brazil.

Geometric morphometrics – Each cranium was photographed in the dorsal, ventral, and left lateral views of the skull and on the left lateral side of the mandible, with a digital camera with 3.1 megapixels (2048 × 1536) of resolution, with macro function and without flash. We used 29 two-dimensional landmarks for dorsal, 30 for ventral, and 21 for lateral views of the skull, as proposed by Fernandes *et al*. (2009), and added 13 more landmarks in the lateral view of the mandible (Figure 2 and Appendix II). The anatomical landmarks were digitized by the same person (R.F.) for each specimen using TPSDig version 1.40 software (Rohlf, 2004; http://life.bio.sunysb.edu/morph). Coordinates were superimposed using a generalized Procrustes analysis (GPA) algorithm (Dryden & Mardia, 1998). GPA removes differences unrelated to shape such as scale, position, and orientation (Rohlf & Slice, 1990; Rohlf & Marcus, 1993; Bookstein, 1996a, 1996b; Adams, Rohlf & Slice, 2004). We symmetrized both sides of the landmarks in dorsal and ventral views of the skull, and only the symmetrical part of the variation was analyzed (Kent & Mardia 2001, Evin *et al*. 2008). The size of each skull was estimated using its centroid size, the square root of the sum of the squares of the distance of each landmark from the centroid (mean of all coordinates) of the configuration (Bookstein 1991). Since each skull had three separate centroid size for each view, we calculated an single value by summing the logarithms of dorsal, ventral, and lateral centroid sizes. We also used form (size plus shape) using log-transformed centroid size plus the PCs matrix of shape variables. Differences in the shape of the skull inferred from statistical analyses were visualized through multivariate regression of shape variables on discriminant axes.

Testing sex, karyotypes, and habitats as determinants of size and shape – Size difference was tested between sexes and among karyotypes with a two-way analysis of variance (ANOVA), and for multiple comparisons we used Tukey's test. Size differences between groups were visualized through box plots. To test for the multiple the factors that

might be causing shape differences we used a multivariate analysis of variance (MANOVA) of shape variables with the following independent categorical variables and their interactions: sex (males and females), chromosomal systems (North, "a", 2n = 42, and "b"; see Fig. 1), karyotypes (2n in Appendix I), populations (see Appendix I), and habitats (fields and dunes of 2n = 46a, see Fig.1 and Appendix I). When testing if different habitats result in morphological changes in the skull, to prevent effects that might be related to chromosomal polymorphisms, we compared skull shape and size only among populations with the same karyotype 2n = 46a (N = 45), which inhabit dunes (localities 24, 27, 28, and 37 in Fig. 1) and sandy fields (localities 26, 19, 22, 23, 31, 35, 65, 71 and 78 in Fig. 1). Populations were grouped to provide a minimal sample size of 5, as a function of geographical proximity reducing the 40 original populations to 20. The Bonferroni correction for multiple comparisons was applied when needed (Wright 1992).

Assessing phenotypic proximity among karyotypes – Principal components analysis (PCA) was calculated on the variance-covariance matrix of generalized least-squares superimposition residuals. The PCs were used as new shape variables, to reduce the dimensionality of the data set as well as to work on independent variables. The matrices of PCA scores for each view of the cranium were combined in one total matrix, and a subsequent matrix was used for a PCA to pool dorsal, ventral, and lateral information in the same analysis (Cordeiro-Estrela *et al*. 2006, Fernandes *et al*. 2009).

Among-group differences in shape were explored by Linear Discriminant Analysis (LDA), calculated on PCs in combination and without centroid size (Cordeiro-Estrela *et al*. 2006). We computed correct classification percentages among chromosomal populations for the skull. Due to a reduced sample size in some populations we used only 10 chromosomal populations (2n = 42, 46a, 46b, 47a, 48a, 48b, 48c, 49a, 50a, and 50b). For the mandible we did not use populations 2n = 49a and 2n = 50a because of small sample size (N = 1).

Mahalanobis distances were used to compute Neighbor-joining trees to visualize the morphological relationship among means of karyotype populations. This representation was favoured over ordination of canonical scores because it provides a distance measure over all the discriminant space whereas ordination is a projection on two or three axes among the nine (10 karyotype populations -1).

Assessing geographical variation – Geographical variation was assessed through partial least squares and by testing the adequacy of the isolation-by-distance model to our data. These two approaches have different aims and are detailed below.

The two-block partial least-squares (2B-PLS) method (Rohlf & Corti 2000) was done to find a set of variables that maximize the covariance between shape and geographical location of the populations of *C. minutus*. Although PLS is related to multivariate regression, it differs from it because it treats both sets of variables symmetrically. Instead of trying to find how shape (dependent variable) changes along geographical coordinates (independent variable), we calculate what is the maximum covariance that can be found between shape and geographical location of populations. This means that geographical distribution of populations might be a function of skull shape fitness. The 2B-PLS will provide a measure in percentage of the covariance between the two sets of variables. The significance of each new variable calculated from the 2B-PLS was assessed through permutation tests with 10,000 randomizations as recommended by Rohlf & Corti (2000).

We tested the adequacy of the isolation-by-distance model to our data. A significant result would favour genetic drift as a main force of the shaping the evolution of the skull of *C. minutus* along the coastal plain. Two different tests were calculated. First, we evaluated the correlation between two pairwise population distance matrices with the RV coefficient randomization test (RV test) (Heo & Gabriel 1997), using 10,000 random permutations. The first is a morphological distance matrix based on Mahalanobis distances, calculated from morphometric data for the skull. The second is a geographic distance matrix based on linear distances of each locality and the program Geographic Distance Matrix Generator version 1.2.3 (Ersts 2009). To test the association between skull size (centroid size) and geographical coordinates (latitude and longitude), we used Pearson's correlation.

Recently, some studies proposed the use of the divergence of heritable quantitative traits (Q_{ST}) or phenotypic data (P_{ST}) in an analogy to F_{ST} which would allow evaluation of the isolation-by-distance model using morphological data (Storz 2002, Palo *et al*. 2003, Saether *et al*. 2007). Therefore, we also tested for the correspondence between shape and geographical structure using an analog of the F_{ST} statistic for quantitative characters, namely Q_{ST} (see Storz, 2002 for the calculation of Q_{ST}). The Q_{ST} statistic was calculated on centroid size and Procrustes distances separately. We used Procrustes distances so as to

calculated pooled within and between population variances. Q_{ST} is the ratio between population variance and pooled-within population variance calculated over morphometric distances. It provides additional information apart from morphometrics distances correlation because it provides information on population differentiation. Populations can be differentiated either because they have high between population variance or because they have low pooled intrapopulation variance. This is especially useful if colonization has been recent. In this case there may have not been enough time to detect significant differentiation between population since the within population variances are expected to be small because of founder effects. We tested for the significance of the correlation between log-transformed Q_{ST} and pairwise geographic distances, in an analogy to the test based on F_{ST}. Q_{ST} values were calculated for dorsal, ventral, and lateral data sets separately, because Procrustes distances could not be computed over the pooled dataset, as each one has to be superimposed separately. Because of the small sample sizes of the mandible compared to the skull sample and because some localities were not sampled, we did not use mandibles in the 2B-PLS and Q_{ST} analysis.

For all statistical analyses and to generate the graphs, we used the "R" language and environment for statistical computing version 2.9.0 for Windows (R Development Core Team, http://www.R-project.org) and the following libraries: MASS (Venables & Ripley, 2002), ape version 1.8-2 (Paradis *et al*. 2004), stats (R Development Core Team, 2009), and ade4 (Dray & Dufour 2007). Geometric morphometrics procedures were carried out with the Rmorph package: a geometric and multivariate morphometrics library for R (Baylac 2008).

Results

Sexual dimorphism – Males and females differed significantly in both cranium and mandible size and shape. The results of the ANOVAs for centroid size were significant for skull ($F = 3.45$, *d.f.* = 1, $P < 0.001$), and for the mandible ($F = 17.3$, *d.f.* = 1, $P < 0.001$). Males were on average larger than females. Interaction between factors (sex, chromosomal systems, karyotypes, populations, and habitats) was not significant, except the interaction between sex and karyotypes, for both cranium and mandible ($P < 0.05$).

The MANOVA showed significant differences between males and females in shape for all skull views separately and pooled, as well as for the mandible ($P < 0.001$) (dorsal: $\lambda_{Wilks} = 0.62$, $F = 7.89$; ventral: $\lambda_{Wilks} = 0.61$, $F = 8.24$; lateral: $\lambda_{Wilks} = 0.67$, $F = 4.82$; three views pooled: $\lambda_{Wilks} = 0.57$, $F = 5.21$; mandible: $\lambda_{Wilks} = 0.71$, $F = 4.1$). In all tests, no significant interaction was detected among factors (sex, chromosomal systems, karyotypes, populations, and habitats). Therefore, males and females were pooled for subsequent analyses.

Chromosomal systems – The centroid size of skull differ significantly among chromosomal systems ($F = 10.26$, *d.f.* = 3, $P < 0.001$). The Tukey pairwise comparison showed significant differences in size between "a" × "b" ($P < 0.001$) and between "a" × 2n = 42 ($P < 0.05$). In both cases "a" system have smaller centroid size than the other groups. For the mandible we found no significant differences among four groups ($P > 0.05$).

The results of the MANOVAs for the chromosomal systems (North, "a", 2n = 42, and "b") were significantly different for the three skull views and the mandible ($P < 0.001$) (dorsal: $\lambda_{Wilks} = 0.14$, $F = 9.06$, *d.f.* = 3; ventral: $\lambda_{Wilks} = 0.26$, $F = 6.61$, *d.f.* = 3; lateral: $\lambda_{Wilks} = 0.102$, $F = 10.67$, *d.f.* = 3; mandible: $\lambda_{Wilks} = 0.27$, $F = 5.89$, *d.f.* = 3). Pairwise MANOVA comparisons among the four groups showed significant differences after Bonferroni correction for the three views of the skull pooled (Table 1).

Karyotypes – Size – The results of the ANOVAs for chromosomal populations showed significant differences for cranium size ($F = 3.69$, *d.f.* = 9, $P < 0.001$), but not for the mandible ($F = 1.04$, *d.f.* = 6, $P > 0.05$). The Tukey test for multiple comparisons indicated only two significant differences for skull size, between 2n = 46a × 50b, and between 2n = 48a × 50b ($P < 0.001$). All significant differences in skull size were between populations from different chromosomal systems ("a" and "b"), and none was between populations of the same chromosomal system. The box plot for skull showed centroid size variation among karyotypes (Fig. 3) and populations of the system "b" have larger skulls than "a" populations.

Karyotypes – Form (shape plus size) – The results of the MANOVAs for karyotypes indicated significant differences for all skull views and for the mandible ($P < 0.001$), (dorsal: $\lambda_{Wilks} = 0.025$, $F = 3.91$, *d.f.* = 9; ventral: $\lambda_{Wilks} = 0.031$, $F = 3.22$, *d.f.* = 9; lateral: $\lambda_{Wilks} = 0.0064$, $F = 4.19$, *d.f.* = 9; mandible: $\lambda_{Wilks} = 0.076$, $F = 3.14$, *d.f.* = 6). The percentage of correct classification using form (size plus shape) provided the highest value

(100%) for the 2n = 48b populations, for the three views of the skull and the mandible (Table 2). The lowest was for the 2n = 47a populations, for the dorsal view of the skull (Table 2). For the means, the three views of the skull pooled had the highest value (86.74%), followed by the lateral view (84.62%), and the mandible, the lowest one (65.08% in mean). Populations 2n = 47a are the hybrids from the 2n = 46a and 2n = 48a parental populations, and our results showed that hybrids were erroneously classified in either parental form. The erroneously classified individuals were assigned to either chromosomal system, irrespective of their original system.

The unrooted neighbor-joining tree of Mahalanobis distances for the dorsal view of the skull data, placed populations 2n = 48c/49a/50a and populations 2n = 50b, as the most divergent (Fig. 4). The 2n = 42 populations appeared as morphologically intermediate between the two groups. This pattern suggests that morphological skull variation is geographically structured, because the 2n = 48c/49a/50a populations are located at the northern end of the species' distribution, and the 2n = 50b population is at its southern extreme (Fig. 4).

Habitats – Fields versus dunes – The ANOVA for centroid size for the skull and the mandible showed no significant differences between individuals that inhabit fields and dunes ($P > 0.05$). However, the results of the MANOVAs showed significant differences in shape between habitats for the dorsal ($\lambda_{Wilks} = 0.52$, $F = 4.57$, *d.f.* = 1, $P < 0.001$), ventral ($\lambda_{Wilks} = 0.43$, $F = 2.55$, *d.f.* = 1, $P < 0.01$), and lateral views ($\lambda_{Wilks} = 0.49$, $F = 4.42$, *d.f.* = 1, $P < 0.001$), and for the three views of the skull pooled ($\lambda_{Wilks} = 0.34$, $F = 4.21$, *d.f.* = 1, $P < 0.001$), but not for the mandible ($P > 0.05$). The field populations had an angle of the rostrum larger than dune populations, and the rostrum was deeper in field specimens (landmarks 1 and 6 in Fig. 2c; and in lateral view of the skull in Fig. 5c). The Q_{ST} values were very low between dune and field for the dorsal ($Q_{ST} = 0.103$), ventral ($Q_{ST} = 0.275$), and lateral ($Q_{ST} = 0.019$) views of the skull.

Geographical variation – Size – We found weak but significant correlation between skull size and latitude ($r = 0.229$, $P < 0.001$), the southern populations had a larger skull than northern ones. We also found weak but significant correlations between skull size and longitude ($r = 0.22$, $P < 0.01$). For mandible size we found no significant correlation between latitude/longitude and centroid size ($P > 0.05$).

Geographical variation – Shape – The RV test showed significant correlations for the dorsal ($r = 0.358$, $P < 0.01$), ventral ($r = 0.146$, $P < 0.05$), and lateral views ($r = 0.51$, $P < 0.01$), and the three views pooled ($r = 0.326$, $P < 0.01$), as well as for the mandible ($r = 0.207$, $P < 0.05$). These results suggest an association between variation in skull shape and linear distances among the populations.

With the RV test, the "a" system populations showed significance only for the ventral ($r = 0.25$, $P < 0.05$), and lateral ($r = 0.32$, $P < 0.01$) views of the skull. The "b" chromosomal system populations showed no significant association between morphometric and geographic distances ($P > 0.05$).

In the following section, dQ_{ST}, vQ_{ST}, and lQ_{ST} are the Q_{ST} values for the dorsal, ventral, and lateral data sets of the skull respectively. Globally, both size and shape Q_{ST} showed significant but weak correlations with geographic distances. For shape, dQ_{ST} ($r = -0.15$, $P < 0.05$) and lQ_{ST} ($r = 0.24$, $P = 0.001$) were significantly correlated with distances. For size, dQ_{ST} ($r = -0.16$, $P < 0.05$), and vQ_{ST} ($r = -0.17$, $P < 0.05$) were significantly correlated with distances. The Q_{ST} calculated for ventral shape and lateral size were not significant. The global Q_{ST} values for size were $dQ_{ST} = 0.51$, $vQ_{ST} = 0.5$, and $lQ_{ST} = 0.68$. Global Q_{ST} values for shape were $dQ_{ST} = 0.41$, $vQ_{ST} = 0.4$, and $lQ_{ST} = 0.5$.

Two-block partial least-squares (2B-PLS) results indicate that 3.34%, 2.86%, and 6.01% of the total possible squared covariance between skull shape of the dorsal, ventral, and lateral views of the skull respectively is due to geography alone. The first PLS vector for the dorsal, ventral, and lateral views explained 99.3%, 99.0%, and 99.5% respectively of the total covariance between shape and geography. For the mandible, the 2B-PLS covariance was 6.47% between shape and geography, and the first PLS vector explained 99.8% of the total covariance.

The geographic variation in PLS projections showed a larger rostrum, and the auditory meatus was anteriorly dislocated in the southwestern populations compared to the northeastern ones (dorsal view in Fig. 6a). The northeastern populations had a longer pterygoid process (ventral view of the skull in Fig. 6b), and a more procumbent rostrum, and the inferior jugal process was larger than in southwestern populations (lateral view in Fig. 6c). Southwestern specimens had a jugal dislocated upwards compared to northeastern populations (Fig. 6c). For the mandible, the body appeared to be larger in southwestern populations, and the mandibular processes were larger in northeastern ones, mainly the

intersection between the mandibular body and the masseteric crest was anteriorly dislocated (landmark 11 in Fig. 2d; and Fig. 6d).

Discussion

In the present study we inspected if chromosomal rearrangments, geographic distribution and environmental heterogeneity affect skull size and shape within populations of the subterranean rodent *Ctenomys minutus*. Our findings tend to infer which factors could be playing a significant role in the intraspecific differentiation of this species. Henceforth we discuss how these factors might affect phenotypic change and enrich the picture about differentiation mechanisms of the speciose subterranean genus *Ctenomys*.

Chromosomal rearrangements and morphological variation – A high chromosomal polymorphism was found in *C. minutus* (Freitas 1995, 1997, 2006) and this variation occurs in chromosomal diploid number along the species geographical distribution. We found significant differences in skull morphology among karyotype populations. Nevertheless, Freitas (2005) postulated that there was no causal relationship between karyotype and skull morphology, and that these characters were independent in *C. minutus*. Since most of the rearrangements are chromosomal fusions and fissions, it is unlikely that these rearrangements cause any modifications in gene expression or macromutations in regulatory genes. Conversely, chromosomal inversions have been shown to alter gene expression and phenotype (Brooks *et al*. 2007).

Instead of a direct effect on phenotype, chromosomal rearrangements can cause a reduction in gene flow (White 1978). Hybrid karyotypes between populations can cause sterility, infertility or heterozygote disadvantage owing to the complex chromosomal configurations that would be produced at meiosis. The presence of these hybrids of reduced fitness would enhance genetic drift which could permit the fixation of new chromosomal rearrangements and allow reproductive isolation (total or partial) among populations (White 1978). Thus, chromosomal evolution can be an efficient mechanism of reproductive isolation (King 1987, Britton-Davidian *et al*. 2000) providing hybrids that could have, in some cases, a lower fitness than parental forms. This hypothesis, viewed in the light of the high karyotypic variation and high speciation rates in *Ctenomys*, has been used to propose that chromosomal speciation is a probable, if not the main, mechanism of

cladogenesis in this genus (Reig *et al*. 1990, Ortells & Barrantes 1994). Nevertheless, there is not enough evidence to support chromosomal speciation in *Ctenomys*. Tomasco & Lessa (2007) discussed several chromosomal speciation models and suggest that fixation of new rearrangements in *Ctenomys* may not be hampered by negative heterosis. Moreover, some works show that chromosomal polymorphism fail to cause sterility in heterozygous animals and many hybrid zones show no evidence of negative heterosis in *Ctenomys* (Freitas 1997, Gava & Freitas 2002, 2003).

Nevertheless, *C. minutus* has a chromosomal inversion in populations of the chromosomal system "b" and that does not occur in system "a". Our results for phenotypic data show a significant difference between these two karyotype systems. King (1987) reinforced the ambiguous effects of chromosomal inversions, which in some cases appear to act as an effective postmating isolation mechanism (i.e. Nevo *et al*. 1994, Taylor 2000) and in others, in balanced polymorphism, appear to have a minor role in speciation.

The analysis of phenotypic structuring of chromosomal populations suggests that the geographic structure of *C. minutus* is divided into three morphological groups, populations at the extreme north, at the extreme south, and all others associated with lakes and lagoons in the middle of the distribution (phenogram in Fig. 4). The chromosomal population 2n = 42 appears to differ from the others, but this might be an artifact of the small sample size and very low variation within this group, which could inflate *F* values and Mahalanobis distances even without large between-group variances.

Isolation by distance – Isolation by distance is a model of population genetics that is characterized by increasing genetic divergence and decreasing gene flow with increasing geographic distance (Wright 1943). The isolation by distance in molecular data is an expected result in some species of coastal subterranean *Ctenomys* such as *C. australis*, *C. talarum*, *C. pearsoni*, and *C. flamarioni*, which are restricted to nearly linear spatial distributions associated with a limited dispersal capability, in the absence of selection (Freitas 1994, Mora *et al*. 2006, Fernández-Stolz, Stolz & Freitas, 2007; Tomasco & Lessa, 2007). The same pattern of linear distribution is observed in *C. minutus*, an almost one-dimensional spatial system along the coast, which increases the chances of detecting isolation by distance (Slatkin & Barton 1989, Mora *et al*. 2006). This pattern is found in *C. talarum* (Cutrera, Lacey & Busch, 2005; Mora *et al*., 2007) and *C. pearsoni* (Tomasco & Lessa 2007) but not in *C. australis* (Mora *et al*., 2006).

We investigated if phenotypic geographic variation in *C. minutus* follows this pattern of isolation by distance, as previously detected in morphological traits in *Sorex* (Ochocinska & Taylor 2003; Yom-Tov & Yom-Tov, 2005; Polly, 2007), rodents (Pessôa & Reis 1991; Reis *et al*., 2002a, 2002b) and bats (Storz, 2002). At this time, only one study has formally evaluated the relationship between skull shape variation and geographic distances in the genus *Ctenomys* (D'Anatro & Lessa, 2006). We found a weak but significant association between morphometric and geographic distances, and our results suggest that differences among populations follow a mild pattern of isolation by distance (less than 10% of the phenotypic covariance) for the analysis using the total range of the distribution. Both the RV test, and the regression of Q_{ST} against linear distances support this weak correlation between morphological and geographic distances. This correlation persisted when tested only in the chromosomal populations within the group of chromosomal system "a" but not in "b", again indicating a phenotypic discontinuity between the groups with or without the chromosomal inversion. Thus, our data showed a discontinuity in skull shape along the spatial distribution of *C. minutus*. The weak pattern of isolation-by-distance might have at least three possible explanations. Firstly, if the phenotypic data evolves mainly neutrally, there is enough migrants to blur a isolation-by-distance signal. Second, if the evolution is not neutral, stabilizing selection might be counterbalancing differentiation forces. Finally, not enough time might have elapsed since colonization for differentiation to have occurred.

Adaptation in skull morphological change – Our results have shown that the phenotypic variation found in *C. minutus* is not totally neutral. The shape changes inferred for the geographical variation by 2B-PLS are located on biomechanically meaningful regions. Thus, the shape changes in the cranium and the mandible inferred along the southwest-northeast distribution appears to be of adaptive nature. The rostrum is more developed, as well as the zygomatic arch and the mandibular process is larger in southwestern field populations than in northeastern ones, which generally occupy sand dunes (Fig. 6). Moreover, when we compared adjacent populations to test specifically for differences related to habitats, we found a significant difference in skull shape between dune and field populations (Fig. 5). We expected that populations that inhabit fields (harder soils) would have more robust zygomatic arches, a deeper rostrum, and a more procumbent incisor angle (for pocket gophers see Lessa & Stein 1991). Mora *et al*. (2003)

found a significant relationship between the angle of incisor procumbency and the length of the diastema in *Ctenomys*. Our data indirectly showed a change in the procumbency angle in field populations that have a more procumbent incisor based on the rostrum angle and a proportionally longer diastema (lateral view in Fig. 5c). Both the larger geographic shape trends and specific tests between phenotypes of different habitats are congruent with excepted soil-shapes associations inferred from biomechanical point of view. These inferences suggest the action of diversifying selection as a source of intraspecific variation in *C. minutus*.

River channels like barriers – For tuco-tucos, watercourses are strong barriers to dispersal, because the swimming capability of *Ctenomys* seems to be very poor (Reig *et al*., 1990). Mora *et al*. (2007) suggested that the major rivers within the range of *C. talarum* appear to be associated with genetic differences. Freitas (2005) examined skull shape using traditional morphometrics in this same species and observed that the Araranguá River divides the geographic distribution of *C. minutus* and the skull form differs in populations to the north and south of the river. Likewise, our results show significant phenotypic differences of northern specimens (2n = 48c, 49a, 50a). The phenogram (Fig. 4) showed large phenotypic differentiation of these populations that can not be explained by habitat differences since they all dig tunnel in sand dunes. The most probable explanation might be that the Araranguá River (located between localities 82 and 37 in Fig. 1) acts as a barrier to gene flow between the extreme northern specimens and the other populations.

The morphological division in chromosomal systems “a” and “b” does not correspond to a presently existing physical barrier. However, in the past, during the Quaternary Period the coastal plain contained innumerable rivers channels prior to the transgressive events that dissected the present coastal zone in southern Brazil. These paleochannels dried during the last transgressive post-glacial event in the Pleistocene (Weschenfelder, 2005). One of these paleochannels was located nearly at the present 2n = 42 populations (locality 38 in the map in Fig. 1), exactly where we found a division in skull morphology and chromosomal hybrid zones. Moreover, another paleochannel was found in the Bojuru region (near locality number 5 on the map in Fig. 1), the Barra Falsa channel. This channel was located just at the present chromosomal hybrid zone, the 2n = 47b populations (Fig. 1). This paleochannel was closed during the last marine transgression

event, about 5,000 years ago (Weschenfelder *et al*., 2008). Furthermore, Marinho & Freitas (2000) examined skull shape in *C. minutus* and suggest that morphological variation could be explained by historical factors such as populations separated by ancient geographic barriers which no longer exist today. Moreover, Gava & Freitas (2002) suggest that the actual pattern of chromosomal distribution of populations of *C. minutus* may resulted by geographic barriers in the past. Therefore, the observed morphological differentiation may be due to the presence of geographical barriers, followed by subsequent chromosomal differentiation and not necessarily by chromosomal inversion.

Thus, the divisions in chromosomal systems could be a result of combination of historical factors (paleochannels), followed by chromosomal evolution. Subsequently, the restored contact zone might have generated hybrids (Marinho & Freitas, 2000; Gava & Freitas, 2002). The morphological differentiation in the northern extreme of the distribution of *C. minutus* could be explained by isolation by a physical barrier, the Araranguá River (Freitas, 2005). The hybrid forms indicate the existence of gene flow, and physical barriers may have had more influence than the chromosomal rearrangements in reducing the gene flow. The physical barrier hypothesis is reinforced by the more-diverse phenotypes in the extreme north and south of the distribution than in the central part (phenogram in Fig. 4).Therefore, our data suggest that both chromosomal polymorphism and skull morphological variation were structured by geographic barriers, and the discrimination by locality and chromosome population are not completely independent.

Modes of raciation – Sympatric speciation via resource specialization or any other mechanism is extremely unlikely for subterranean rodents, as well as parapatric speciation (Steinberg & Patton 2000). Thus, they undergone one of the several types of allopatric divergence, such as peripheral isolation (Steinberg & Patton, 2000). Therefore, we suggest that *C. minutus* follows an allopatric raciation model with *a posteriori* chromosomal differentiation and independent skull morphological evolution in heterogeneous habitats. Moreover, Gava & Freitas (2002) suggested that data from protein analysis and geological evolution of south coastal plain of Brazil are compatible with the hypothesis of divergence in allopatry in *C. minutus*.

In conclusion, our data lead us to suggest that the evolution of skull shape in *C. minutus* followed weakly an isolation-by-distance model that was shaped by selection and historical factors (geological evolution of the coastal plain, including river formation and

paleochannels). Intrinsic factors such as robertsonian chromosomal rearrangements seem to have played a minor role in the evolution of the shape of the skull and mandible of *C. minutus*. The role of the chromosomal inversion as a barrier to gene flow will have to be tested using neutral molecular markers (Lopes *et al*. in press).

Figure Legends

Figure 1. Map of the coastal plain of southern Brazil showing the sample localities of *Ctenomys minutus*, with indication of karyotypes (diploid number) and schematic view of chromosomal rearrangements in the boxes.

Figure 2. Landmark locations on the skull of *Ctenomys* for dorsal (a), ventral (b), and lateral (c) views of the cranium and lateral view of the mandible (d).

Figure 3. Box plot showing variability of centroid size among chromosomal population groups of *Ctenomys minutus* for the sum of logarithms transformed centroid size for dorsal, ventral and lateral views of the skull, ordered from north (50a) to south (50b). The horizontal line represents the mean, box margins are at the 25th and 75th percentiles, bars extend to the 5th and 95th percentiles, and circles are outliers.

Figure 4. Neighbor-joining tree of Mahalanobis distances among chromosomal populations of *Ctenomys minutus*, for three views of the skull pooled using form data (size plus shape).

Figure 5. Skull shape differences for *Ctenomys minutus* for dorsal, ventral, and lateral views of the skull for different habitats, dune (dotted lines) and field (solid lines). Mandible is not significant for habitat (see the text for more details).

Figure 6. Skull shape differences for *Ctenomys minutus* for dorsal, ventral, and lateral views of the cranium, and for lateral view of the mandible for northeast and southwest differences. Northeastern populations (dotted lines) and southwestern populations (solid lines).

Tables

Table 1 - Pairwise MANOVA results among four groups of populations (North = extreme northern populations with 2n = 48c, 49a, 50a; A = chromosomal system "a"; B = chromosomal system "b"; and 2n = 42 populations) of *C. minutus* for cranial shape (results for dorsal, ventral, and lateral skull views pooled).

Comparison	λ_{Wilks}	*d.f.*	*F*	*P*
A × B	0.281	1	12.868	1.32×10^{-15}**
A × North	0.428	1	9.55	1.32×10^{-15}**
A × 2n = 42	0.366	1	6.443	1.08×10^{-13}**
B × North	0.121	1	15.701	4.02×10^{-12}**
B × 2n = 42	0.461	1	4.468	0.00018**
North × 2n = 42	0.154	1	12.645	7.73×10^{-7}**

*$P < 0.05$; **$P < 0.01$; after Bonferroni correction.

Table 2 - Percentage of correct classification from Linear Discriminant Analysis (LDA) for chromosomal populations of *C. minutus* for dorsal, ventral, lateral, and three views of the skull pooled, and mandible using form (size plus shape). Karyotype populations arranged from north (2n = 50a) to south (2n = 50b).

	50a	49a	48c	46a	47a	48a	42	46b	48b	50b
Dorsal	83.3	100	100	75.4	25	79	71.4	71.4	100	100
Ventral	66.6	66.6	85.7	77.1	37.5	74.4	71.4	92.8	100	100
Lateral	100	66.6	100	80.7	62.5	72	85.7	85.7	100	92.8
3 views	83.3	100	100	78.9	62.5	79	85.7	78.5	100	100
Mandible	-	-	100	52.6	20	60	100	85.7	66.6	85.7

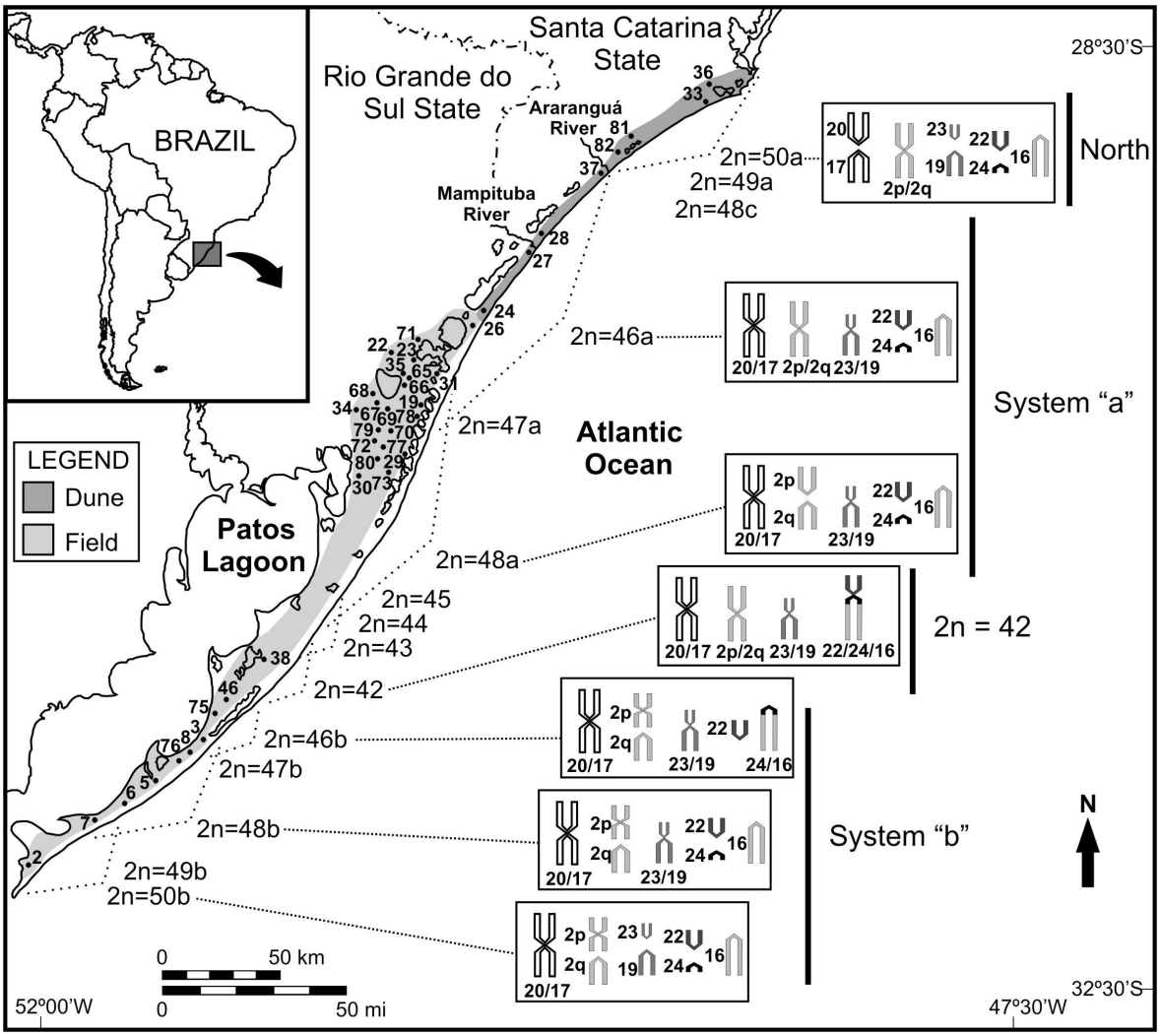

Figure 1. Map of the coastal plain of southern Brazil showing the sample localities of *Ctenomys minutus*, with indication of karyotypes (diploid number) and schematic view of chromosomal rearrangements in the boxes.

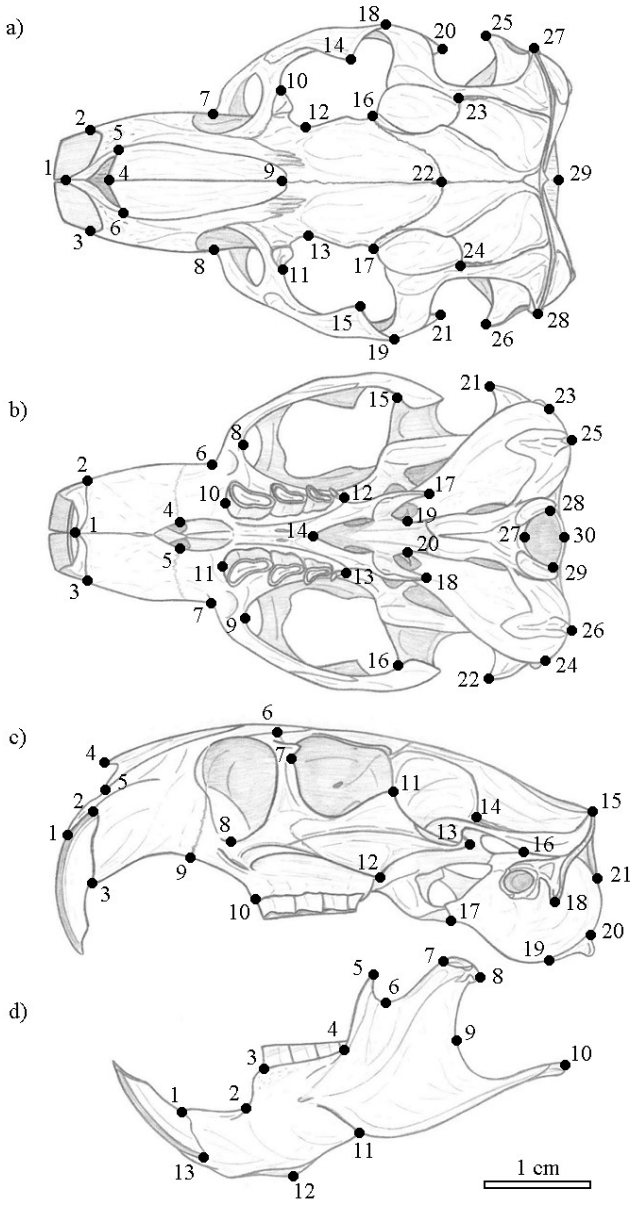

Figure 2. Landmark locations on the skull of *Ctenomys* for dorsal (a), ventral (b), and lateral (c) views of the cranium and lateral view of the mandible (d).

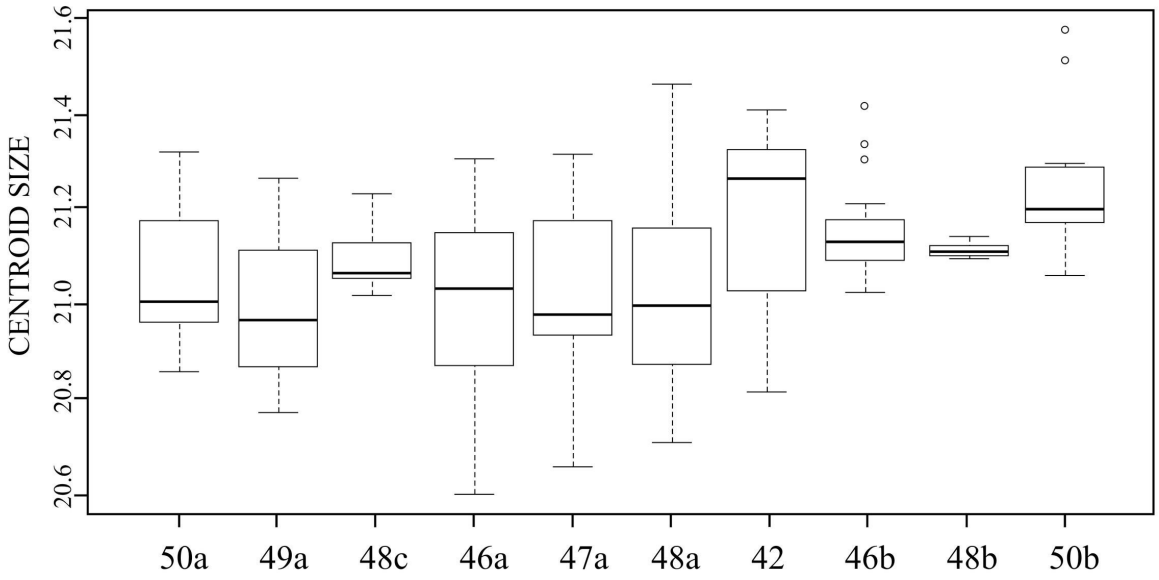

Figure 3. Box plot showing variability of centroid size among chromosomal population groups of *Ctenomys minutus* for the sum of logarithms transformed centroid size for dorsal, ventral and lateral views of the skull, ordered from north (50a) to south (50b). The horizontal line represents the mean, box margins are at the 25th and 75th percentiles, bars extend to the 5th and 95th percentiles, and circles are outliers.

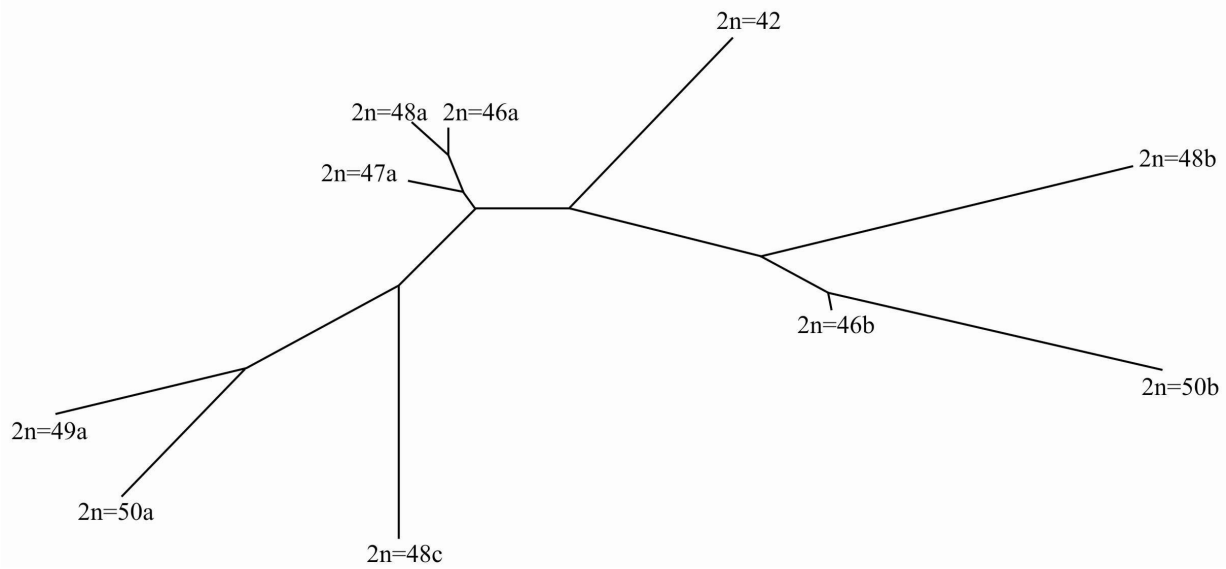

Figure 4. Neighbor-joining tree of Mahalanobis distances among chromosomal populations of *Ctenomys minutus*, for three views of the skull pooled using form data (size plus shape).

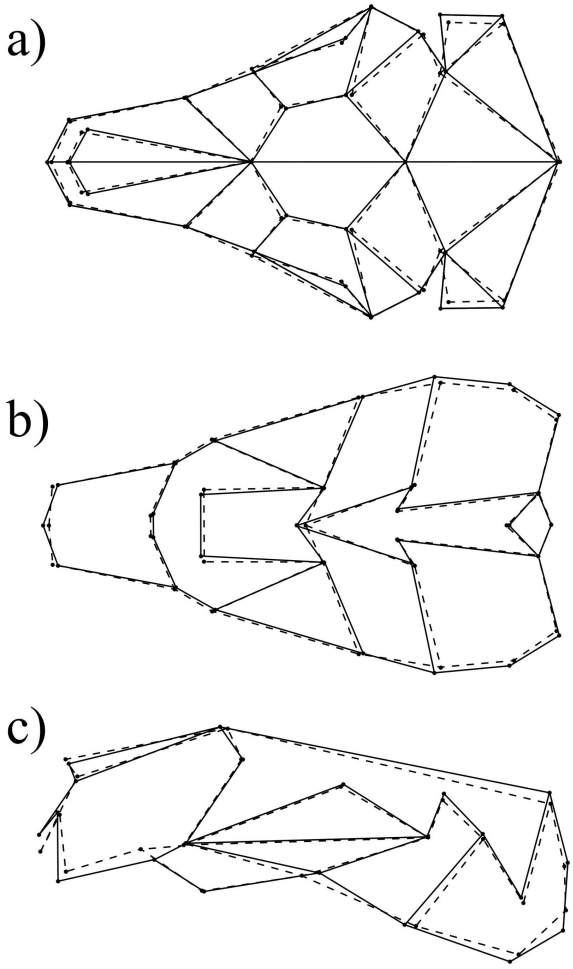

Figure 5. Skull shape differences for *Ctenomys minutus* for dorsal, ventral, and lateral views of the skull for different habitats, dune (dotted lines) and field (solid lines). Mandible is not significant for habitat (see the text for more details).

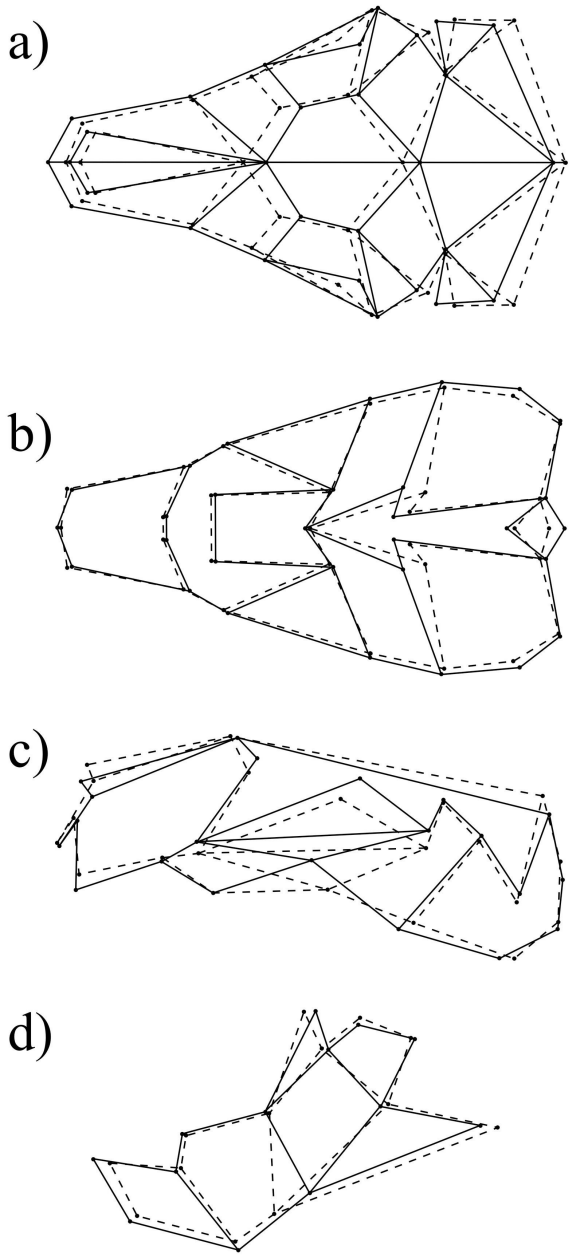

Figure 6. Skull shape differences for *Ctenomys minutus* for dorsal, ventral, and lateral views of the cranium, and for lateral view of the mandible for northeast and southwest differences. Northeastern populations (dotted lines) and southwestern populations (solid lines).

Appendix I

Specimens of *Ctenomys minutus* examined. N-S = order number from north to south; Nº Loc = Locality number on the map (Fig. 1); Pop = population number; 2n = chromosomal diploid number; N_{SKULL} = sample size of skulls; $N_{MANDIBLE}$ = sample size of mandibles; Habitat = dune or field.

N-S	Locality	Nº Loc	Pop	2n	N_{SKULL}	$N_{MANDIBLE}$	Habitat
1	Jaguaruna (Beach)	36	1	50a	4	-	Dune
2	Jaguaruna (Field)	33	1	49a/50a	9	6	Dune
3	Esteves Lake	81	2	48c	3	2	Dune
4	Ilhas	82	2	48c	3	3	Dune
5	Morro dos Conventos	37	3	46a	6	5	Dune
6	Passo de Torres	28	4	46a	3	2	Dune
7	Torres	27	4	46a	3	2	Dune
8	Praia do Barco	24	5	46a	3	-	Dune
9	Capão Novo	26	5	46a	3	-	Field
10	Traíras Lake	23	6	46a	3	-	Field
11	Caiera Lake	22	6	46a	2	-	Field
12	Osório-Capivarí 1	65	6	46a	5	-	Field
13	Barros Lake	35	7	46a/47a/48a	8	7	Field
14	Osório-Capivarí 2	66	8	47a/48a	6	-	Field
15	Weber Ranch	71	8	46a	4	-	Field
16	Emboaba Lake	19	9	46a	5	-	Field
17	Osório	31	10	46a	12	4	Field
18	West Barros Lake	69	11	48a	6	-	Field
19	South Barros Lake 1	67	12	48a	10	2	Field
20	Passinhos	34	13	48a	4	4	Field
21	Passo do Paulo	79	13	48a	1	1	Field
22	Estância Velha	70	13	46a	3	-	Field
23	Pitangueira	72	14	46a/48a	6	3	Field
24	East Manuel Nunes Lake	78	14	46a	2	1	Field
25	Rincão da Fortaleza	77	14	46a/48a	3	3	Field
26	Fortaleza Lake 2	80	15	46a/47a/48a	5	4	Field
27	Suzana Lake	73	15	46a/47a	4	4	Field
28	Fortaleza Lake 1	29	15	47a/48a	17	13	Field
29	Palmares do Sul	30	16	48a	9	7	Field
30	South Barros Lake 2	68	16	48a	4	-	Field
31	Mostardas	38	17	42	10	5	Field
32	South Mostardas	46	18	42/43/44/45	6	6	Field
33	Tavares-Bojuru 1	75	19	46b	4	4	Field
34	Tavares 1	3	19	46b	12	12	Field
35	Tavares 2	8	19	46b	2	2	Field
36	Tavares-Bojuru 2	76	19	46b	1	1	Field
37	Bojuru	5	19	48b	3	3	Field
38	South Bojuru 1	6	20	49b/50b	1	1	Field
39	South Bojuru 2	7	20	50b	1	1	Field
40	São José do Norte	2	20	50b	14	14	Field
					210	122	

Appendix II

Definition of landmarks with numbers and locations for each view of the cranium and lower jaw of *Ctenomys minutus* (represented in Figure 2).

Dorsal view of the cranium: 1. anterior tip of the suture between premaxillas; 2-3. anterolateral extremity of incisor alveolus; 4. anterior extremity of the suture between nasals; 5-6. anteriormost point of the suture between nasal and premaxilla; 7-8. anteriormost point of the root of zygomatic arch; 9. suture between nasals and frontals; 10-11. anterolateral extremity of lacrimal bone; 12-13. point of least width between frontals; 14-15. tip of extremity of superior jugal process; 16-17. anterolateral extremity of suture between frontal and squamosal; 18-19. lateral extremity of suture between jugal and squamosal; 20-21. tip of posterior process of jugal; 22. suture between frontals and parietals; 23-24. anterolateral extremity of suture between parietal and squamosal; 25-26. anterior tip of external auditory meatus; 27-28. point of maximum curvature on mastoid apophysis; 29. posteriormost point of occipital along the midsagittal plane.

Ventral view of the cranium: 1. anterior tip of suture between premaxillas; 2-3. anterolateral extremity of incisor alveolus; 4-5. lateral edge of incisive foramen in suture between premaxilla and maxilla; 6-7. anteriormost point of root of zygomatic arch; 8-9. anteriormost point of orbit in inferior zygomatic root;10-11. anteriormost point of premolar alveolus; 12-13. posterior extremity of III molar alveolus; 14. posterior extremity of suture between palatines; 15-16. anteriormost point of intersection between jugal and squamosal; 17-18. posteriormost point of pterygoid; 19-20. anterior extremity of tympanic bulla; 21-22. anterior tip of external auditory meatus; 23-24. posterior extremity of mastoid apophysis; 25-26. posterior extremity of paraoccipital apophysis; 27. anteriormost point of foramen magnum; 28-29. posterior extremity of occipital condyle in foramen magnum; 30. posteriormost point of foramen magnum along midsagittal plane.

Lateral view of the cranium: 1. anteriormost point of premaxilla; 2. posteriormost point of incisor alveolus; 3. inferiormost point of incisor alveolus; 4. anterior tip of nasal; 5. anteriormost point of the suture between nasal and premaxilla; 6. suture between premaxilla, maxilla and frontal in superior zygomatic root; 7. inferiormost point of suture between lacrimal and maxilla; 8. inferiormost point of infraorbital foramen in inferior zygomatic root; 9. inferiormost point of suture between premaxilla and maxilla; 10. anteriormost point of premolar alveolus; 11. extremity of superior jugal process; 12. extremity of inferior jugal process; 13. tip of posterior jugal process; 14. medial point of suture between parietal and squamosal; 15. superior extremity of lambdoidal crest; 16. posterior extremity of postglenoid fossa; 17. inferior extremety in suture between pterygoid and tympanic bulla; 18. inferior extremity of mastoid apophysis; 19. anteriormost margin of paraoccipital apophysis; 20. posteriormost margin of paraoccipital apophysis; 21. posterior extremity of intersection between occipital and tympanic bulla.

Lateral view of the mandible: 1. upper extreme anterior border of incisor alveolus; 2. extreme of the diastema invagination; 3. anterior edge of the premolar alveolus; 4. intersection between molar alveolus and coronoid process; 5. tip of the coronoid process; 6. maximum of curvature between the coronoid and condylar processes; 7. anterior edge of the articular surface of the condylar process; 8. tip of the postcondyloid process; 9. maximum curvature between condylar and angular processes; 10. tip of the angular process; 11. intersection between mandibular body and masseteric crest; 12. posterior extremity of the mandibular symphysis; 13. posterior extremity border of incisor alveolus.

Capítulo V

Manuscrito em preparação

A variable and functionally constrained structure: skull shape in *Ctenomys lami* (Rodentia: Ctenomyidae)

Rodrigo Fornel[1,2], Pedro Cordeiro-Estrela[1,2], Michel Baylac[3], Daniela Sanfelice[4] and Thales Renato O de Freitas[1,2]

[1]Programa de Pós-Graduação em Genética e Biologia Molecular – Universidade Federal do Rio Grande do Sul, Av. Bento Gonçalves 9500, CEP 91501-970, Porto Alegre, RS, Brazil.
[2]Departamento de Genética, Instituto de Biociências, Universidade Federal do Rio Grande do Sul, Av. Bento Gonçalves 9500, CEP 91501-970, Porto Alegre, RS, Brazil.
[3]Entomologie, CNRS UMR 7502 and UMS 2700 Plate-forme Morphométrie, Départment Systématique et évolution, Muséum National d'Histoire Naturelle, 45 rue Buffon, F-75005 Paris, France.
[4]Museu de Ciências Naturais, Fundação Zoobotânica do Rio Grande do Sul, Av. Salvador França, 1427, CEP 90690-000, Porto Alegre, RS, Brazil.

Email addresses:

RF: rodrigofornel@hotmail.com
PCE: pedroestrela@yahoo.com
MB: baylac@mnhn.fr
DS: daniela.sanfelice@fzb.re.gov.br
TROF: thales.freitas@ufrgs.br

Running Title: Skull shape variation in *Ctenomys lami*

Keywords: chromosomal polymorphism, cranium, genetic drift, geometric morphometrics, natural selection.

Abstract

Ctenomys lami is a subterranean rodent that occurs in a narrow strip of fossil sand dunes on the coastal plain of southern Brazil. This species shows high karyotypic variation, with diploid numbers ranging from 2n = 54 to 2n = 58. Based on different chromosome rearrangement frequencies along its geographical distribution, four population blocks were previously proposed (A, B, C and D). In this study, we explored dorsal, ventral and lateral views of the skull related to shape and size variation for sex, population blocks, karyotypes, and chromosome rearrangements, using geometric morphometrics. Our results showed significant differences in skull shape for all factors tested, and there was no correlation between morphological and geographical distances. Moreover, we found drift, diversifying and stabilizing selection acting on variation in skull shape in four chromosomal population blocks. Diversifying patterns involve structures related to digging, compatible with biomechanical models proposed for *Ctenomys*. Stabilizing patterns involve a compromise in the proportions of the auditory bulla, between hearing ability and the mandibular opening. Our findings suggested that a combination of drift and selection (diversifying and stabilizing) is acting on skull shape. We do not found an positive association between chromosomal diploid number and skull morphology.

Introduction

The phenotypic evolution of subterranean organisms has fascinated evolutionary biologists because the invasion of the underground habitat led to changes at the morphological, ethological, ecological and molecular levels (Lacey *et al*. 2000, Lessa *et al*. 2008). In the speciose mammalian order Rodentia, the independent acquisition of an underground mode of life has occurred at different taxonomic levels. Predominantly fossorial taxa are found in the families Bathyergidae, Geomyidae, Muridae, Ctenomyidae, and Octodontidae, and in the subfamilies Arvicolinae, Myospalacinae, Rhizomyinae, Spalacinae, and Sigmodontinae (Nevo & Reig 1990, Lacey *et al*. 2000, Bezerra *et al*. 2007). The taxonomic diversity of subterranean taxa has provided an opportunity for evolutionary biologists to study the diversity of adaptations (Stein 2000) and evolutionary constraints (Lessa 1990, Lessa & Stein 1992, Cook *et al*. 2000, Nevo *et al*. 2000, Lessa *et al*. 2008) arising in underground habitats.

One striking observation about underground adaptations is that they seem to emerge very rapidly (Cook *et al*. 2000). The absence of transitional forms seems to indicate that once the basic structural adaptations have been acquired, they are maintained by stabilizing selection or by developmental constraints acquired during the adaptation process.

Therefore, the maintenance by constant selection of phenotypic characters at their optima for underground life activities or the inability to revert to the above ground habitat may explain the morphological similarity within the speciose subterranean genus *Ctenomys*. Few studies have, however, paid attention to the degree of variation of complex integrated morphological structures at the infra-specific levels in subterranean or fossorial taxa (but see D'Anatro & Lessa 2006). The importance of such an assessment is crucial to determine how microevolutionary processes act on hypothetically functionally constrained structures (Martins & Hansen 1997, Simons 2002).

In the subterranean genus *Ctenomys,* which is the model of our study, skull shape can be viewed as an integrated tool for excavation (Mora *et al*. 2003, Lessa *et al*. 2008). Traditional morphometric analyses at the genus level have shown little variation in cranial characters, with the noteworthy exception of the angle of incisor procumbency, which permits variable attack angles for chisel-tooth digging (Mora *et al*. 2003). By contrast, the

application of geometric morphometrics methods (Bookstein 1991, Dryden & Mardia 1998, Monteiro & Reis 1999) has revealed an unexpected variation in skull shape at the within and among species levels in *Ctenomys* (D'Anatro & Lessa 2006, Fernandes *et al*. 2009a). These observations raise many evolutionary questions about phenotypic evolution (Arnold *et al*. 2008), especially if the phenotypic variance/covariance matrix can be viewed as a rough surrogate of the genetic variance/covariance matrix (G-matrix).

In the present study, we analyzed through geometric morphometrics methods, the patterns of variation in skull shape and size of *Ctenomys lami*, a member of the speciose genus *Ctenomys*. The tuco-tucos, as they are commonly known, with their 60 species (Reig *et al*. 1990, Nowak & Paradiso 1991, Woods 1993, Wilson & Reeder 2005) and their Lower Pliocene origin are acknowledged as an example of explosive radiation (Verzi 2008). This rapid diversification within different South American biomes has been imputed to chromosomal modes of speciation because of their considerable karyotypic diversity, both inter- and intra-specifically, with diploid numbers ranging from 2n = 10 to 2n = 70 (Reig & Kiblisky 1969, Kiblisky *et al*. 1977, Reig *et al*. 1990, Freitas & Lessa 1984, Massarini *et al*. 1991, Freitas 1997, 2001, Slamovits *et al*. 2001). In fact, their patchy distribution and solitary mode of life (with the exception of *C. sociabilis*) would favor the fixation of chromosomal rearrangements acting as post-zygotic barriers to gene flow. This genus is among the most speciose mammalian genera, with probably the highest rate of chromosomal evolution among mammals (Cook & Lessa 1998, Lessa & Cook 1998, Mascheretti *et al*. 2000).

In *C. lami*, these common characteristics of tuco-tucos have evolved to an extreme: this species shows the widest chromosomal variability within the smallest geographic distribution (Freitas 2007). It is found endemically in a region of sandy soils of approximately 940 km^2 (El Jundi & Freitas 2004) surrounded by marshes and lakes, known as the Coxilha das Lombas, on the coastal plain of Rio Grande do Sul state in southern Brazil (Figure 1).

Seven different diploid numbers have been described for this species, 2n = 54, 55a, 55b, 56a, 56b, 57 and 58, involving the fission/fusion of chromosomes 1 and/or 2 (Freitas 1995b, 2001, 2006, 2007) (Figure 2). As expected under a model of chromosomal speciation, karyotypes are not randomly distributed in space. Freitas (2007) divided the species into four population blocks based on the spatial distribution of its karyotypes in the

Coxilha das Lombas: block A with 2n = 54, 55a and 56a; block B with 2n = 57 and 58; block C with 2n = 54 and 55a; and block D with 2n = 55b and 56b (Figure 1). We preserve the term population block in this article essentially for historical reasons (Freitas 2007); however the term metapopulation might be more accurate, because each sampling site is a population (Figure 1) and the blocks represent a group of populations separated by chromosomal rearrangements that limit gene flow. Gene flow between blocks can be quantified by the presence of hybrids between blocks. Freitas (2007) found one hybrid form between blocks A and B (2n = 57 results from 2n = 56a × 2n = 58) and five between blocks C and D (2n = 55b results from 2n = 54 × 2n = 56b), but none between blocks B and C. However, Moreira *et al*. (1991) using protein polymorphisms in *C. lami*, did not find four population blocks, but two large groups instead. The first group is formed by populations of blocks A and B, and the second by blocks C and D. These two large groups are separated by a natural barrier, the connection between two swamps in the middle of the range of *C. lami* (see the map in Figure 1).

The main objective of our study was to quantify shape and size variation in the skull of *Ctenomys lami*, and to relate these findings to generalizations on phenotypic evolution. We used comparisons of within and among patterns of phenotypic covariance matrices (P-matrix) (Ackermann & Cheverud 2002, Marroig & Cheverud 2004, Harmon & Gibson 2006) as surrogates of matrix of genetic variances and covariances (G-matrix) (Marroig & Cheverud 2004, Arnold *et al*. 2008). Our study is important because it addresses these questions at a microevolutionary scale. In a first step, we tested for significant differences in the size and shape of skulls of *C. lami* between sexes, among population blocks, and chromosomal populations, and related them to homozygotes and heterozygotes for the different rearrangements of chromosome pairs 1 and 2 (# 1 and # 2 respectively). In a second step, we tested whether these differences can be imputed to selection, drift, or both. We can expect to find a small phenotypic variability due to i) functionally integrated characters possibly under strong stabilizing selection, as attested by small variation between populations; and ii) a supposed homogeneous adaptive landscape (homogeneity of habitat). On the other hand, sources of divergence might arise from strong drift due to small population size (as attested by the restricted geographic range and low densities) acting on chromosomal blocks, on either side of the connection of the two swamps, which constitutes another barrier to gene flow.

Material and Methods

Sample – We examined 89 specimens of *C. lami*. All of them were adults according to definitions by El Jundi and Freitas (2004). The sample used in this study is deposited in the collection of the Laboratório de Citogenética e Evolução of the Departamento de Genética, Instituto de Biociências, Universidade Federal do Rio Grande do Sul, Porto Alegre, Brazil. The sex and karyotype of the individuals used in this study were known and were collected at the sites shown in Figure 1. The specimens examined are listed in Appendix I.

Geometric Morphometrics – Each cranium was photographed in dorsal, ventral, and lateral views with a digital camera at 3.1 Megapixels of resolution (2048 × 1536). We used the same landmarks proposed by Fernandes *et al*. (2009a) for *C. torquatus* and *C. pearsoni* congeneric species, which defined 29, 30, and 21 two-dimensional morphological landmarks for dorsal, ventral, and lateral views of the skull respectively (see Figure 3 for landmark location and Appendix II for description). The coordinates of each landmark were obtained using TPSDig 1.40 software (Rohlf 2004). Coordinates were superimposed using a generalized Procrustes analysis (GPA) algorithm (Dryden & Mardia 1998). GPA removes differences unrelated to shape, such as scale, position, and orientation (Rohlf & Slice 1990, Rohlf & Marcus 1993, Bookstein 1996a, 1996b, Adams *et al*. 2004). We symmetrized both sides of the landmarks in dorsal and ventral views of the skull, and only the symmetrical part of the variation was analyzed (Kent & Mardia 2001, Klingenberg *et al*. 2002). The size of each skull was estimated using its centroid size, the square root of the sum of the squares of the distances of each landmark from the centroid (Bookstein 1991).

Statistical Analysis – Size difference was tested between sexes, population blocks, and karyotypes with an analysis of variance (ANOVA). Size differences between groups were visualized through box plots. Shape differences between sexes, blocks, and karyotypes, as well as their interactions, were tested through multivariate analysis of variance (MANOVA). The Bonferroni correction for multiple comparisons was applied (Wright 1992). To test for significant shape differences induced by rearrangements of chromosomal pairs 1 and 2, separate MANOVAs were used. In these two designs, the categories compared were metacentric homozygotes, acrocentric homozygotes, and

heterozygotes. Because sample sizes were relatively small, pairwise differences between mean shapes of blocks were assessed through resampling tests with and without permutation. In the first case, the permutation is carried out without replacement from the pooled samples; and in the second case; a bootstrap resampling is carried out within each group. Three statistics were computed which make different assumptions about the distribution and properties of covariance matrices: (1) Hotelling's T^2, assuming normality and equal covariance matrices; (2) James' J, assuming normality and unequal covariance matrices; and (3) Lambda, based on the asymptotic Chi-square distribution, assuming large population sizes (Amaral *et al*. 2007).

Principal components analysis (PCA) was carried out using the variance-covariance matrix of generalized least-squares superimposition residuals. PCs of the covariance matrix of superimposition residuals were used as new shape variables, to reduce the dimensionality of the data set as well as to work on independent variables. The matrices of PCA scores for each view of the cranium were combined in one total matrix, and a subsequent matrix was used for a PCA to pool dorsal, ventral, and lateral information in the same analysis (Cordeiro-Estrela *et al*. 2006, Fernandes *et al*. 2009a).

To choose the number of PCs to be included in the linear discriminant analysis (LDA), we computed correct classification percentages with each combination of PCs (Baylac & Friess 2005). We selected the subset of PCs giving the highest overall correct classification percentage. We used a leave-one-out cross-validation procedure that allows an unbiased estimate of classification percentages (Ripley 1996, Baylac & Friess 2005). Cross-validation is used to evaluate the performance of classification by LDA. Mahalanobis distances were used to compute neighbor-joining trees to visualize the morphological relationships among population blocks and among chromosomal populations. The visualization of shape differences for the three views of the skull was obtained through multivariate regression of shape variables on principal component axes. The karyotype 2n = 54 occurs in block A and C, so we termed it 2n = 54 (A) and 2n = 54 (C) populations respectively, to test for differences between them.

Geographical Variation – We calculated Mahalanobis distance (D^2) for morphometric data from the skull among karyotypes and estimated for each population. We used Mantel's test (Mantel 1967) using 10,000 random permutations and the

randomization test (RVtest) using 10,000 random permutation (Heo & Gabriel 1997) to evaluate the correlation between morphometric and geographical distance matrices.

Selection / Drift Test – To infer processes acting on shape differences, we used the procedure described by Marroig and Cheverud (2004) (but see also Ackermann & Cheverud 2002, Harmon & Gibson 2006) which tests for the proportionality and the correlations between principal directions of the covariance matrices within and among groups.

This is a two-step test, which first compares the variances, then contrasts the principal directions of the Within and the Between group covariance matrices. In the first step, the logged eigenvalues of the Within-pooled covariance matrix (**Wp**) are regressed against the logged variances of the projections of the Between-group matrix (**B**) onto the **Wp** PCs (here termed **BWp**). Under a drift model of multivariate phenotypic evolution (Lande 1976), a proportionality of these pairs of matrices is expected, whereas departure from proportionality would indicate the potential action of selection. In the second step, we tested for the correlation between the n-1 (where n corresponds to the number of groups) **BWp** projections values using the Bartlett's test for sphericity. The PCs of **Wp** are independent by construction, and under drift the **BWp** should equally be independent. Any significant correlation within **BWp** would be indicative of a correlational selection (selection of a covariance pattern, a shape change in this case). The selection/drift test was calculated for chromosomal population blocks. Although we acknowledge that this test was designed for interspecies data, i.e. in the absence of gene flow, continuous field work has shown that the gene flow among blocks is small. Due to the low number of degrees of freedom, equal to the group number minus one (i.e. equal to three of the four population blocks), the power of the correlation and sphericity tests will be dramatically reduced. We therefore set the alpha level to 0.1 and following Arnold *et al*. (2008) rejected the null hypothesis (drift) only if both steps led to rejection. The unexpectedly large morphological diversity that was found (see results) clearly helped us to interpret our results.

The statistical analyses and graphs used the "R" language and environment for statistical computing version 2.2.1 for Linux (R Development Core Team, http://www.R-project.org) and the following libraries: MASS (Venables & Ripley 2002), APE version 1.8-2 (Paradis *et al*. 2006) and Shapes (Dryden 2007). Geometric morphometrics

procedures and the drift test were carried out with the Rmorph package: a geometric and multivariate morphometrics library for R (Baylac 2008).

Results

Size – We found highly significant differences in centroid size related to sexual dimorphism for dorsal ($F = 153.5$, *d.f.* = 1, $P < 0.001$), ventral ($F = 125.5$, *d.f.* = 1, $P < 0.001$), and lateral ($F = 151.1$, *d.f.* = 1, $P < 0.001$) views of the skull; males were on average larger than females in all population blocks (Figure 4). The F tests in the ANOVAs for population block, karyotypes, and chromosome pairs 1 and 2 were not significant for centroid size ($P > 0.05$).

Shape – Sexual Dimorphism – Tests for shape differences (MANOVA) indicated significant sexual dimorphism for three views of the skull. The MANOVA results for skull shape were significant for dorsal (Wilks'$\lambda = 0.31$, $F = 7.5$, $P < 0.001$), ventral (Wilks'$\lambda = 0.36$, $F = 12.4$, $P < 0.001$), and lateral (Wilks'$\lambda = 0.22$, $F = 7.8$, $P < 0.001$), and for the three views pooled (Wilks'$\lambda = 0.31$, $F = 6.7$, $P < 0.001$). MANOVA interactions among sex, population blocks, karyotypes, and chromosomal rearrangements (# 1 and # 2) were not significant for skull shape ($P > 0.05$).

Shape – Two Population Blocks – For the two large groups AB and CD, separated by the intervening swamps, we found significant shape differences in the three views of the skull and in the pooled analysis (MANOVA: dorsal: Wilks'$\lambda = 0.45$, $F = 3.84$, $P < 0.001$; ventral: Wilks'$\lambda = 0.44$, $F = 7.8$, $P < 0.001$; lateral: Wilks'$\lambda = 0.55$, $F = 5.2$, $P < 0.001$; pooled: Wilks'$\lambda = 0.52$, $F = 3.8$, $P < 0.001$). The dorsal view of the skull showed the highest percentage of correct classification for two blocks (89.65%), and the lateral view showed the lowest (82.05%).

Shape – Four Population Blocks – Significant differences in skull shape were also found among the four population blocks for the three views and the pooled analysis (MANOVA: dorsal: Wilks'$\lambda = 0.21$, $F = 4.17$, $P < 0.001$; ventral: Wilks'$\lambda = 0.13$, $F = 3.82$, $P < 0.001$; lateral: Wilks'$\lambda = 0.28$, $F = 2.43$, $P < 0.001$; pooled: Wilks'$\lambda = 0.28$, $F = 2.43$, $P < 0.001$). Pairwise MANOVA comparisons revealed significant differences between all blocks (Table 1). The F value was higher for the A × D comparison (the extremes of distribution), and the F value was lower for the C × D blocks (Table 1). The

smallest percentage of correct classification was for the ventral view of the skull (75.8%), and the highest percentage was for the dorsal view (85.7%). The population block that showed the smallest percentage of correct classification was block C (76.3%), and block D showed the highest (87.0%). The permutation test among the four population blocks indicated statistically significant differences for skull shape (Table 2).

Morphological distances among four population blocks gave distinct topologies for the different views of the skull. Mahalanobis distances were larger between A and B blocks for the dorsal and three views of the skull integrated. For the ventral and lateral views, the larger distances blocks were between A and C (Figure 5).

Shape – Karyotypes – MANOVA results indicated significant differences in skull shape for dorsal (Wilks'$\lambda = 0.18$, $F = 2.78$, $P < 0.001$), ventral (Wilks'$\lambda = 0.2$, $F = 2.32$, $P < 0.001$), lateral (Wilks'$\lambda = 0.05$, $F = 1.97$, $P < 0.001$), and the three views pooled (Wilks'$\lambda = 0.03$, $F = 2.06$, $P < 0.001$). Pairwise MANOVA comparisons among karyotypes (including the cytotype 2n = 54 occurring in two blocks A and C) were significant for six of the 15 comparisons (Table 3). There were significant differences among karyotypes 2n = 54, 2n = 56b, and 2n = 58 and among 2n = 54 populations of blocks A and C. On the other hand, the hybrid forms 2n = 55a and 2n = 55b karyotypes were not significantly different from any other population (Table 3). For different karyotypes, the percentage of correct classification for three integrated views of the skull was 89.7% the highest value, and for the ventral view was the lowest, 58.4%. Morphological distances among population karyotypes generated distinct phenogram topologies for the different views of the skull. Furthermore, there is a distinct pattern: the karyotypes 2n = 54 and 2n = 55a (both from block A) always appeared together (Figure 5).

Shape – chromosomal rearrangements (# 1 and # 2) – Chromosomal pairs 1 showed significant differences in shape for the dorsal and lateral views, and for the three views of the skull pooled. Pairwise MANOVA comparisons showed significant differences among all rearrangements for pair 1 only for the dorsal view: metacentric homozygote versus heterozygote (MM × MA: Wilks'$\lambda = 0.51$, $F = 2.62$, $P < 0.05$); metacentric homozygote versus acrocentric homozygote (MM × AA: Wilks'$\lambda = 0.63$, $F = 3.6$, $P < 0.01$); and heterozygote versus acrocentric homozygote (MA × AA Wilks'$\lambda = 0.78$, $F = 2.8$, $P < 0.05$). For chromosomal pair 2, we found significant differences in skull shape only for the comparison between two homozygote chromosome forms (MM × AA), for

dorsal (Wilks'λ = 0.62, $F = 5.5$, $P < 0.001$), ventral (Wilks'λ = 0.6, $F = 4.1$, $P < 0.001$), lateral (Wilks'λ = 0.95, $F = 0.64$, $P > 0.05$), and three views of the skull pooled (Wilks'λ = 0.43, $F = 5.25$, $P < 0.001$). No MANOVA interaction was found among chromosomal pairs 1 and 2, and population blocks.

Correlation between morphological and geographical distances – The Mantel's test showed no significant correlation between morphological and geographic matrices for the dorsal ($P = 0.54$), ventral ($P = 0.32$), lateral ($P = 0.11$) and three views of the skull pooled ($P = 0.41$). Randomization tests showed no significant correlation for the dorsal ($P = 0.18$), ventral ($P = 0.13$), and three views pooled ($P = 0.38$); but there was a significant correlation for the lateral view of the skull ($P = 0.007$). These results suggest that there was no association between skull shape and linear distances among populations.

Selection / Drift Test – The regression test (**BWp** variances over **Wp** eigenvalues) led to a slope value of 0.53, which did not differ from one ($t = 1.58$, *d.f.* = 25, $P = 0.127$), or from zero ($t = 1.76$, *d.f.* = 25, $P = 0.091$). Figure 6a illustrates the regression plot of **B** variances on **Wp** eigenvalues with the associated 95% confidence interval of the regression line. The low power of the test as well as the deviation from a strict drift model are clearly due to at least four diverging PCs: 3, 13, 15, and 16. All are characterized by smaller than expected values for the **BWp** variances and may be indicative of selective pressures. The Bartlett's test for sphericity is significant at the 0.1 level ($P = 0.095$): because of the small number of degrees of freedom, equal to 3, this result indicates that the **BWp** and **Wp** principal directions are not congruent. If we restrict the analysis to the first three PCs, which correspond to the number of degrees of freedom of the **B** covariance matrix, both PC2 and PC3 deviated from the neutral model, contrarily to PC1 (Figure 6a). PC2 is more variable than expected, and may be driven by diversifying selection (Figure 6a). PC3 is below the confidence interval, indicating a strong stabilizing selection (Figure 6a). Examination of the plots of the **BWp** scores (Figures 6b to 6d) shows that block B differed from the other blocks in PC1 scores (Figures 6b and 6c), block A differed in PC2 scores (Figures 6b and 6d), while PC3 highlighted the lack of differences between blocks (Figures 6c and 6d). The percent of variance explained for each PC was 17.48% for PC1, 10.19% for PC2, and 5.77% for PC3. All these results tend, therefore, to indicate that the evolution of the skull shape in *Ctenomys lami* resulted from both drift and selection.

Drift acts on PC1 – Landmark configuration projections from PC1 scores indicated that members of population block B have a more robust skull than those in other blocks (Figure 7, column 1). Block B has a larger rostrum in dorsal view of the skull, a deeper rostrum and larger jugal bone in lateral view and a proportionally smaller tympanic bulla in ventral view (dashed lines in Figure 7, column 1).

Selection acts on PC2 and PC3 – Morphological landmark projections from PC2 scores showed that the skull shape of population block A differed from the other three blocks (Figure 7, column 2). Block A showed a narrow zygomatic arch in dorsal view, a less procumbent angle of the rostrum, an upwards displaced jugal, and a proportionally larger paraoccipital apophysis in lateral view; and a shorter tympanic bulla in ventral view (solid lines in Figure 7, column 2). The landmark projections on PC3 scores showed changes in tympanic bulla shape in lateral view (Figure 7, column 3).

Population block B showed a larger centroid size than the other blocks (Box plot Figure 4). Although this difference was not significant, we found a highly significant negative correlation between centroid size and PC1 scores (R = -0.83, $P < 0.001$). The increase in skull size led to an increase in rostrum and jugal bone proportions (see Figures 6b, 6c and Figure 7, column 1). Therefore, PC1 is an allometric vector representing variation in cranial shape associated with size.

Discussion

Wide variation in organisms at the microevolutionary scale (Arnold *et al*. 2008) compared to the stasis observed at the geological level (Hansen & Houle 2004) is a well-known phenomenon in evolution. Unfortunately, we can only directly observe evolution either within a human lifespan or through the paleontological record. It is not surprising that the most successful attempts to solve this apparent paradox came from mathematical modeling and simulation studies (Lande 1976, Lande 1971, Hansen & Martins 1996, Arnold 2001, Polly 2004, Hohenlohe & Arnold 2008). Interestingly the blurring of the micro/macro evolutionary distinction has come both from quantitative genetics and from the comparative phylogenetic method. These conceptual reformulations attempt not only to explain this transition of patterns, but also to allow us to infer the action of evolutionary processes from observed patterns (Lande 1976, Venables 2002, Ackermann 2004, Paradis

et al. 2006). In the present study, we have addressed such an evolutionary phenomenon and propose both proximal and distal causes for this large amount of variation.

The subterranean rodent *Ctenomys lami* provides an ideal experimental model to inspect microevolutionary patterns. On one hand, we did not expect to find much variation, since we analyzed a functionally constrained structure the skull, which is used as a digging tool (Lessa & Stein 1992, Mora *et al*. 2003). Moreover, the distributional area of this species is fairly homogeneous and spatially restricted, which led us to hypothesize a flat adaptive landscape, which lessened the probability of the presence of disruptive selection. On the other hand, the potential source of differentiation lay in the supposed small effective population size, a geographical barrier, and on the spatially structured chromosomal variability, which attestedly limits gene flow between chromosomal blocks (Freitas 2007). Given this balance between diversifying and homogenizing forces, we decided to test which evolutionary forces might be acting on the skull, and more interestingly, what shape changes they caused. This last point is particularly useful, since we have a fair amount of information to define an explicit biomechanical model and thus, to interpret shape changes functionally (Lessa & Stein 1992, Mora *et al*. 2003, Fernandes *et al*. 2009a).

Our study indicated significant variation in both skull shape and size in *C. lami*, in a small area, perhaps the smallest distribution area for a species of *Ctenomys*. The intraspecific morphological differentiation shown was found at many levels, which are detailed in the following paragraphs.

Sexual Dimorphism – Our results detected strong sexual dimorphism in skull size. This was an expected result, because sexual size dimorphism is well documented in genus *Ctenomys* (Pearson 1959, Pearson *et al*. 1968, Cook *et al*. 1990, Malizia & Busch 1991, Gastal 1994, Zenuto & Busch 1998, Marinho & Freitas 2006, Fernandes *et al*. 2009a). Sexual dimorphism in size has been associated with sexual selection or niche divergence within species (Hood 2000). Following the former alternative, El Jundi and Freitas (2004) suggested that the dimorphism in *C. lami* might be associated with competition for resources and/or reproduction, since males show territoriality and aggressive behavior with other males to access receptive females (Zenuto *et al*. 2001). More interestingly, our results also showed a sexual dimorphism in skull shape, as previously documented only by

Fernandes *et al*. (2009a) for *C. torquatus* and *C. pearsoni*, and probably related to the same factors as sexual dimorphism in size.

Population Blocks – Additional significant variation was found between the two large-group blocks (AB) and (CD), which are isolated by the connection of two swamps (see the map in Figure 1). Moreira *et al*. (1991) previously demonstrated this dichotomy using biochemical polymorphisms. This isolation hypothesis was reinforced by Freitas (2007), who did not find hybrids between the two groups. Our data indicate that this isolation promotes not only biochemical differentiation but also morphological differences at a microevolutionary scale.

Dealing with the four population blocks proposed by Freitas (2007), our results confirmed their shape differences in pairwise and overall comparisons among blocks. The hypothesis of four blocks is related to the frequency of different karyotypes found along the distribution of *C. lami*. Despite this structure, Freitas (2007) found hybrid forms between the A and B blocks (2n = 57 result from 2n = 56a × 2n = 58) and between the C and D blocks (2n = 55b result from 2n = 54 × 2n = 56b), but the high F_{ST} values and rarity of hybrids indicate very low gene flow among blocks. Thus, both the channel between the swamps (physical obstacle) and the chromosomal polymorphism (unbalanced gametes, or fitness disadvantage of chromosomal heterozygotes) may be acting as reproductive isolating factors. Our results of MANOVA among the four blocks revealed statistically significant differences in skull shape. Moreover, F values decreased from blocks A-D to A-C to A-B, in what appeared to be an isolation by distance pattern. This would be an expected pattern in *Ctenomys* (low dispersal, small effective population size), but the only study addressing this issue for the skull with geometric morphometrics methods did not detect a correlation between geographical and morphological distances for *C. rionegrensis* (D'Anatro & Lessa 2006). Likewise, we did not find a correlation between morphological and geographic distances in Mantel and randomization tests (an exception was the lateral view of the skull with $P < 0.01$). Thus, there seems not to exist a constant gradual morphological variation in skull shape in the almost linear distribution of *C. lami*.

If an isolation by distance model does not explain cranial morphological variation, chromosome rearrangements may provide an adequate model. Two hypotheses can be proposed. First, different karyotypes act in reproductive isolation, and morphological variation evolves by random drift. Second, chromosome rearrangements originate

phenotypic variation by independently acting on genes of small effect, especially in quantitative trait loci (Albert *et al*. 2007). Many previous studies have related karyotype variation to morphological differences in rodents (Márquez et al. 2000, Corti & Rohlf 2001) or in Lipotyphla (Polly 2007). Nevertheless, Chondropoulos *et al*. (1996) proposed that morphological variation is associated with geography and not with karyotype in *Mus musculus*. Comparisons among the skull shapes of *C. lami* for different karyotypes agreed with a subdivision into four population blocks. Furthermore, significant differences were found only in karyotypes from different blocks, never within the same block. We did not find differences between hybrid karyotypes 2n = 55a, 2n = 55b and other chromosomal forms. This could be due to a small sample of only two hybrid cytotypes, or to the similarity of the cranial morphology of hybrids to one of the parental forms. Marinho and Freitas (2000) studied craniometric variation in *Ctenomys minutus* with linear measurements, and found that hybrid form 2n = 47 was more similar to 2n = 48 than to 2n = 46. As this species is very similar to *C. lami* (Freitas 2001, 2006), a similar pattern could have occurred.

Interestingly, two population blocks (A and C) had the same 2n = 54 karyotype but their skull shapes differed. This could result from the absence of gene flow rather than chromosomal rearrangements as the diversifying cause. In chromosomal evolution theory, fusions are expected to occur more frequently than fissions (King 1993). Therefore, the population of *C. lami* 2n = 58 could be at the origin of all the other karyotypic polymorphism of this species, by fusions and inversions in chromosome pairs 1 and 2. Our results reinforce this hypothesis, because PCA block B (2n = 58) is more different in skull shape than any other population blocks (Figures 6b and 6c), and Mahalanobis distances are larger in the majority of cases for block B and 2n = 58 karyotype (Figure 5). Thus, if we assume that 2n = 58 is the ancestral form, the 2n = 54 karyotype could evolved twice independently to produce the two separated blocks A and C. Nevertheless, two blocks with the same karyotype (2n = 54) but with significant differences in skull shape reinforce the hypothesis from Tomasco & Lessa (2007) that there is no correlation between chromosomal rearrangements and speciation.

Chromosomal Rearrangements as Source of Morphological Variation – We tested differences among chromosome rearrangements for pairs 1 and 2, and obtained unexpected results. For pair 1, we found differences in skull shape only in the dorsal view. This result

is expected in traits related to QTL (quantitative trait loci) which could cause cranium changes in only one view (Klingenberg & Leamy 2001, Klingenberg *et al*. 2001). In chromosome pair 2, we also found significant differences only between the homozygote forms. This probably occurred because we were comparing karyotypes from the A, C, and D blocks (metacentric homozygotes) with the only acrocentric homozygote block B (2n = 58), which also has the most different skull shape in *C. lami*. Furthermore, the absence of interaction between chromosome rearrangements and population blocks in the MANOVA is noteworthy. Thus, some kinds of chromosome changes, such as fusion and inversions, can lead to perceptible or measurable phenotypic modifications. Our hypothesis is that the species *C. lami* has undergone chromosome rearrangements that acted as a reproductive isolation mechanism of populations, but also directly triggered some phenotypic changes. Moreover, reproductive isolation by new mutations could arise in different populations, allowing population blocks to evolve independently by drift and natural selection.

Genetic Drift and Selection as Sources of Variation – Despite the functional constraints related to the cranium, our results suggest that the main trend (PC1) of variation in skull shape may be generated by drift, but that subsequent patterns (PCs 2 and 3) may have been generated by diversifying and stabilizing selection, respectively (Figures 6 and 7). In the selection/drift test, the lack of significance for the regression slope was related to the least two PCs which differed strongly within and among groups. These two PCs were congruent with disruptive and stabilizing selection, respectively.

Drift may be an important evolutionary force in skull shape in *Ctenomys*. Marroig and Cheverud (2004) studied New World primate skulls, and showed that morphological evolution of Neotropical monkeys can in some instances be nonadaptive. We found similar results, but on a microevolutionary scale. Likewise, Fernandes *et al*. (2009a) suggested that genetic drift has an important role as an evolutionary force driving both morphological and karyotypic evolution in *C. torquatus* and *C. pearsoni*. Furthermore, they indicated that drift and selection may be acting in combination in cranial shape evolution, and our data for *C. lami* support this view. Moreover, centroid size did not show significant differences among the population blocks, contrasting with the significant differences in skull shape. The hypothesis that size is a line of least evolutionary resistance (Klingenberg *et al*. 2001, Marroig & Cheverud 2005) does not seem to find support in this case study; however, we emphasize that we are working on an intraspecific scale. Nevertheless, we did find some

variation, as population block B had the largest size (see results and box plot in Figure 4) and the most robust skull (Figure 7, column 1), and we found a strong significant correlation between shape and size in this population block. Thus, for the patterns described by PC1, genetic drift can act on skull shape characters that are directly influenced by changes in size, or in other words, on an allometric component of the cranium.

Biomechanical Arguments for Selective Changes – Our results suggest that stabilizing selection acts on the auditory bulla (PC3) and that this pattern is less variable than would be expected under drift (see results and Figures 6a, 6d and 7). This result suggests that a strong stabilizing selection acts to preserve the bulla shape. This may be explained by the craniomandibular joint, which imposes mechanical constraints on the size and shape of the tympanic bulla. Verzi and Olivares (2006) suggest that a small bulla reduces the capacity of the ear to respond to low-frequency sounds, and that an inflated bulla prevents a satisfactory opening of the mandible. Therefore, the craniomandibular joint constrains the shape of the auditory bulla in *Ctenomys*, and stabilizing selection supports this hypothesis.

Our results also support the view that diversifying selection is acting to shape some patterns (PC2). The angle of incisor procumbency seems to be an adaptive trait in the *Ctenomys* skull for chisel-tooth digging (Vassallo 1998, 2000, Mora *et al*. 2003). Our results is consistent this view, at least for the angle of the rostrum (Figures 6a, 6b and 7). This trait appears to be more variable than expected, suggesting that diversifying selection acts directly on the angle of incisor procumbency. At the same time, the depth and width of the rostrum seem to be driven by drift. We do not have enough information about the ecological variation in the environmental of *C. lami*. Therefore, adaptive radiation could be responsible for skull shape variation in *C. lami*.

We found that both drift and selection are acting on the skull shape of *C. lami*. The literature suggests that *Ctenomys* has morphofunctional and adaptive traits for digging and for life underground (Lacey *et al*. 2000, Lessa *et al*. 2008, Verzi 2008). Thus, the cranial shape of *Ctenomys* can evolve in a mosaic model, parts by drift, other parts by natural selection, and still others by two forces acting simultaneously in different ways.

Where do these variations come from? – Any specific morphological character (such as the mammal skull) is a product of complex processes of temporal and spatial

expression of many interacting genes in development (Nei 2007). Our results revealed statistically significant differences in skull shape of *C. lami* at all factors tested: sexual dimorphism, population blocks, karyotype populations, and chromosome rearrangements of pairs 1 and 2. Despite this, none of these factors showed significant interaction with the others. Therefore, each factor apparently contributes independently at some level in cranial shape evolution. The elevated variation found in the skull shape of *C. lami*, may be due to intrinsic factors such as high mutation rates, rapid recombination levels, horizontal gene transfer (transposons), chromosome rearrangements, or historical factors. Alternatively this variation might also result from the action of extrinsic factors such as stochastic events, environmental changes, or anthropic influence (Arnold 2001).

Two hypotheses can be put forward to explain the high variation found in *C. lami*. First, a high ancestral polymorphism: in the past the species might have occupied a large area and had high morphological diversity, conserved after some event reduced its distribution to the present area. Unpublished data and ongoing research from our group confirm that *C. lami* possesses high levels of intraspecific variation, not only in karyotypes and morphology but also at the molecular level. Secondly, a huge M-matrix (mutational effects on the variance/covariance matrix) increases variation with new mutations (Jones *et al*. 2007, Arnold *et al*. 2008) and action of natural selection in adaptive radiation.

Conclusions

The skull shape of *Ctenomys lami* was found to be more variable than we expected for a functionally constrained structure. This morphological variation can be attributed to many factors as sexual dimorphism, chromosomal population blocks, karyotypes and chromosome rearrangements (Freitas 2001, 2007).

Sexual dimorphism is present in skull shape and size with a pattern similar to the one described for *C. torquatus* and *C. pearsoni* (Fernandes *et al*. 2009a). The four chromosomal population blocks are significantly different in skull shape and also among karyotypes and chromosome rearrangements. Even though the three factors are biologically related their effects show no interaction. Besides there is no correlation between morphological and geographical distances in *C. lami*. Our results suggest that chromosomal rearrangements can lead to phenotypic modifications in cranial shape. Thus,

the four population blocks could have evolved independently due to reproductive isolation by new chromosomal rearrangements and also by small effects of rearrangements in morphology as in quantitative trait loci (QTL) (Klingenberg & Leamy 2001, Klingenberg *et al*. 2001). Each of these factors, sexual dimorphism, population blocks, karyotypes, and chromosome rearrangements contributes in some level and in different ways to morphological skull shape variation.

Moreover, our findings suggest that a combination of drift and selection (diversifying and stabilizing) acted on the skull shape variation in four chromosomal population blocks. The covariance patterns associated with selection are compatible with biomechanical models proposed for *Ctenomys* (Vassallo 1998, Mora *et al*. 2003, Lessa *et al*. 2008). The diversifying patterns involve structures related to digging as the angle of incisors (Mora *et al*. 2003) and jugal proportion. Stabilizing patterns involve a compromise in the auditory bulla proportion between hearing ability and mandibular opening like suggested by Verzi and Olivares (2006). All of these variations can be due to chromosome evolution, small effective size and characteristics of subterranean adaptations.

Further work will allow us to determine which modes of evolution have been prevalent during the radiation of *Ctenomys*. Phylogenetic comparative analysis of morphological data would constitute a powerful approach to determine these modes, provided the existence of a supported phylogeny. Moreover, the estimation of mutational rates could be relevant to understand the origin of the large amount of unexpected phenotypic variation found in the genus *Ctenomys*.

Legend Figures

Figure 1. Map with sample localities for populations of *C. lami* (1-18) from southern Brazil. Circles indicate the karyotypic frequencies in our sample for each population block (A, B, C and D). The references for each locality number are listed in Additional file 1.

Figure 2. Schematic view of rearrangements in chromosomes pairs 1 and 2 (# 1 and # 2) which determined karyotype variation in *C. lami* based on data shown by Freitas (2007), "M" indicate metacentric chromosome and "A" indicates acrocentric chromosome. *Chromosome form not observed.

Figure 3. The location of landmarks defined on the skull of *C. lami* for a) dorsal; b) ventral; and c) lateral views of the skull.

Figure 4. Skull centroid size variability for dorsal view of the skull of *C. lami* for each population block for each sex. The horizontal line represents the mean; box margins are at 25th and 75th percentiles; bars extend to 5th and 95th percentiles; and circles are outliers.

Figure 5. Neighbor-joining tree phenograms for *Ctenomys lami*. Phenograms computed from Mahalanobis distances among four population blocks in the left column (blocks A, B, C and D); and among karyotypes in the right column: 2n = 54, 55a (from block A), 2n = 58 (from block B), 2n = 54 (from block C), 2n = 55b and 56b (from block D) for *C. lami*. Trees are made by using the neighbor-joining method with branch length proportional to morphological distances.

Figure 6. Selection / drift test. a) Regression straight line of **B** (Between-group matrix) variances on **Wp** (Within-pooled covariance matrix) eingenvalues and associated 95% confidence interval (dashed lines) for the population blocks (A, B, C and D) of *C. lami*. b) Principal components analysis for PC1 and PC2 scores; c) PC1 and PC3; and d) PC2 and PC3.

Figure 7. Landmark configuration projections for the first three principal components (PCs) for: a) dorsal, b) ventral and c) lateral views of the skull of *C. lami*. The first column shows PC1 under neutral selection (17.48% of the variance explained), the second column PC2 under diversifying selection (10.19% of the variance explained), and the third column PC3 under stabilizing selection (5.77% of the variance explained). Dashed lines indicate negative scores, and solid lines positive scores. For description of the skull shape see the text.

Tables

Table 1 - Pairwise MANOVA among four population blocks (A, B, C and D) of *C. lami* for cranial shape (results for dorsal, ventral and lateral views integrated).

Comparison	λ_{Wilks}	*d.f.*	*F*	*P*
A × B	0.18	1	5.71	4.23×10^{-4}**
A × C	0.47	1	7.59	3.23×10^{-4}**
A × D	0.42	1	12.84	4.69×10^{-7}**
B × C	0.40	1	4.48	0.00595**
B × D	0.28	1	3.19	0.00818**
C × D	0.43	1	2.26	0.0288*

*$P < 0.05$; **$P < 0.01$; after Bonferroni correction.

Table 2 - Pairwise test for shape differences with bootstrap (Boot) and permutation (Perm) results among four population blocks (A, B, C, and D) of *C. lami*. H - Hotelling's T^2 assuming normality and equal covariance matrices; J - James' J assuming normality and unequal covariance matrices; Lambda based on the asymptotic Chi-square distribution assuming large population sizes.

		B		C		D	
		Boot	Perm	Boot	Perm	Boot	Perm
A	H	-6.5×10^{14} ns	-6.5×10^{14} ns	-5.4×10^{14} ns	-5.4×10^{14} ns	-1×10^{11}**	-1×10^{11} ns
	J	7.15×10^{16} ns	7.15×10^{16}**	2.4×10^{17} ns	2.4×10^{17}**	7×10^{13} ns	7×10^{13}**
	Lambda	375.8**	375.8**	383.3*	383.3**	423.6**	3.4**
B	H			-1×10^{15} ns	-1×10^{15} ns	-3.6×10^{13}**	-3.6×10^{13}**
	J			1.3×10^{17}ns	1.3×10^{17}**	2.4×10^{16} ns	2.4×10^{16}**
	Lambda			216.3 ns	216.2 ns	236.8 ns	236.8**
C	H					-2.5×10^{14} ns	-2.5×10^{14} ns
	J					1.25×10^{16}ns	1.25×10^{16}**
	Lambda					186.4 ns	186.4*

*$P < 0.05$; **$P < 0.01$; ns = statistically not significant.

Table 3 - MANOVA resume with *F* and *P* values respectively among six different diploid numbers compared pair to pair for cranial shape of *C. lami* (integrated results for dorsal, ventral and lateral views). Parentheses indicate the population block for each karyotype.

	54 (A)	55a (A)	58 (B)	54 (C)	55b (D)
55a (A)	ns	-			
58 (B)	5.0 / 0.01*	ns	-		
54 (C)	4.96 / 0.009**	ns	4.48 / 0.02*	-	
55b (D)	ns	ns	ns	ns	-
56b (D)	7.26 / 0.0003**	ns	5.31 / 0.006**	1.91 / 0.009**	ns

*$P < 0.05$; **$P < 0.01$; ns = statistically not significant; after Bonferroni correction.

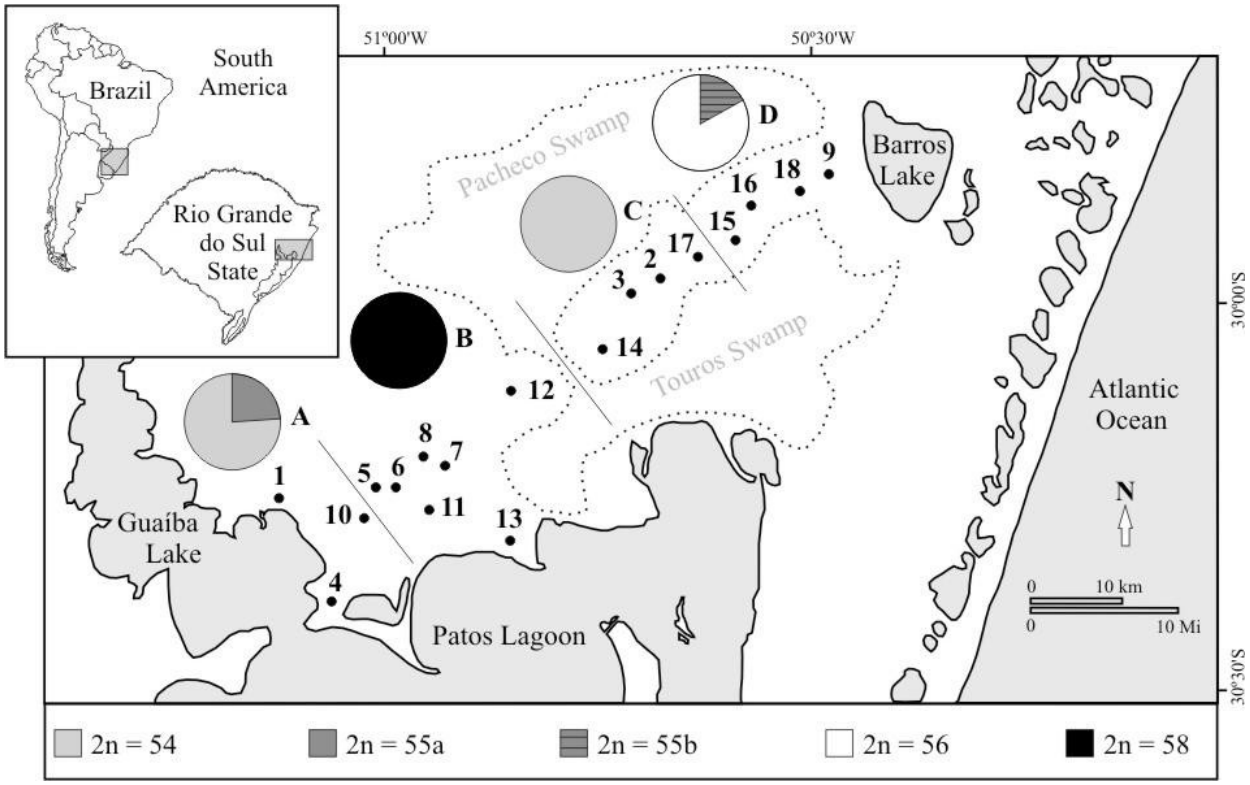

Figure 1. Map with sample localities for populations of *C. lami* (1-18) from southern Brazil. Circles indicate the karyotypic frequencies in our sample for each population block (A, B, C and D). The references for each locality number are listed in Additional file 1.

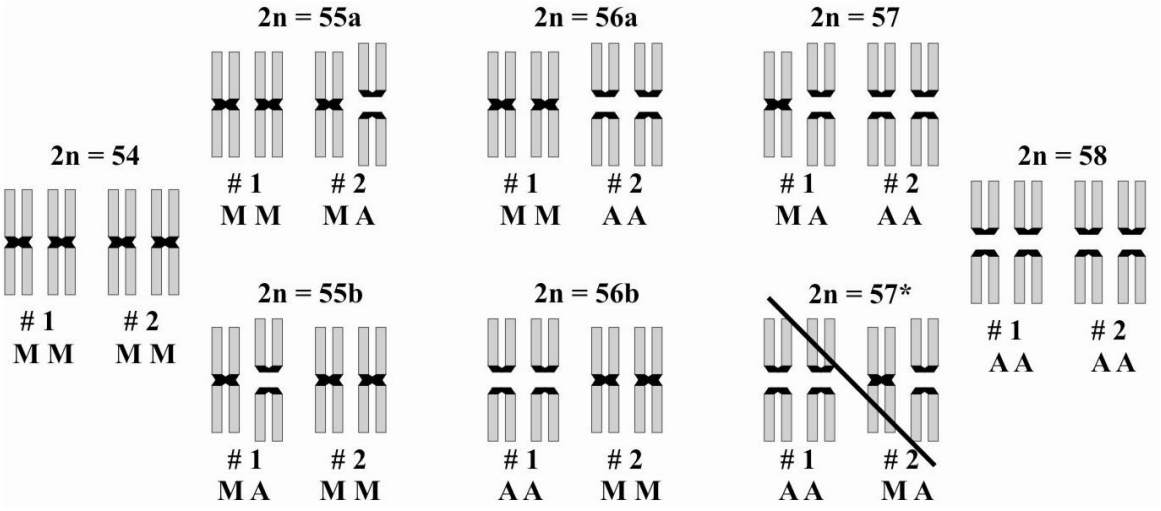

Figure 2. Schematic view of rearrangements in chromosomes pairs 1 and 2 (# 1 and # 2) which determined karyotype variation in *C. lami* based on data shown by Freitas (2007), "M" indicate metacentric chromosome and "A" indicates acrocentric chromosome. *Chromosome form not observed.

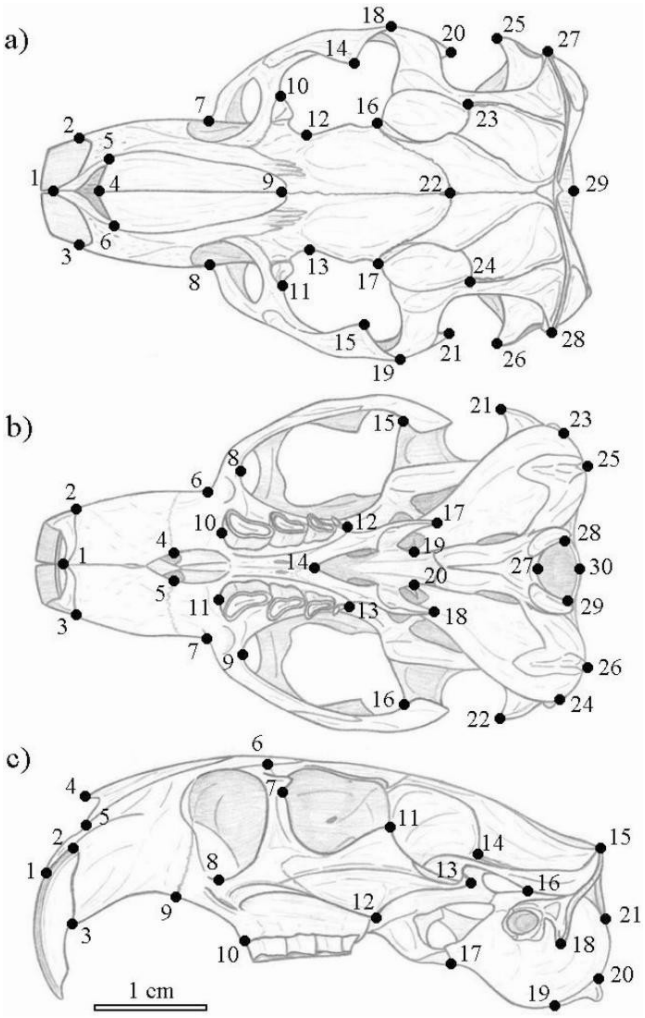

Figure 3. The location of landmarks defined on the skull of *C. lami* for a) dorsal; b) ventral; and c) lateral views of the skull.

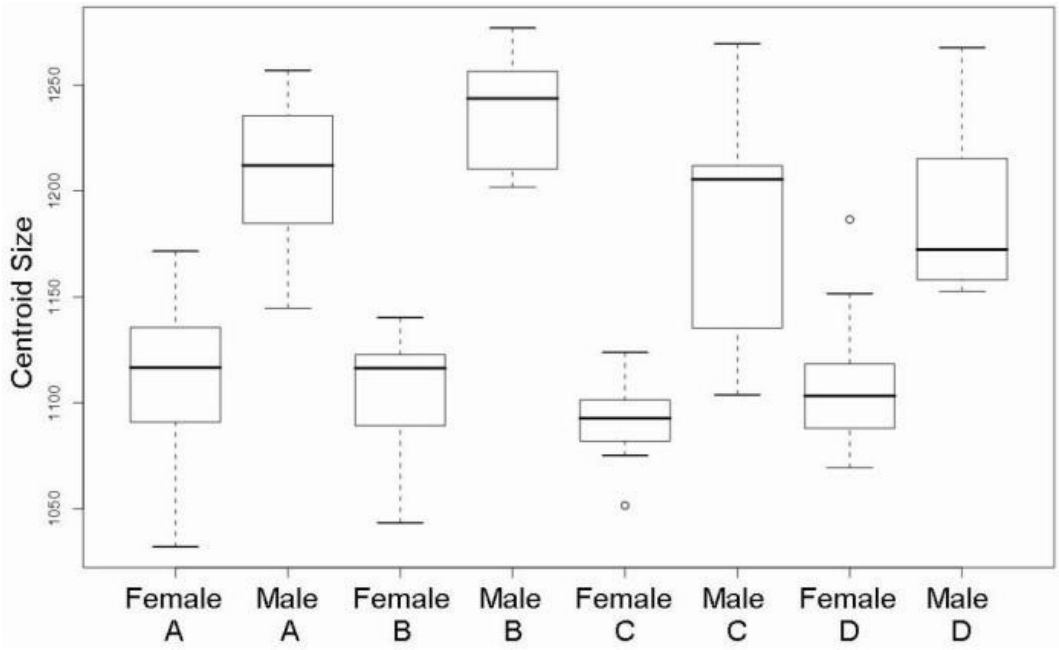

Figure 4. Skull centroid size variability for dorsal view of the skull of *C. lami* for each population block for each sex. The horizontal line represents the mean; box margins are at 25th and 75th percentiles; bars extend to 5th and 95th percentiles; and circles are outliers.

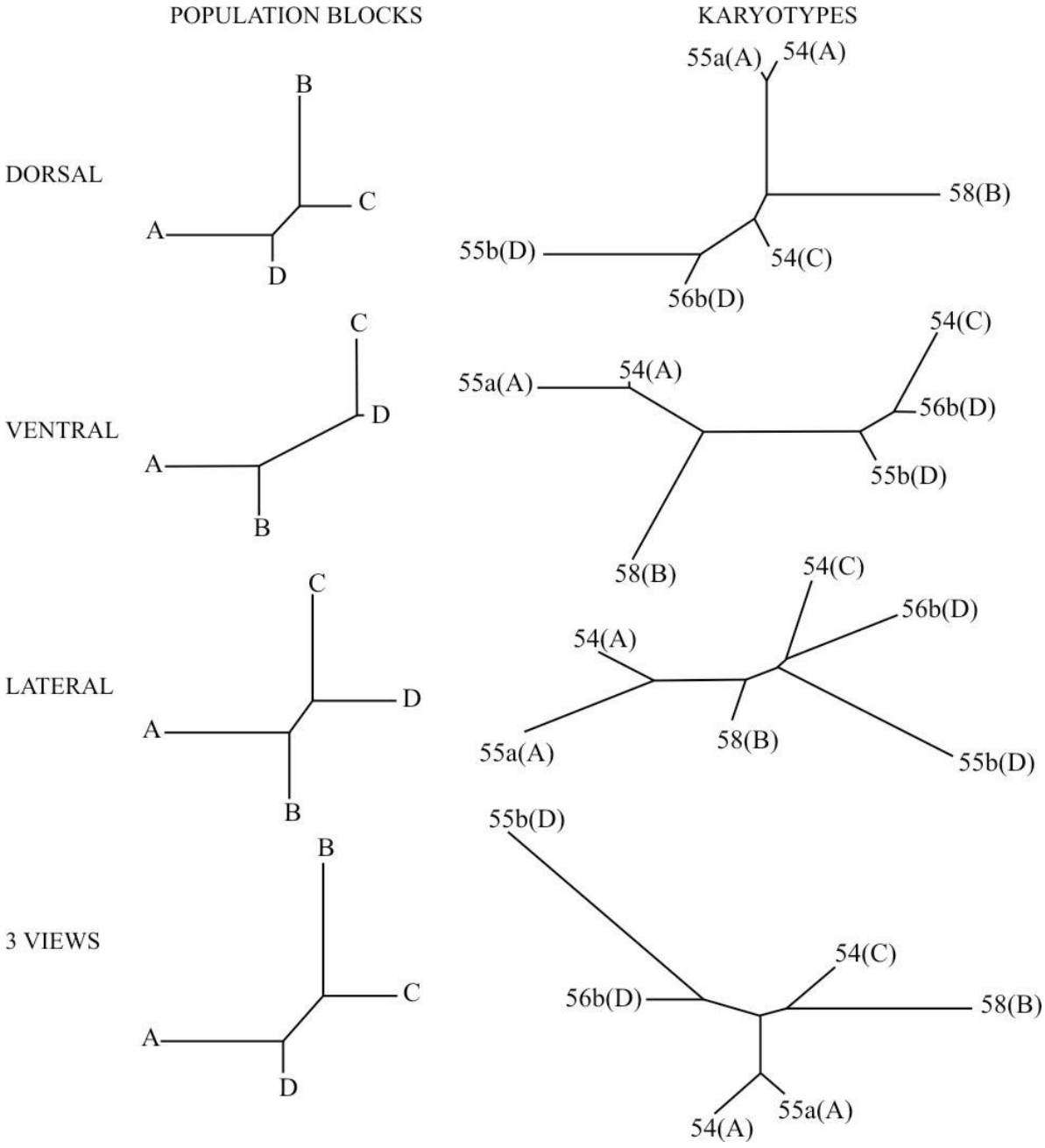

Figure 5. Neighbor-joining tree phenograms for *Ctenomys lami*. Phenograms computed from Mahalanobis distances among four population blocks in the left column (blocks A, B, C and D); and among karyotypes in the right column: 2n = 54, 55a (from block A), 2n = 58 (from block B), 2n = 54 (from block C), 2n = 55b and 56b (from block D) for *C. lami*. Trees are made by using the neighbor-joining method with branch length proportional to morphological distances.

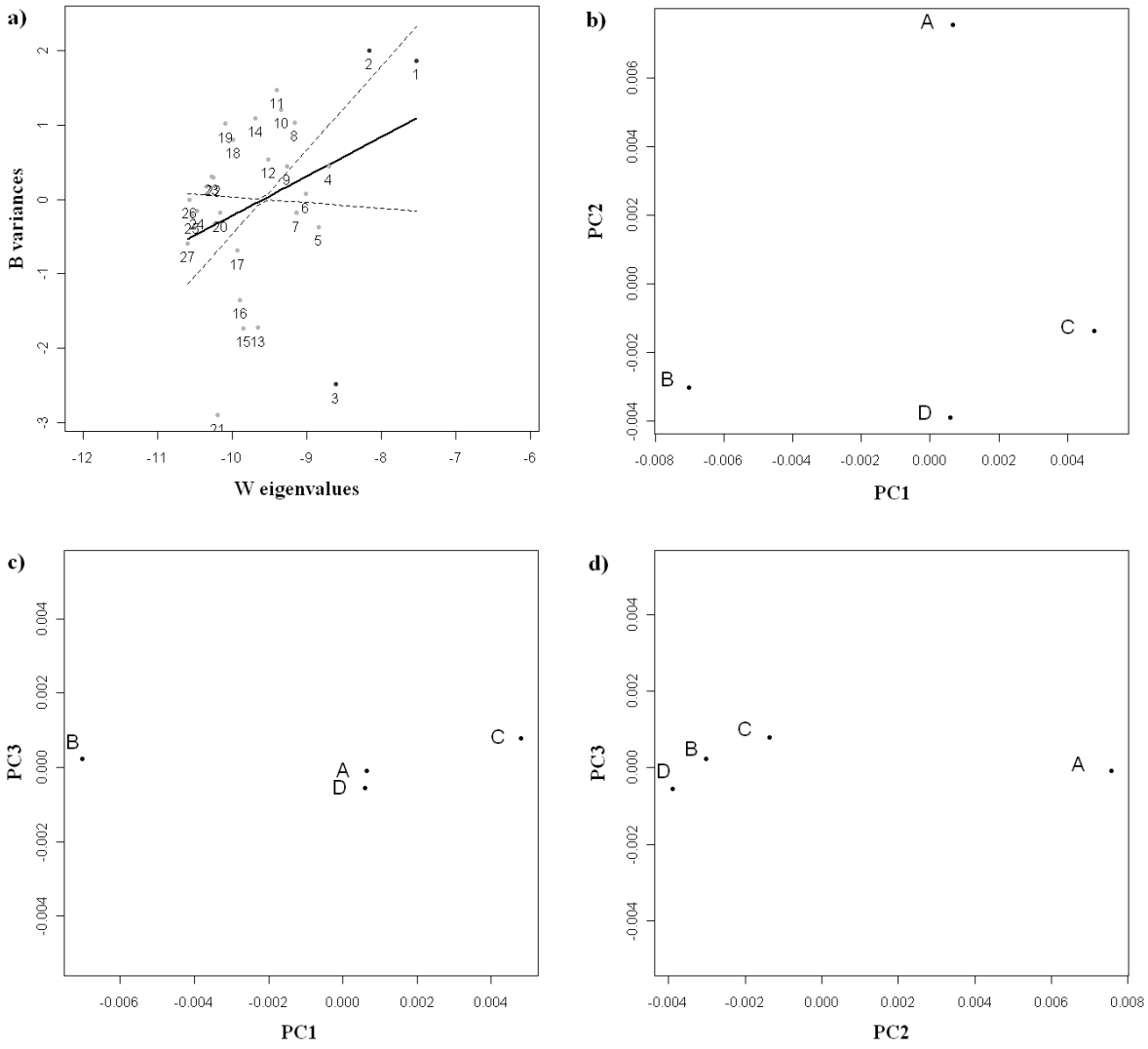

Figure 6. Selection / drift test. a) Regression straight line of **B** (Between-group matrix) variances on **Wp** (Within-pooled covariance matrix) eingenvalues and associated 95% confidence interval (dashed lines) for the population blocks (A, B, C and D) of *C. lami*. b) Principal components analysis for PC1 and PC2 scores; c) PC1 and PC3; and d) PC2 and PC3.

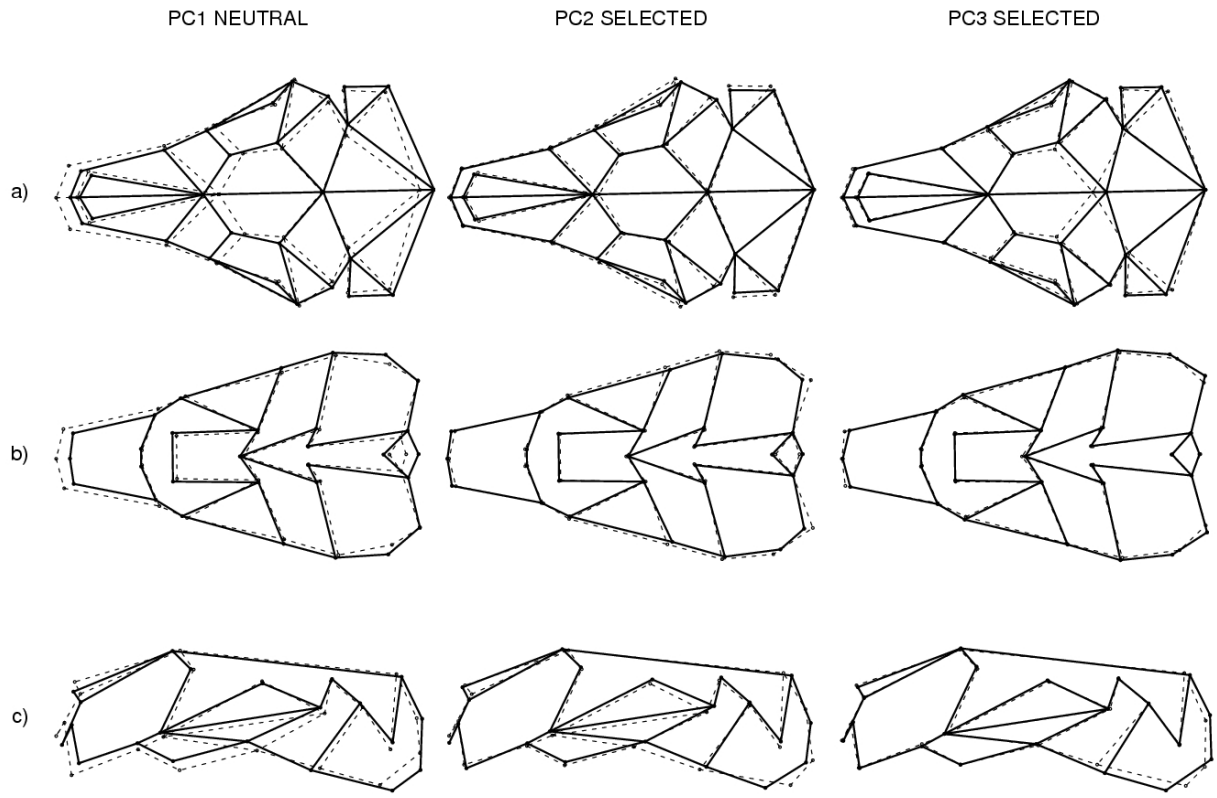

Figure 7. Landmark configuration projections for the first three principal components (PCs) for: a) dorsal, b) ventral and c) lateral views of the skull of *C. lami*. The first column shows PC1 under neutral selection (17.48% of the variance explained), the second column PC2 under diversifying selection (10.19% of the variance explained), and the third column PC3 under stabilizing selection (5.77% of the variance explained). Dashed lines indicate negative scores, and solid lines positive scores. For description of the skull shape see the text.

Appendix I

Number of specimens examined of *Ctenomys lami*.

Population block	Number of collection site*	Karyotype (2n)	Year of collection	*N* males	*N* females	*N* total
A	1	54/55a	1981/82 /83	5	11	16
	4	54/55a	1984	4	2	6
	10	54	1984	1	2	3
B	5	58	1984	2	3	5
	6	58	1984	-	1	1
	7	58	1984	1	-	1
	8	58	1984	1	-	1
	11	58	1984	-	3	3
	12	58	1983/85	2	2	4
	13	58	1983	2	-	2
C	2	54	1984	3	2	5
	3	54	1984	2	4	6
	14	54	1983/85	1	3	4
	17	54	1985	3	-	3
D	9	55b	1992	1	1	2
	15	56b	1983/84/85	3	8	11
	16	56b	1983/90	1	4	5
	18	55b/56b	1985	5	6	11
				37	52	89

* See the map in Figure 1 for details.

Appendix II

Definition of landmarks with numbers and locations for each view of the skull of *Ctenomys lami* (represented in Figure 3).

Dorsal view of the cranium: 1. anterior tip of the suture between premaxillas; 2-3. anterolateral extremity of incisor alveolus; 4. anterior extremity of the suture between nasals; 5-6. anteriormost point of the suture between nasal and premaxilla; 7-8. anteriormost point of the root of zygomatic arch; 9. suture between nasals and frontals; 10-11. anterolateral extremity of lacrimal bone; 12-13. point of least width between frontals; 14-15. tip of extremity of superior jugal process; 16-17. anterolateral extremity of suture between frontal and squamosal; 18-19. lateral extremity of suture between jugal and squamosal; 20-21. tip of posterior process of jugal; 22. suture between frontals and parietals; 23-24. anterolateral extremity of suture between parietal and squamosal; 25-26. anterior tip of external auditory meatus; 27-28. point of maximum curvature on mastoid apophysis; 29. posteriormost point of occipital along the midsagittal plane.

Ventral view of the cranium: 1. anterior tip of suture between premaxillas; 2-3. anterolateral extremity of incisor alveolus; 4-5. lateral edge of incisive foramen in suture between premaxilla and maxilla; 6-7. anteriormost point of root of zygomatic arch; 8-9. anteriormost point of orbit in inferior zygomatic root;10-11. anteriormost point of premolar alveolus; 12-13. posterior extremity of III molar alveolus; 14. posterior extremity of suture between palatines; 15-16. anteriormost point of intersection between jugal and squamosal; 17-18. posteriormost point of pterygoid; 19-20. anterior extremity of tympanic bulla; 21-22. anterior tip of external auditory meatus; 23-24. posterior extremity of mastoid apophysis; 25-26. posterior extremity of paraoccipital apophysis; 27. anteriormost point of foramen magnum; 28-29. posterior extremity of occipital condyle in foramen magnum; 30. posteriormost point of foramen magnum along midsagittal plane.

Lateral view of the cranium: 1. anteriormost point of premaxilla; 2. posteriormost point of incisor alveolus; 3. inferiormost point of incisor alveolus; 4. anterior tip of nasal; 5. anteriormost point of the suture between nasal and premaxilla; 6. suture between premaxilla, maxilla and frontal in superior zygomatic root; 7. inferiormost point of suture between lacrimal and maxilla; 8. inferiormost point of infraorbital foramen in inferior zygomatic root; 9. inferiormost point of suture between premaxilla and maxilla; 10. anteriormost point of premolar alveolus; 11. extremity of superior jugal process; 12. extremity of inferior jugal process; 13. tip of posterior jugal process; 14. medial point of suture between parietal and squamosal; 15. superior extremity of lambdoidal crest; 16. posterior extremity of postglenoid fossa; 17. inferior extremety in suture between pterygoid and tympanic bulla; 18. inferior extremity of mastoid apophysis; 19. anteriormost margin of paraoccipital apophysis; 20. posteriormost margin of paraoccipital apophysis; 21. posterior extremity of intersection between occipital and tympanic bulla.

Capítulo VI - Discussão Geral

Neste trabalho foi possível abordar uma série de questões a respeito da evolução morfológica dos tuco-tucos. Entre elas, uma visão mais ampla da variação craniana entre um número de espécies como nunca antes havia sido explorada. Podemos notar que os tuco-tucos quanto a morfologia geral não variam só em tamanho, coloração e ângulo de procumbência dos incisivos, mas que a forma do crânio também é altamente variável, tanto no nível inter quanto intra-específico.

O dimorfismo sexual, que já havia sido registrado em uma longa série de trabalhos foi mais uma vez observado no gênero *Ctenomys* (Pearson 1959, Pearson *et al*. 1968, Cook *et al*. 1990, Malizia & Busch 1991, Gastal 1994, Zenuto & Busch 1998, Marinho & Freitas 2006, Fernandes *et al*. 2009a). Apesar da ocorrência de dimorfismo sexual ser bem conhecido, a sua origem e manutenção permanecem alvo de especulação. Ainda não se tem uma idéia clara à respeito do quanto este dimorfismo pode ser explicado por seleção sexual ou por diferenças ecológicas entre os sexos. E ainda mais, se este dimorfismo segue o mesmo padrão em diferentes espécies.

Com esta ampla amostragem, proveniente de várias coleções, fomos capazes de explorar a congruência entre dados morfológicos e moleculares. De maneira inesperada, encontramos um sinal filogenético no chamado grupo *torquatus* (Parada 2007). Além da forma, este grupo apresentou baixa diferenciação quanto ao tamanho. Esta restrição morfológica não foi observada nos outros grupos propostos para *Ctenomys*. A baixa variação no tamanho dentro do grupo *torquatus* pode ter origens ecológicas ou ser devida a ancestralidade comum muito recente deste grupo.

Nos fenogramas gerados com distâncias de Mahalanobis para 47 espécies do gênero, foi possível observar uma forte associação entre os grupos Patagônico e *mendocinus*. Estes dois grupos apresentam o mesmo tipo de morfologia de espermatozóide, o chamado simples-assimétrico (Feito & Gallardo 1982, Vitullo *et al*. 1988). D'Elia *et al*. (1999) baseados em filogenias geradas à partir de dados usando citocromo *b*, sugeriram que a forma simples-assimétrica de espermatozóide poderia ter evoluido independentemente por duas vezes na linhagem Ctenomyidae. Assim, a similaridade morfológica que encontramos no crânio dos grupos Patagônico e *mendocinus* poderia ser um caso de convergência evolutiva, ou por outro lado, atestar a retenção de caracteres

plesiomórficos. Portanto, os dois grupos podem ter tido uma origem comum com um mesmo ancestral de espermatozóide simples-assimétrico como hoje é encontrado nos dois grupos. Não estamos afirmando aqui que o tipo assimétrico evoluiu apenas uma vez na linhagem de *Ctenomys* apenas baseado na morfometria craniana, mas sim, que esta seria uma hipótese mais parcimoniosa, (mais provável ocorrer um dado evento ao acaso uma vez do que duas) lembrando ainda que tal polimorfismo nos gametas masculinos não tem par entre outras linhagens de mamíferos.

Quando analisamos as relações entre a morfologia do sincrânio dos oito grupos, encontramos uma estruturação geográfica em um gradiente leste-oeste e norte-sul. No norte encontramos crânios mais robusto nos grupos Bolivianos e ao sul um crânio mais grácil no grupo Patagônico. Esta diferenciação morfológica ao longo da latitude pode ser um resultado congruente com os dados de Medina *et al*. (2007) que sugerem que *Ctenomys* segue o inverso da regra de Bergmann. No entanto, encontramos uma grande variação de tamanho do centróide dentro de cada grupo. Esta grande variabilidade de tamanho (com exceção do grupo *torquatus*) poderia se encaixar na hipótese do tamanho como sendo a menor linha de resistência evolutiva (Klingenberg *et al*. 2001, Marroig & Cheverud 2005), por outro lado o tamanho influencia pouco na estruturação dos dados. A estruturação geográfica encontrada no nível de grupos pode ser apoiada pelo que vem sendo descrito para muitas espécies de tuco-tuco. De que estes animais apresentam territorialidade, baixa vagilidade e populações com pequeno tamanho efetivo (Reig *et al*. 1990) e assim formar um padrão de isolamento pela distância numa escala maior. A grande variação na forma do crânio pode nos estar indicando uma grande radiação adaptativa no gênero *Ctenomys* ao longo de uma heterogeneidade de habitats ao longo da porção meridional da América do Sul.

De maneira geral a mandíbula mostrou-se menos variável que o crânio. Essa menor variação morfológica pode ser devido a uma menor plasticidade ou a uma restrição evolutiva relacionada ao modo de escavação, alimentação ou comportamento agonístico.

Também analisamos a variação na forma e tamanho do crânio de espécies dos grupos *mendocinus* e *torquatus*. Esperávamos encontrar maior variação fenotípica no grupo *torquatus* devido ao maior polimorfismo cromossômico e a hipótese de que rearranjos cromossômicos poderiam influenciar no isolamento reprodutivo e possibilitar diversificação (por deriva genética ou seleção natural) entre as populações (Contreras &

Bidau 1999). No entanto, nossos dados mostraram maior variação morfológica no grupo *mendocinus* (tamanho do crânio) que possui baixíssima variação cariotípica. Diferentes hipóteses podem ser conjecturadas para responder a essa variação. Uma delas é a maior distribuição e distância entre as espécies do grupo *mendocinus* em relação ao grupo *torquatus*; esse padrão geográfico poderia levar ao maior isolamento entre as espécies. Além disso, o grupo *mendocinus* é encontrado em uma grande variedade de habitats, desde dunas na costa do oceano Atlântico até as bases da Cordilheira dos Andes, podendo ter diferente disponibilidade de alimento ou diferenças na pressão de predação (Reig *et al*. 1990, Massarini *et al*. 19991). Esses fatores demográficos e ecológicos podem influenciar direta e indiretamente na variação na forma e tamanho do crânio do grupo *mendocinus*. Mais ainda, existe a possibilidade do grupo *torquatus* ter uma ancestralidade mais recente que o grupo *mendocinus* e não ter acumulado diferenças no tamanho do crânio nesse período de tempo.

No nível intra-específico *C. minutus* mostrou-se altamente variável quanto à forma do crânio e mandíbula. O padrão de variação observado parece ser mais influenciado pelas formas cariotípicas e mudanças de habitat do que pela geografia. Mais ainda, a atual distribuição do polimorfismo cromossômico na planície costeira do sul do Brasil pode ter sido moldada por rios tanto atuais como antigos. As zonas híbridas encontradas hoje em dia coincidem com os registros de paleo-rios como aqueles descritos por Weschenfelder (2005) e Weschenfelder *et al*. (2008). Nossos dados mostram variação adaptativa na forma do crânio que difere significativamente na forma entre os habitats de duna e campo.

Para *C. lami* foram encontrados vários níveis de diferenciação morfológica, desde dimorfismo sexual até diferenciação dos blocos cromossômicos populacionais (Freitas 2007), passando pelos rearranjos cromossômicos, o que sugere associação entre polimorfismo cariotípico e diferenciação morfológica (associação fraca). No entanto, encontramos diferenças significativas na forma do crânio entre populações com o mesmo cariótipo (2n = 54) em regiões diferentes. Isto pode reforçar a hipótese de Tomasco & Lessa (2007) de que não há relação entre rearranjos cromossômicos e especiação em *Ctenomys*. Entre os quatro conjuntos de populações foi demonstrado a ação de deriva, seleção diversificadora e seleção estabilizadora na forma de *C. lami*. O padrão de seleção diversificadora envolve estruturas relacionadas a escavação, que são compatíveis com modelos biomecânicos propostos para *Ctenomys*. O padrão de seleção estabilizadora

envolve um ajuste das proporções da bula timpânica, entre a capacidade auditiva e a abertura mandibular.

A presente tese mostra um panorama geral da variação morfológica do crânio no gênero *Ctenomys*. Em um nível macro (gênero) observamos um claro padrão geográfico na mudança craniana ao longo da distribuição das diferentes espécies. Em um nível micro (intra-específico) registramos influência de seleção estabilizadora, seleção diversificadora e deriva na variação da morfologia craniana.

Resumidamente, os dados com *C. lami* e *C. minutus* mostram um cenário complexo de evolução morfológica. Os dois capítulos mostram que não há uma influência direta dos arranjos cromossômicos na morfologia craniana. Os dois mostram ação de deriva, *C. minutus* com o isolamento pela distância e *C. lami* com o teste de seleção/deriva. Ainda, os dois mostram ação de seleção natural, *C. minutus* com as diferenças na forma do crânio entre as populações que habitam duna e campo, e para *C. lami* o teste de seleção/deriva que indica tanto seleção estabilizadora quanto diversificadora em diferentes regiões do crânio.

No panorama geral tanto macro quanto microevolutivo nossos dados com este "marcador fenotípico", o crânio de *Ctenomys*, fomos capazes de dar suporte aos achados de Tomasco e Lessa (2007) usando marcadores moleculares que sugerem que os rearranjos cromossômicos não são a principal razão da grande especiação observada no gênero *Ctenomys*. Nossos dados interespecíficos mostram uma grande variação na forma do crânio que pode ser devido a fatores históricos ou irradiação adaptativa (seleção natural).

Novos trabalhos, com melhor amostragem, com maior número de espécies e com mais marcadores moleculares nos próximos anos deverão nos dar uma visão mais completa das relações filogenéticas entre as aproximadamente 60 espécies atuais de *Ctenomys* (Woods & Kilpatrick 2005).

Mas antes disso, uma profunda revisão taxonômica no gênero *Ctenomys* ainda se faz necessária (Lessa & Cook 1998). Muitas espécies do gênero são conhecidas e foram descritas à partir de um único exemplar. Um bom exemplo disto é *Ctenomys brasiliensis*, que é a primeira espécie descrita para o gênero. H. M. D. Blainville em 1826 descreveu *C. brasiliensis*, cujo a localidade tipo permanece uma incerteza e esta espécie nunca mais foi encontrada. O exemplar tipo de *C. brasiliensis* não passa de um crânio quebrado, uma mandíbula e de uma pele no Museu de Ciências Naturais de Paris (Fernandes *et al*. In prep). Além do problema das espécies que foram descritas no passado necessitarem de

revisão, novas espécies de tuco-tucos ainda estão sendo descritas. Assim, pode-se perceber que muito trabalho ainda deve ser feito com este grupo antes de se ter uma visão completamente satisfatória da evolução do gênero *Ctenomys*.

Perspectivas

Esta tese não resolve todos os problemas relacionados a evolução do gênero *Ctenomys* mas certamente abre portas para novas abordagens a serem exploradas. Entre os temas que poderão ser explorados a partir desse trabalho inicial destacamos:

- Testar e avaliar a presença de assimetria flutuante na forma do crânio em zonas híbridas intra e inter-específicas para *Ctenomys lami* e *C. minutus*;
- Fazer uma síntese com os dados de micro e macroevolução craniana em *Ctenomys*;
- Estimar caracteres ancestrais para a morfologia do crânio do gênero *Ctenomys*;
- Estimar taxas de evolução fenotípica no gênero *Ctenomys*;
- Explorar a biomecânica da escavação no crânio de espécies de *Ctenomys* com diferente comportamento escavador.

Referências Bibliográficas

Ackermann RR, Cheverud JM (2002) Discerning evolutionary processes in patterns of tamarin (genus *Saguinus*) craniofacial variation. *Am J Phys Anthropol* **117**: 260-271.

Ackermann RR, Cheverud JM (2004) Detecting genetic drift versus selection in human evolution. *PNAS* **101**: 17946-17951.

Adams DC, Rohlf FJ, Slice DE (2004): Geometric Morphometrics: ten years of progress following the "revolution". *Ital J Zool* **71**: 5-16.

Agrawal VC (1967) Skull adaptations in fossorial rodents. *Mammalia* **31**: 300-312.

Albert AYK, Sawaya S, Vines TH, Knecht AK, Miller CT, Summers BR, Balabhadra S, Kingsley DM, Schuluter D (2007) The genetics of adaptive shape shift in stickleback: pleiotropy and effect size. *Evolution* **62**: 76-85.

Amaral GJA, Dryden IL, Wood ATA (2007) Pivotal Bootstrap Methods for k -Sample Problems in Directional Statistics and Shape Analysis. *Journal of the American Statistical Association* **102**: 695-707.

Anderson S, Jones JK Jr (1985) *Orders and families of Recent mammals of the world*. New York: John Wiley & Sons. 389-446.

Arnold SJ, Bürger R, Hohenlohe PA, Ajie BC, Jones AG (2008) Understanding the evolution and stability of the G-matrix. *Evolution* **62**: 2451-2461.

Arnold SJ, Pfrender ME, Jones AG (2001) The adaptive landscape as a conceptual bridge between micro- and macroevolution. *Genetica* **112-113**: 9-32.

Ashton KG, Tracy MC, Queiroz A (2000) Is Bergmann's rule valid for mammals? *Am Nat* **156:** 390-415.

Atchley WR, Hall BK (1991) A model for development and evolution of complex morphological structures. *Biological Review Cambridge Philosophy Society* **66**: 101-157.

Azurduy HF (2005) Una nueva especie fósil de *Ctenomys* (Rodentia) y breve panorama paleontológico del género en Bolivia. *Kemppfiana* **1**: 29-39.

Barton NH (1999) Clines in polygenic traits. *Genetics Research, Cambridge* **74**: 223–236.

Baylac M (2008) Rmorph: a R geometric and multivariate morphometrics library.

Baylac M, Friess M (2005) Fourier Descriptors, Procrustes Superimposition and Data Dimensionality: An Example of Cranial Shape Analysis in Modern Human

Populations. In *Modern morphometrics in physical anthropology*. Edited by Slice DE. Springer-Verlag, New York 145-166.

Bezerra AM, Carmignotto AP, Nunes AP, Rodrigues FH (2007) New data on the distribution, natural history and morphology of *Kunsia tomentosus* (Lichtenstein, 1830) (Rodentia: Cricetidae: Sigmodontidae). *Zootaxa* **1505**: 1-18.

Bidau CJ, Gimenez MD, Contrras JR (1996) Especiación cromosómica y la conservacion de la variabilidad genética: El caso del género *Ctenomys* (Rodentia, Caviomorpha, Ctenomyidae). *Mendeliana* **12**: 25-37.

Blackburn TM, Gaston KJ, Loder N (1999) Geographic gradients in body size: a clarification of Bergmann's rule. *Diversity and Distributions* **5:** 165-174.

Bock WJ (2007) Explanations in evolutionary theory. *J Zool Syst Evol Res* **45**: 89-103.

Bookstein FL (1991) *Morphometric Tools for Landmark Data: Geometry and Biology*. London, United Kingdom: Cambridge University Press.

Bookstein FL (1996a) Biometrics, biomathematics and the morphometric synthesis. *Bulletin of Mathematical Biology* **58**: 313-365.

Bookstein FL (1996b) Combining the tools of geometric morphometrics. In *Advances in Morphometrics*. Edited by Marcus LF, Corti M, Loy A, Naylor G, Slice DE. New York: Plenum Publishing Corporation 131-151.

Britton-Davidian J, Catalan J, Ramalhinho MG, Ganem G, Auffray J-C, Capela R, Biscoito M, Searle JB, Mathias ML (2000) Rapid chromosomal evolution in island mice. *Nature* **403**: 158.

Brooks S, Lear T, Adelson D, Bailey E (2007) A chromosome inversion near the *KIT* gene and the Tobiano spotting pattern in horses. *Cyt Gen Res* **119:** 225-230.

Cardini A, O'Higgins P (2004) Patterns of morphological evolution in *Marmota* (Rodentia, Sciuridae): geometric morphometrics of the cranium in context of marmot phylogeny, ecology and conservation. *Biol J Lin Soc* **82**: 385-407.

Cardini A, Thorington RD (2006) Postnatal ontogeny of Marmot (Rodentia, Sciuridae) Crania: Allometric trajectories and species divergence. *J Mammal* **87**: 201-215.

Castillo AH, Cortinas MN, Lessa EP (2005) Rapid diversification of South American Tuco-tucos (*Ctenomys*: Rodentia, Ctenomyidae): contrasting mitochondrial and nuclear intron sequences. *J Mammal* **86**: 170-179.

Catley KM, Novick LR (2009) Digging Deep: Exploring College Students' Knowledge of Macroevolutionary Time. *Journal of Research in Science Teaching* **46**: 311-332.

Cheverud JM (1996) Quantitative genetic analysis of cranial morphology in the cotton-top (*Saguinus oedipus*) and saddle-back (*S. fuscicollis*) tamarins. *J Evol Biol* **9**: 5-42.

Chondropoulos BP, Fraguedakis-Tsolis SE, Markakis G, Giagia-Athanaspoulou E (1996) Morphometric variability in karyologically polymorphic populations of the wild *Mus musculus domesticus* in Greece. *Acta Theriol* **41**: 375-382.

Contreras JR (1996) Acerca de la distribuicion geografica de la morfología espermática en el genero *Ctenomys* (Rodentia: Ctenomyidae). *Notulas Faunisticas* **88**: 1-5.

Contreras JR & Bidau CJ (1999) Líneas generales del panorama evolutivo de los roedores excavadores sudamericanos del genero *Ctenomys* (Mammalia, Rodentia, Caviomorpha: Ctenomyidae). *Ciencia Siglo XXI*, Buenos Aires, Nº1. Fundación Bartolomé Hidalgo. 22 pp.

Cook JA, Lessa EP, Hadly E (2000) Paleontology, phylogenetics patterns, and macroevolutionary processes in subterranean rodents. In *Life Underground: The Biology of Subterranean Rodents*. Edited by Lacey EA, Patton JL, Cameron GN. Chicago: University of Chicago Press; 332-369.

Cook JA, Lessa EP (1998) Are rates of diversification in subterranean South American tuco-tucos (genus *Ctenomys*, Rodentia: Octodontidae) unusually high? *Evolution* **52:**1521-1527.

Cook JA, Salazar-Bravo J (2004) Heterochromatin variation among the chromosomally diverse tuco-tucos (Rodentia: Ctenomyidae) From Bolivia. In *Contribuciones Mastozoológicas en Homenaje a Bernardo Villa*. Eds: Sánchez-Cordero V. and Medellín RA. México.

Cook JA, Anderson S, Yates A (1990) Notes on Bolivian mammals 6: The genus *Ctenomys* (Rodentia, Ctenomyidae) in the highlands. *American Museum Novitates* **2980**: 1-27.

Cordeiro-Estrela P, Baylac M, Denys C, Marinho-Filho J (2006) Interspecific patterns of skull variation between sympatric Brazilian vesper mice: geometric morphometrics assessment. *J Mammal* **87**: 1270-1279.

Corti M, Fadda C, Simson S, Nevo E (1996) Size and shape variation in the mandible of the fossorial rodent *Spalax ehrehbergi*: A Procrustes analysis of three dimensions. In

Advances in Morphometrics: 303-320. Marcus LF, Corti M, Loy A, Naylor G & Slice DE (Eds). New York: Plenum Publishing Corp.

Corti M, Rohlf FJ (2001) Chromosomal speciation and phenotypic evolution in the house mouse. *Biol J Lin Soc* **73**: 99-112.

Crispo E, Hendry AP (2005) Does time since colonization influence isolation by distance? A meta-analysis. *Conservation Genetics* **6**: 665-682.

Crow JF, Kimura N (1970) *An Introduction to Population Genetics Theory*. Minneapolis MN: Burgess.

Cutrera AP, Lacey EA, Busch C (2005) Genetic structure in a solitary rodent (*Ctenomys talarum*): implications for kinship and dispersal. *Mol Ecol* **14:** 2511-2523.

Cwynar LC, MacDonald GM (1987) Geographical Variation of Lodgepole Pine in Relation to Population History. *Am Nat* **129**: 463-469.

D'Anatro A, Lessa EP (2006) Geometric morphometric analysis of geographic variation in the Río negro tuco-tuco, *Ctenomys rionegrensis* (Rodentia: Ctenomyidae). *Mammalian Biology* **71**: 288-298.

Davidson EH, Erwin DH (2006) Gene Regulatory Networks and the Evolution of Animal Body Plans. *Science* **311**: 796-800.

De Robertis EM (2008) Evo-Devo: Variations on Ancestral Themes. *Cell* **132**: 185-195.

D'Elía G, Lessa EP, Cook JA (1999) Molecular Phylogeny of Tuco-Tucos, Genus *Ctenomys* (Rodentia: Octodontidae): Evaluation of the *mendocinus* Species Group and the Evolution of Asymmetric Sperm. *Journal of Mammalian Evolution* **6**: 19-38.

Dray S, Dufour AB (2007) The ade4 package: implementing the duality diagram for ecologists. Journal of Statistical Software. **22**: 1-20.

Dryden IL (2007): Shapes: Statistical shape analysis. R package version 1.0-1.2.

Dryden IL, Mardia KV (1998): Statistical Shape Analysis. John Wiley & Sons, Inc., New York.

El Jundi TARJ, Freitas TRO (2004) Genetic and demographic structure in a population of *Ctenomys lami* (Rodentia-Ctenomyidae). *Hereditas* **140**: 18-23.

Emmons LH, Feer F (1990) *Neotropical Rainforest Mammals: A Field Guide*. The University of Chicago Pres. Chicago, 281.

Ersts PJ (2009) Geographic Distance Matrix Generator (version 1.2.3). American Museum of Natural History, Center for Biodiversity and Conservation. http://biodiversityinformatics.amnh.org/open_source/gdmg. Acessado em 8-4-2009.

Erwin DH (2000) Macroevolution is more than repeated rounds of microevolution. *Evolution & Development* **2**: 78-84.

Erwin DH, Davidson EH (2009) The evolution of hierarchical gene regulatory networks. *Nat Rev Genet* **10**: 141-148.

Evin A, Baylac M, Ruedi M, Mucedda M, Pons J-M (2008) Taxonomy, skull diversity and evolution in a species complex of *Myotis* (Chiroptera: Vespertilionidae): a geometric morphometric appraisal. *Biol J Lin Soc* **95**: 529-538.

Feito R, Gallardo M (1982) Sperm morphology of the Chilean species of *Ctenomys* (Octodontidae). *J Mammal* **63**: 658-661.

Fernandes FA, Fornel R, Cordeiro-Estrela P, Freitas TRO (2009a) Intra- and interspecific skull variation in two sister species of the subterranean genus *Ctenomys* (Rodentia, Ctenomyidae): coupling geometric morphometrics and chromosomal polymorphism. *Zool J Lin Soc* **155**: 220-237.

Fernandes FA, Gonçalves GL, Ximenes SSF, Freitas TRO (2009b) Karyotypic and molecular polymorphisms in *Ctenomys torquatus* (Rodentia: Ctenomyidae): taxonomic considerations. *Genetica* **136**: 449-459.

Fernández-Stolz GP, Stolz JFB, Freitas TRO (2007) Bottlenecks and dispersal in the tuco-tuco das dunas *Ctenomys flamarioni* (Rodentia: Ctenomyidae), in southern Brazil. *J Mammal* **88**: 935-945.

Freitas TRO (1990) Estudos citogenéticos e craniométricos em três espécies do gênero *Ctenomys*. Curso de Pós-Graduação em Genética e Biologia Molecular, UFRGS: Porto Alegre. (Tese de Doutorado).

Freitas TRO (1994) Geographical variation of heterochromatin in *Ctenomys flamarioni* (Rodentia-Octodontidae) and its cytogenetic relationships with other species of the genus. *Cytogenetics and Cell Genetics* **67**: 193-198.

Freitas TRO (1995a) Geographical distribution of sperm forms in the genus *Ctenomys* (Rodentia-Octodontidae). *Rev Bras Genética* **18**: 43-46.

Freitas TRO (1995b) Geographic distribution and conservation of four species of the genus *Ctenomys* in southern Brazil. *Studies on Neotropical Fauna and Environment* **30**: 53-59.

Freitas TRO (1997) Chromosome polymorphism in *Ctenomys minutus* (Rodentia-Octodontidae). *Braz J Genetics* **20**: 1-7.

Freitas TRO (2001) Tuco-tucos (Rodentia, Octodontidae) in southern Brazil: *Ctenomys lami* spec. nov. separated from *C. minutus* Nehring 1887. *Studies on Neotropical Fauna and Environment* **36**: 1-8.

Freitas TRO (2005) Analysis of Skull Morphology in 15 Species of the Genus *Ctenomys*, Including Seven Karyologically Distinct Forms of *Ctenomys minutus* (Rodentia: Ctenomyidae). In *Mammalian Diversification From Chromosomes to Phylogeography (A Celebration of the Career of James L. Patton)*. Lacey EA, Myers P (eds.) University of California, 131-154.

Freitas TRO (2006) Cytogenetics status of four *Ctenomys* species in the south of Brazil. *Genetica* **126**: 227-235.

Freitas TRO (2007) *Ctenomys lami*: The highest chromosome variability in *Ctenomys* (Rodentia, Ctenomyidae) due to a centric fusion/fission and pericentric inversion system. *Acta Theriol* **52**: 171-180.

Freitas TRO, Lessa EP (1984) Cytogenetics and morphology of *Ctenomys torquatus* (Rodentia-Octodontidae). *J Mammal* **65**: 637-642.

Freygang CC, Marinho JR, Freitas TRO (2004) New karyotypes and some considerations about the chromosomal diversification of *Ctenomys minutus* (Rodentia: Ctenomyidae) on the coastal plain of the Brazilian state of Rio Grande do Sul. *Genetica* **121**: 125-132.

Galis F (1996) The application of functional morphology to evolutionary studies. *TREE* **11:** 124-129.

Gastal MLA (1994) Density, sexual rate and biometrics data from one population of *C. minutus* Nehring, 1887 (Rodentia, Caviomorpha, Ctenomyidae). *Iheringia* **77**: 25-34.

Gava A, Freitas TRO (2002) Characterization of a hybrid zone between chromosomally divergent populations of *Ctenomys minutus* (Rodentia: Ctenomydae). *J Mammal* **83**: 843-851.

Gava A, Freitas TRO (2003) Inter and intra-specific hybridization in tuco-tucos (*Ctenomys*) from Brazilian coastal plains (Rodentia: Ctenomydae). *Genetica* **119**: 11-17.

Grantham T (2007) Is macroevolution more than successive rounds of microevolution? *Paleontology* **50**: 75-85.

Hanken J, Thorogood P (1993) Evolution and development of the vertebrate skull–the role of pattern formation. *TREE* **8**: 9-15.

Hansen TF, Houle D (2004) Evolvability, stabilizing selection, and the problem of stasis. In *Phenotypic integration: Studying the ecology and evolution of complex phenotypes.* Pigliucci M, Preston K, Oxford University Press. 130-150.

Hansen TF, Martins EP (1996) Translating between microevolutionary process and macroevolutionary patterns: the correlation structure of interspecific data. *Evolution* **50**: 1404-1471.

Harmon LJ, Gibson R (2006) Multivariate phenotypic evolution among island and mainland populations of the ornate day gecko, *Phelsuma ornata*. *Evolution* **60**: 2622-2632.

He J, Deem MW (2010) Hierarchical evolution of animal body plans. *Developmental Biology* **337**: 157-161.

Heo M, Gabriel KR (1997) A permutation test of association between configurations by means of RV coefficient. *Communications in Statistics – Simulation and Computation* **27**: 843-856.

Heth G (1991) Evidence of aboveground predation and age determination of the preyed in subterranean mole rats (*Spalax ehreenbergi*) in Israel. *Mammalia* **55:** 529-542.

Hildebrand M (1995) *Análise da Estrutura dos Vertebrados*. Atheneu, São Paulo. Pp. 499-518.

Hohenlohe PA, Arnold SJ (2008) MIPoD: A hypothesis-testing framework for microevolutionary inference from patterns of divergence. *Am Nat* **171**: 366-385.

Honeycutt RL (2009) Rodents (Rodentia). In *The Timetree of Life*, SB. Hedges & Kumar (eds). Pp. 490-494.

Hood CS (2000) Geometric morphometric approaches to the study of sexual size dimorphism in mammals. *Hystrix* **11**: 77-90.

Jablonski D (2007) Scale and hierarchy in macroevolution. *Paleontology* **50**: 87-109.

Jones AG, Arnold SJ, Bürger R (2007) The mutation matrix and the evolution of evolvability. *Evolution* **61**: 727-745.

Kardong KV (1995) *Vertebrates: comparative anatomy, function, evolution*. Oxford: W.C. Brown.

Kent JT, Mardia K (2001) Shape, Procrustes tangent projections and bilateral symmetry. *Biometrika* **88**: 469-485.

Kiblisky P, Brum-Zorrilla N, Perez G, Saez FA (1977) Variabilidad cromossómica entre diversas poblaciones uruguayas del roedor cavador del género *Ctenomys* (Rodentia-Octodontidae). *Mendeliana* **2**: 85-93.

Kim HJ, Rice DP, Kettunen PJ, Thesleff I (1998) FGF-, BMP- and Shh-mediated signalling pathways in the regulation of cranial suture morphogenesis and calvarial bone development. *Development* **125**: 1241-1251.

King M (1987) Chromosomal rearrangements, speciation and the theoretical approach. *Heredity* **59**: 469-485.

King M (1993) *Species Evolution, the Role of Chromosomal Changes*. Cambridge: Cambridge University Press.

Kittlein MJ, Vassallo AI, Busch C (2001) Differential predation upon sex and age classes of tuco-tucos (*Ctenomys talarum*, Rodentia: Octodontidae) by owls. *Mammalian Biology* **66**: 281-289.

Klingenberg CP, Barluenga M, Meyer A (2002) Shape analysis of symmetric structures: quantifying variation among individuals and asymmetry. *Evolution* **56**: 1909-1920.

Klingenberg CP, Leamy LJ (2001) Quantitative genetics of geometric shape in the mouse mandible. *Evolution* **55**: 2342-2352.

Klingenberg CP, Leamy LJ, Routman EJ, Cheverud JM (2001) Genetic Architecture of Mandible Shape in Mice: Effects of Quantitative Trait Loci Analyzed by Geometric Morphometrics. *Genetics* **157**: 785-802.

Klingenbeg CP, Mebus K; Auffray J-C (2003) Developmental integration in a complex morphological structure: how distinct are the modules in the mouse mandible? *Evolution & Development* **5**: 522-531.

Koots KR, Gibson JP (1996) Realized sampling variances of estimates of genetic parameters and the differences between genetic and phenotypic correlations. *Genetics* **143**: 1409-1416.

Lacey EA, Patton JM, Cameron GN (2000) *Life Underground: The Biology of Subterranean Rodents*. Chicago and London: The University of Chicago Press.

Lande R (1976) Natural selection and random genetic drift in phenotypic evolution. *Evolution* **30**: 314-334.

Lande R (1977) Statistical tests for natural selection on quantitative characters. *Evolution* **31**: 442-444.

Lande R (1979) Quantitative genetic analysis of multivariate evolution, applied to brain: body size allometry. *Evolution* **33**: 402-416.

Lande R (1991) Isolation by Distance in a Quantitative Trait. *Genetics* **128**: 443–452.

Leamy L, Routman E, Cheverud J (1999) Quantitative trait loci for early and late developing skull characters in mice: a test of the genetic independence model of morphological integration. *Am Nat* **153**: 201-214.

Lessa EP, Vassallo AI, Verzi DH, Mora MS (2008) Evolution of morphological adaptations for digging in living and extinct Ctenomyid and Octodontid Rodents. *Biol J Lin Soc* **95**: 267-283.

Lessa EP (1990) Morphological evolution of subterranean mammals: integrating structural, functional, and ecological perspectives. In *Evolution of the Subterranean Mammals at the Organismal and Molecular levels*. Edited by Nevo E, Reig OA. New York: Alan Liss; 211-230.

Lessa EP, Stein BR (1992) Morphological constraints in the digging apparatus of pocket gophers (Mammalia: Geomyidae). *Biol J Lin Soc* **47**: 439-453.

Lessa EP, Cook JA (1998) The molecular phylogenetics of tuco-tucos (genus *Ctenomys*, Rodentia: Octodontidae) suggests as early burst of speciation. *Mol Phylogenet Evol* **9**: 88-99.

Lessa EP (2000) The Evolution of Subterranean Rodents: A Synthesis. In *Life Underground: The Biology of Subterranean Rodents*. Edited by Lacey EA, Patton JL, Cameron GN. Chicago: University of Chicago Press; 389-420.

Malizia AI, Busch C (1991) Reproductive parameters and growth in the fossorial rodent *Ctenomys talarum* (Rodentia: Octodontidae). *Mammalia* **55**: 193-305.

Mantel N (1967) The detection of disease clustering and a generalized regression approach. *Cancer Research* **27**: 209-220.

Marcus LF, Corti M, Loy A, Naylor GJP, Slice DE (1996) *Advances in Morphometrics*. NATO ASI series A: Life Sciences Vol. 284.

Marinho JR, Freitas TRO (2000) Intraspecific craniometric variation in a chromosome hybrid zone of *Ctenomys minutus* (Rodentia, Hystricognathi). *Mammalian Biology* **65**: 226-231.

Marinho JR, Freitas TRO (2006) Population structure of *Ctenomys minutus* (Rodentia, Ctenomyidae) on the coastal plain of Rio Grande do Sul, Brazil. *Acta Theriol* **51**: 53-59.

Marivaux L, Vianey-Liaud M, Welcomme JL, Jaeger JJ (2002) The role of Asia in the origin and diversification of hystricognathous rodents. *Zool Scripta* **31**: 225-239.

Márquez EJ, Aguilera M, Corti M (2000) Morphometric and chromosomal variation in populations of *Oryzomys albigularis* (Muridae: Sigmodontinae) from Venezuela: multivariate aspects. *Mammalian Biology* **65**: 84-99.

Marroig G, Cheverud JM (2001) A comparison of phenotypic variation and covariation patterns and the role of phylogeny, ecology, and ontogeny during cranial evolution on new world monkeys. *Evolution* **12**: 2576-2600.

Marroig G, Cheverud JM (2004) Did Natural Selection or Genetic Drift Produce the Cranial Diferentiation of Neotropical Monkeys? *Am Nat* **163**: 417-428.

Marroig G, De Vivo M, Cheverud JM (2004) Cranial evolution in sakis (*Pithecia*, Platyrrhini) II: evolutionary processes and morphological integration. *J Evol Biol* **17**: 144-155.

Marroig G, Cropp S, Cheverud JM (2004) Systematics and Evolution of the Jacchus Group of Marmosets (Platyrrhini). *Am J Phys Anthropol* **123**: 11-22.

Marroig G, Cheverud JM (2005) Size as a line of least evolutionary resistance: diet and adaptive morphological radiation in New World monkeys. *Evolution* **59**: 1128-1142.

Martins EP, Hansen TF (1997) Phylogenies and the comparative method: A general approach to incorporating phylogenetic information in to the analysis of interspecific data. *Am Nat* **149**: 646-667.

Mascheretti S, Mirol PM, Giménez MD, Bidau CJ, Contreras JR, Searle JB (2000) Phylogenetics of the speciose and chromosomally variable rodent genus *Ctenomys* (Ctenomyidae: Octodontidae), based on mitochondrial cytochrome *b* sequences. *Biol J Lin Soc* **70**: 361-376.

Massarini A, Barros MA, Ortells M (1991) Evolutionary biology of fossorial Ctenomyinae rodents (Caviomorpha: Octodontidae). I. Cromosomal polymorphism and small karyotypic differentiation in Central Argentinian populations of tuco-tucos. *Genetica* **83**: 131-144.

Massarini AI, Freitas TRO (2005) Morphological and cytogenetics comparison in species of the *mendocinus*-group (genus *Ctenomys*) with emphasis in *C. australis* and *C. flamarioni* (Rodentia-ctenomyidae). *Caryologia* **58**: 21-27.

Massarini AI, Dyzenchauz FJ, Tiranti SI (1998) Geographic variation of chromosomal polymorphism in nine populations of *Ctenomys azarae*, Tuco-tucos of the *Ctenomys mendocinus* group (Rodentia: Octodontidae). *Hereditas* **128**: 207-211.

Medina AI, Martí DA, Bidau CJ (2007) Subterranean rodents of the genus *Ctenomys* (Caviomorpha, Ctenomyidae) follow the converse to Bergmann's rule. *J Biogeogr* **34**: 1439-1454.

Monteiro LR, Reis SF (1999) *Princípios de Morfometria Geométrica.* Ribeirão Preto: Holos Editora.

Monteiro LR, Reis SF (2005) Morphological evolution in the mandible of spiny rats, genus *Trinomys* (Rodentia: Echimyidae). *J Zool Syst Evol Res* **43**: 332-338.

Moore W (1981) *The Mammalian Skull*. Cambridge University Press, Cambridge.

Mora M, Olivares AI, Vassallo AI (2003) Size, shape and structural versatility of the skull of the subterranean rodent *Ctenomys* (Rodentia, Caviomorpha): functional and morphological analysis. *Biol J Lin Soc* **78**: 85-96.

Mora MS, Lessa EP, Kittlein MJ, Vassallo AI (2006) Phylogeography of the Subterranean Rodent *Ctenomys australis* in sand-dune habitats: Evidence of Population Expansion. *J Mammal* **87**: 1192-1203.

Mora MS, Lessa EP, Cutrera AP, Kittlein MJ, Vassallo AI (2007) Phylogeographical structure in the subterranean tuco-tuco *Ctenomys talarum* (Rodentia: Ctenomyidae): contrasting the demographic consequences of regional and habitat-specific histories. *Mol Ecol* **16**: 3453-3456.

Moreira DM, Franco MHLP, Freitas TRO, Weimer TA (1991) Biochemical polymorphisms and phenetic relationships in rodents of the genus *Ctenomys* from southern Brazil. *Biochemical Genetics* **29**: 601-615.

Morriss-Kay GM (2001) Derivation of the mammalian skull vault. *J Anat* **199**: 143-151.

Morton NE (1973) Isolation by distance. In *Genetic Structure of Populations*. Edited by Morton NE. Honolulu: University of Hawaii. 76-79.

NABT – American National Association of the American National Association of Biology Teachers (2003) http://www.oklascience.org/NABTstatmnt.html. Acessado em 20 de agosto de 2009.

Nagylaki T (1994) Geographical Variation in a Quantitative Character. *Genetics* **136**: 361–381.

Navarro A, Barton NH (2003) Accumulating postzygotic isolation genes in parapatry: a new twist on chromosomal speciation. *Evolution* **57**: 447–459.

Nehring A (1887) Über eine *Ctenomys* – Art aus Rio Grande do Sul (Süd Brasilien). *Sitzungsberichte der Gesellschaft Naturforschender Freunde zu Berlin* **4**: 45–47.

Nei M (2007) The new mutation theory of phenotypic evolution. *PNAS* **104**: 12235-12242.

Nevo E (1979) Adaptive convergence and divergence of subterranean mammals. *Annual Review of Ecology Systematics* **10:** 269-308.

Nevo E, Filippucci MG, Reidi C, Korol A, Beiles A (1994) Chromosomal speciation and adaptive radiation of mole rats in Asia Minor correlated with increased ecological stress. *PNAS* **91:** 8160-8164.

Nevo E, Reig OA (1990) *Evolution of Subterranean Mammals at the Organismal and Molecular Levels. Progress in Clinical and Biological Research. Volume 335*. New York: Wiley-Liss.

Nevo E, Ivanitskaya E, Filippucci MG, Beiles A (2000) Speciation and adaptive radiation of subterranean mole rats, *Spalax ehrenbergi* superspecies, in Jordan. *Biol J Lin Soc* **69:** 263-281.

Nicola PA, Monteiro LR, Pessoa LM, Von Zuben J, Rohlf FJ, Reis SF (2003) Congruence of hierarchical, localized variation in cranial shape and molecular phylogenetic structure in spiny rats, genus *Trinomys* (Rodentia: Echimydae). *Biol J Lin Soc* **80**: 385-396.

Noden DM, Trainor PA (2005) Relations and interactions between cranial mesoderm and neural crest populations. *J Anat* **207**: 575-601.

Novello A, Altuna CA (2002) Cytogenetics and distribution of two new karyomorphs of the *Ctenomys pearsoni* complex (Rodentia, Octodontidae) from southern Uruguay. *Mammalian Biology* **67**: 188-192.

Nowak RM, Paradiso JL (1991) *Walker's Mammals of the World.* Baltimore and London: Johns Hopkins University Press.

Nowak RM (1999) *Walker's Mammals of the World*. Vol.2. 6ª ed. Baltimore & London, Johns Hopkins University Press, 1243-1681.

Ochocinska D, Taylor JRE (2003) Bergmann's rule in shrews: geographical variation of body size in Paleartic *Sorex* species. *Biol J Lin Soc* **78**: 365-381.

Ortells MO, Contreras JR, Reig OA (1990) New *Ctenomys* karyotypes (Rodentia, Octodontidae) from north-east Argentina and from Paraguay confirm the extreme chromosomal multiformity of the genus. *Genetica* **82**: 189-201.

Ortells MO, Barrantes GE (1994) A study of genetic distances and variability in several species of the genus *Ctenomys* (Rodentia: Octodontidae) with special reference to a probable causal role of chromosomes in speciation. *Bio J Linn Soc* **53**: 189-208.

Osgood WH (1946) A new octodont rodent from the Paraguayan chaco. *Fieldiana Zool* **31**: 47-49.

Osumi-Yamashita N, Eto K (1990) Mammalian Cranial Neural Crest Cells and Facial Development. *Development Growth & Differentiation* **35**: 451-459.

Palo JU, Ohara RB, Laugen AT, Laurila A, Primer CR, Merilä J (2003) Latitudinal divergence of common frog (*Rana temporaria*) life history traits by natural selection: evidence from a comparison of molecular and quantitative genetic data. *Mol Ecol* **12**: 1963-1978.

Parada A (2007) Sistemática molecular de *Ctenomys* (Rodentia, Ctenomyidae): Límites y grupos de especies abordados con un muestro taxonómico y geográfico denso. Faculdad de Ciencias UDELAR. Tesis de Maestría.

Paradis E, Strimmer K, Claude J, Jobb G, Open-Rhein R, Dultheil J, Bolker NB (2006) APE: Analyses of phylogenetics and Evolution in R. R package version 1.8-2.

Pearson OP (1959) Biology of the subterranean rodents, *Ctenomys*, in Peru. *Memorias del Museu de Historia Natural "Javier Prado"* **9**: 1-56.

Pearson OP, Binsztein N, Boiry I, Busch C, Dipace M, Gallopin G, Penchaszadeh P, Piantanida M (1968) Estructura social, distribución espacial e composición por edades de una población de tuco-tucos (*Ctenomys talarum*). *Investigaciones Zoologicas Chilenas* **13**: 47-80.

Pessôa LM, Reis SF (1991) Cranial infraspecific differentiation in *Proechimys iheringi* Thomas (Roentia: Echimyidae). *Mammalian Biology* **56**: 34-40.

Polly PD (2004) On the simulation of the evolution of morphological shape: multivariate shape under selection and drift. *Paleontologia Electronica* **7**: 28.

Polly PD (2007) Phylogeographic differentiation in *Sorex araneus*: morphology in relation to geography and karyotype. *Russian J Theriol* **6**: 73-84.

Reig OA, Contreras JR, Piantanida MJ (1966) *Contribución a la elucidación de la sistematica de las entidades del genero* Ctenomys *(Rodentia, Octodontidae). Contribuiciones Cientificas – Serie Zoologica*. Faculdad de Ciencias Exactas y Naturales Universidad de Buenos Aires **2**: 297-352.

Reig OA, Kiblisky P (1969) Chromosome multiformity in the genus *Ctenomys* (Rodentia: Octodontidae). *Chromosoma* **28**: 211-244.

Reig OA, Busch C, Ortells MO, Contreras JR (1990) An overview of evolution, systematics, population biology, cytogenetics, molecular biology and speciation in *Ctenomys*. In *Evolution of the Subterranean Mammals at the Organismal and Molecular Levels. Progress in Clinical and Biological Research.* Volume 335. Edited by Nevo E, Reig OA. New York: Wiley-Liss; 71-96.

Reis SF, Duarte LC, Monteiro LR, Von Zuben FJ (2002a) Geographic variation in cranial morphology in *Thrichomys apereoides* (Rodentia: Echimyidae). I. Geometric descriptors and patterns of variation in shape. *J Mammal* **83**: 333-344.

Reis SF, Duarte LC, Monteiro LR, Von Zuben FJ (2002b) Geographic variation in cranial morphology in *Thrichomys apereoides* (Rodentia: Echimyidae). II. Geographic units, morphological discontinuities, and sampling gaps. *J Mammal* **83**: 345-353.

Relenthford JH (2004) Global Patterns of Isolation by Distance Based on Genetic and Morphological Data. *Hum Biol* **76**: 499-513.

Ripley BD (1996) *Pattern recognition and neural networks*. Cambridge: Cambridge University Press.

Rieseberg LH (2001) Chromosomal rearrangements and speciation. *TREE* **16**: 351–358.

Rohlf FJ (2004) TPSDig, ver. 1.40 software, F. James Rohlf. Dept. Ecology and Evolution, State University of New York Stony Brook. [http://life.bio.sunysb.edu/morph/].

Rohlf FJ, Slice D (1990) Extensions of the Procrustes Method for the Optimal Superimposition of Landmarks. *Syst Zool* **39**: 40-59.

Rohlf FJ, Marcus LF (1993) A revolution in morphometrics. *TREE* **8**: 129-132.

Rohlf FJ, Corti M (2000) Use of Two-Block Partial Least-Square to Study Covariation in Shape. *Syst Biol* **49**: 740-753.

Saether SA, Fiske P, Kalas JA, Kuresso A, Luigujõe L, Piertney SB, Sahlman T, Höglund J (2007) Inferring local adaptation from Q_{ST}-F_{ST} comparisons: neutral genetic and quantitative trait variation in European populations of great snipe. *J Evol Biol* **20**: 1563-1576.

Simons AM (2002) The continuity of microevolution and macroevolution. *J Evol Biol* **15**: 688-701.

Simpson GG (1944) *Tempo and Mode in Evolution.* New York: Columbia University Press.

Slamovits CH, Cook JA, Lessa EP, Rossi MS (2001) Recurrent amplifications and deletions of satellite DNA accompanied chromosomal diversification in South American tuco-tucos (Genus *Ctenomys*, Rodentia: Octodontidae): a phylogenetic approach. *Mol Biol Evol* **18**: 1708-1719.

Slatkin M, Barton NH (1989) Comparison of three indirect methods for estimating average levels of gene flow. *Evolution* **43**: 1349-1368.

Stein BR (2000) Morphology of subterranean rodents. In *Life Underground: The Biology of Subterranean Rodents.* Edited by Lacey EA, Patton JL, Cameron GN. Chicago: University of Chicago Press; 19-61.

Steinberg EK, Patton JL (2000) Genetic Structure and the Geography of Speciation in Subterranean Rodents: Opportunities and Constraints for Evolutionary Diversification. In *Life Underground: The Biology of Subterranean Rodents.* Edited by Lacey EA, Patton JL, Cameron GN. Chicago. University of Chicago Press; 301-331.

Storz JF (2002) Contrasting patterns of divergence in quantitative traits and neutral DNA markers: analyis of clinal variation. *Mol Ecol* **11**: 2537-2551.

Sutton DA, Patterson BD (2000) Geographic variation of the western chipmunks *Tamias senex* and *T. siskiyou*, with two new subspecies from California. *J Mammal* **81**: 299-316.

Taylor PJ (2000) Patterns of chromosomal variation in southern African Rodents. *J Mammal* **81:** 317-331.

Thomas O (1916) Two new Argentine rodents, with a new subgenus of *Ctenomys*. *Ann Mag Nat Hist* **18**: 303-306.

Tiranti SI, Dyzenchauz FJ, Hasson ER, Massarini AI (2005) Evolutionary and systematic relationships among tuco-tucos of the *Ctenomys pundti* complex (Rodentia: Octodontidae): a cytogenetic and morphological approach. *Mammalia*. **69**: 69-80.

Tomasco I, Lessa EP (2007) Phylogeography of the tuco-tuco *Ctenomys pearsoni*: mtDNA variation and its implication for chromosomal differentiation. In *The Quintessential Naturalist: Honoring the Life and Legacy of Oliver P. Perason*. Edited by Kelt DA, Lessa EP, Salazar-Bravo JA, Patton JL. University of California Publication in Zoology Series, Berkeley, California.

Vassallo AI (1998) Functional morphology, comparative behaviour, and adaptation in two sympatric subterranean rodents genus *Ctenomys* (Caviomorpha: Octodontidae). *J Zool Lond* **244**: 415-427.

Vassallo AI, Kittlein MJ, Busch C (1994) Owl predation on two sympatric species of tuco-tucos (Rodentia: Octodontidae). *J Mammal* **75**: 725-732.

Vassallo AI (2000) Alometría e Isometría em varias especies de roedores caviomorfos, con comentarios sobre la estructura del aparato masticatorio del orden Rodentia. *J Neotrop Mammal* **7**: 37-46.

Vassallo AI, Mora MS (2007) Interspecific scaling and ontogenetic growth patterns of the skull in living and fossil Ctenomyid and Octodontid rodents (Caviomorpha: Octodontidea). In *The Quintessential Naturalist: Honoring the Life and Legacy of Oliver P. Pearson*. Eds, Kelt DA, Lessa EP, Salazar-Bravo J, Patton JL. University of California Publications in Zoology, California, **134**: 945-968.

Venables WN, Ripley BD (2002) MASS: Modern applied statistics with S. 4th ed., New York: Springer.

Verzi DH (2002) Patrones de evolución morfológica en Ctenomyinae (Rodentia, Octodontidae). *J Neotrop Mammal* **9**: 309-328.

Verzi DH (2008) Phylogeny and adaptive diversity of rodents of the family Ctenomyidae (Caviomorpha): delimiting lineages and genera in the fossil record. *J Zool Lond* 1-9.

Verzi DH, Olivares AI (2006) Craniomandibular joint in South American burrowing rodents (Ctenomyidae): adaptations and constraints related to a specialized mandibular position in digging. *J Zool Lond* **270**: 488-501.

Verzi DH, Olivares AI, Morgan CC (2010) The oldest South American tuco-tuco (late Pliocene, northwestern Argentina) and the boundaries of the genus *Ctenomys* (Rodentia, Ctenomyidae). *Mammalian Biology* **75**: 243-252.

Vitullo AD, Roldan ERS, Merani MS (1988) On the morphology of spermatozoa of tuco-tucos, *Ctenomys* (Rodentia: Ctenomyidae): New data and its implications for the evolution of the genus. *J Zool Lond* **215**: 675-683.

Weschenfelder J (2005) Processos sedimentares e variação do nível do mar na região costeira do Rio Grande do Sul, Brasil. Universidade Federal do Rio Grande do Sul (Tese de doutorado).

Weschenfelder J, Medeanic S, Corrêa ICS, Aliotta S (2008) Holocene Paleointel of the Bojuru Region, Lagoa dos Patos, Southern Brazil. *Journal of Coastal Research* **24**: 99-109.

White MJD (1978) *Modes of Speciation*. W.H. Freeman and Company. San Francisco.

Whitlock MC (1999) Neutral additive genetic variance in a metapopulation. *Genetics Research, Cambridge* **74**: 215–221.

Wilson DE, Reeder DM (1993) *Mammal species of the world: A Taxonomic and Geographic Reference*. 2nd ed. Washington, DC: Smithsonian Institution Press.

Wilson DE, Reeder DM (2005) *Mammal Species of the World. A Taxonomic and Geographic Reference.* 3rd ed. Johns Hopkins University Press.

Wlasiuk G, Garza JC, Lessa EP (2003) Genetic and geographic differentiation in Rio Negro tuco-tuco (*Ctenomys rionegrensis*): inferring the roles of migration and drift from multiple genetic markers. *Evolution* **57**: 913-926.

Woods CA (1993) Suborder Hystricognathi. In *Mammal Species of the World.* Edited by Wilson DE, Reeder DM. Washington: Smithsonian Institute Press; 771-807.

Woods CA, Kilpatrick CW (2005) Infraorder Hystricognathi Brandt, 1855. In: Wilson DE, Reeder DM, eds. *Mammal Species of the World*. Baltimore: Johns Hopkins University Press, 1538-1600.

Wright S (1943) Isolation by distance. *Genetics* **28**: 114-138.

Wright SP (1992) Adjusted P-values for simultaneous inference. *Biometrics*, **48**: 1005–1013.

Yom-Tov Y, Yom-Tov J (2005) Global warming, Bergmann's rule and body size in the masked shrew *Sorex cinereus* Kerr in Alaska. *Journal of Animal Ecology* **74**: 803-808.

Zenuto RR, Busch C (1998) Population biology of the subterranean rodent *Ctenomys australis* (Tuco-tuco) in a coastal dunefield in Argentina. *Mammalian Biology* **63**: 357-367.

Zenuto RR, Vassallo AI, Busch C (2001) A method for studying social and reproductive behavior of subterranean rodents in captivity. *Acta Theriol* **46**: 161-170.